The Role of Intracellular Galectin-3 in the CD8 T Cell Response

By

Mohammad Farhad Amani

A DISSERTATION

Presented to the Department of Cell, Developmental & Cancer Biology, Oregon Health & Science University

School of Medicine

Submitted in partial fulfillment of the requirements for

the degree of

DOCTOR OF PHILOSOPY

January, 2020

Oregon Health and Science University

Portland, Oregon

School of Medicine

Oregon Health & Science University

CERTIFICATE OF APPROVAL

This is to certify that the PhD dissertation

Mohammad Farhad Amani

has been approved

Mentor – Dr. William L. Redmond

Chair – Dr. Bernard A. Fox

Member – Dr. Ann B. Hill

Member – Dr. Evan F. Lind

Member – Dr. Owen J.T. McCarty

TABLE OF CONTENTS

List of Tables

List of Figures

List of Abbreviations

HSC: hematopoietic stem cell

LPS: lipopolysaccharide

B cells: B lymphocytes

T cells: T lymphocytes

APC: antigen presenting cells

Ig: immunoglobulin

BCR: B cell receptors

FO: follicular

MZ: marginal zone

CD40L: CD40 ligand

TCR: T cell receptors

MHC: major histocompatibility complex

NK cells: natural killer cells

mTEC: epithelial cells in the medulla

AIRE: autoimmune regulator genes

DRs: death receptors

APAF-1: apoptotic protease activating factor 1

DISC: death-inducing signaling complex

pMHC: TCR- peptide-MHC

LCMV: lymphocytic choriomeningitis virus

ALPS: Autoimmune Lymphoproliferative Syndromes

LCK: lymphocyte-specific protein-tyrosine kinase

SH2: SRC-homology 2

ITAMs: immunoreceptor tyrosine-based activation motifs

NFAT: nuclear factor of activated T cells

MAPK: mitogen-activated protein kinase

Th: T helper

Tfh: T follicular helper

Treg: T regulatory

CTLs: cytotoxic lymphocytes

HEV: high endothelial venules

CCR7: CC-chemokine receptor 7

LFA1: lymphocyte function-associated antigen 1

ICAM1: intracellular adhesion molecule 1

T_E: effector T cell

IFN- γ: effector cytokine

T_{CM}: central memory

T_{EM}: effector memory

γc: gamma chain

IL-2: interleukin-2

JAK: Janus family kinase

STAT: signal transducers and activators of transcription

GAS: gamma interferon-activated sequence

FoxP3: forkhead box P3

T-bet: T-box transcription factor

Gata3: GATA binding protein 3

FOXO1: forkhead box O1

SOS: Ras guanine nucleotide exchange protein

SHC: Src homology 2 domain containing

GRB2: growth factor receptor-bound protein 2

GDP: guanosine diphosphate

GTP: guanosine triphosphate

mTOR: mammalian target of rapamycin

HIF1A: hypoxia inducible factor 1 subunit alpha

S1P1: sphingosine-1-phosphate receptor 1

PI 3-K: phosphoinositol 3-kinase

TNFR: tumor necrosis factor receptor

TRAF: TNF receptor associated factor

OX40L: OX40 ligand

NF-kB: nuclear factor kappa-light-chain-enhancer of activated B cells

TME: tumor microenvironment

EGF: epidermal growth factor

CSF-1: colony stimulating factor 1

FGF: fibroblasts growth factor

HB-EGF: heparin-binding EGF

NRG: neuregulin

TGF: transforming growth factor

VEGF: vascular endothelial growth factor

FDA: US Food and Drug Administration

CAR: chimeric antigen receptor

mAbs: monoclonal antibodies

CTLA-4: cytotoxic T-lymphocyte-associated protein 4

PD-1: programed cell death-1

PD-L1: programed death-ligand 1

rIL-2: recombinant IL-2

Fyn: tyrosine-protein kinase Fyn

ZAP-70: zeta-chain-associated protein kinase 70

IFN-γ: interferon-γ

LAG-3: lymphocyte activation gene 3

TIM-3: T cell membrane protein 3

BTLA: B and T lymphocyte attenuator

TIGIT: T cell immunoreceptor with Ig and ITIM domains

VISTA: V-domain Ig suppressor of T cell activation

gp100: glycoprotein 100 vaccine

BRAF: serine/threonine-protein kinase

MSI-hi: microsatellite instability-high

Gal-3: galectin-3

CRDs: carbohydrate-recognition-binding domain

MMP: matrix metalloproteinases

SCLC: small cell lung cancer

NNK: 4-(methylnitrosamino)-1-(3-pyridyle)-1-butanone

polyLacNAc: poly-N-acetyllactosamine

CLL: chronic lymphocytic leukemia

IL-2R: IL-2 receptor

Ag: antigen

LN: lymph nodes

Erdr1: erythroid differentiation regulator 1

CT: center of the tumor

IM: invasive margin

IHC: immunohistochemistry

mIHC: multiplex IHC

ABC: avidin–biotin complex

LSAB: Labeled Streptavidin–Biotin

MICSSS: multiplexed immunohistochemical consecutive staining on single slide

FFPE: formalin-fixed paraffin-embedded

MSI: multispectral images

TSA: tyramide signal amplification

HRP: horseradish peroxidase

10% NBF: 10% neutral buffered formalin

PLP: Periodate-lysine-paraformaldehyde

NSCLC: non-small cell lung cancer

CK: cytokeratin

MIBI: multiplexed ion beam imaging

IMC-CyTOF: imaging mass cytometry

DSP: digital spatial profiling

Acknowledgments

First and foremost, I would like to thank my family living in Kabul, Afghanistan for their support and help in pursuing my education in the United States. They have all sacrificed to give me the strength to continue my education and succeed. None of my achievements would have been possible without my family. Mike Manaton, my American brother, has been an inspiration, a mentor, and a friend, who has always been there to help me in reaching my goals from the day I stepped into the United States. He was always there to celebrate my achievements or counsel me when I was homesick. Thank you, Mike, for your unwavering support. I would like to thank all the friends I have made in the United States for their support and being there for me in rough times.

Dr. Redmond, it has been a great privilege to be your first graduate student. Thank you for taking a chance on me and giving me the opportunity to work in your lab. You have made my graduate school experience memorable. I have not only benefited from your depth of scientific knowledge but also your positive attitude, patience and willingness to listen. You have made me feel like a colleague and have given me every opportunity to express my scientific curiosity. I have truly learned what open-door policy is from you. You have never disappointed me even when I asked you for money and you gave me one penny, because I had not specified how much. It has been a great honor to be your student.

Earle A. Chiles Research Institute has been and will always be a very special place for me. At our institute, I have been lucky enough to interact with and learn from the best and brightest of the immunology field. Each member of EACRI was willing and available to give help and guidance throughout my graduate school. I will always cherish

memories of belonging to this great group of scientists striving to find a cure for cancer. Special thanks go to the past and present members of the Redmond lab. Melissa Kasiewicz is the best lab manager anyone could ask for. She always made sure that everything was available and ready for experiments and was willing to help in the mouse room with lightning speed. Dr. Annah Rolig has been a tremendous help in reviewing and editing my scientific writing. Annah has always been available and willing to discuss even minute points of my data. She has been a tremendous guide in expressing my scientific communication.

Dr. Bernard Fox, thank you for believing in me. I had lost my confidence in graduate school when I first came to your office. When you gave me an opportunity to rotate in your lab, I truly learned the meaning of the word mentor. Although I ended up joining Redmond Lab, you never stopped encouraging, advising, and supporting me throughout my graduate school. Thank you for being a great co-mentor, Dr. Fox. I also have to mention that Fox lab became my second home lab, and that every member of the Fox lab was always willing to help me in any way they could, specially Dr. Jenson. Shawn has been always available to discuss my project or just talk about life.

Last but not least, I would like to thank my thesis committee (Drs. Evan Lind, Bernard Fox, Will Redmond, Ann Hill and Owen McCarty) for their time commitments and critical analyses of my project. They have pushed me to be a better scientist.

Abstract

The ability of tumors to induce immunosuppression and inhibit the cytolytic function of tumor-infiltrating lymphocytes (TIL) is a major obstacle to creating effective immunotherapies for cancer patients. The levels of galectin-3 (Gal-3) protein, which contribute to the immunosuppression, are increased during tumor progression in many cancers. Gal-3 contributes to immunosuppression by inducing M2 (wound healing) polarization of tumor-associated macrophages and playing a role in the survival and metastasis of cancer cells.

The biology of extracellular Gal-3 has been extensively studied, however, the function of and mechanisms by which intracellular Gal-3 regulates $CD8^+$ T cell responses are poorly understood. We demonstrate that antigen-specific Gal-$3^{-/-}$ OT-I $CD8^+$ T cells exhibited no defects in early activation and proliferation. Additionally, Gal-$3^{-/-}$ OT-I T cells exhibited decreased survival and transition to memory in response to cognate antigen plus agonist anti-OX40 (aOX40) mAb therapy *in vivo* and abrogated the efficacy of agonist aOX40 therapy in a tumor model. Together, these data implicate intracellular Gal-3 as a critical mediator of $CD8^+$ T cell survival and memory formation following antigen exposure.

Chapter 1: A brief review of immune system

1 Immune System

The immune system is comprised of organs, tissues, cells, and molecular components that work in concert to protect the host from foreign pathogens and self-derived cellular abnormalities and can evolve to match ever-changing threats. Immune system function is divided into two arms of response: innate and adaptive immunity. The cellular components of both the innate and adaptive immune systems originate from pluripotent hematopoietic stem cells (HSCs) in the bone marrow (Fig. 1). Innate immunity is the first line of defense and has a nonspecific response to foreign organisms, and there is no memory developed. While adaptive immunity is versatile and builds memory of the encountered specific pathogen for future enhanced specific responses. Although innate and adaptive immunity are categorized separately, the two arms interact in order to defend the organism from foreign pathogens.

1.1 Innate immunity

Innate immunity, found in all multicellular organisms, is evolutionarily the most ancient part of the immune system (3, 4). Innate immunity is the first line of defense in vertebrates and responds to pathogens in the early hours of infection in a nonspecific manner (5). Innate immunity uses different mechanisms to limit or, in some cases, eliminate pathogens and is comprised of three components: physical barriers, cellular immunity, and humoral immunity. Physical barriers include skin, epithelial and mucous membrane, mucus itself, and anatomical barriers, which physically bar pathogens from entering the host. Macrophages, neutrophils, eosinophils, basophils, mast cells, natural

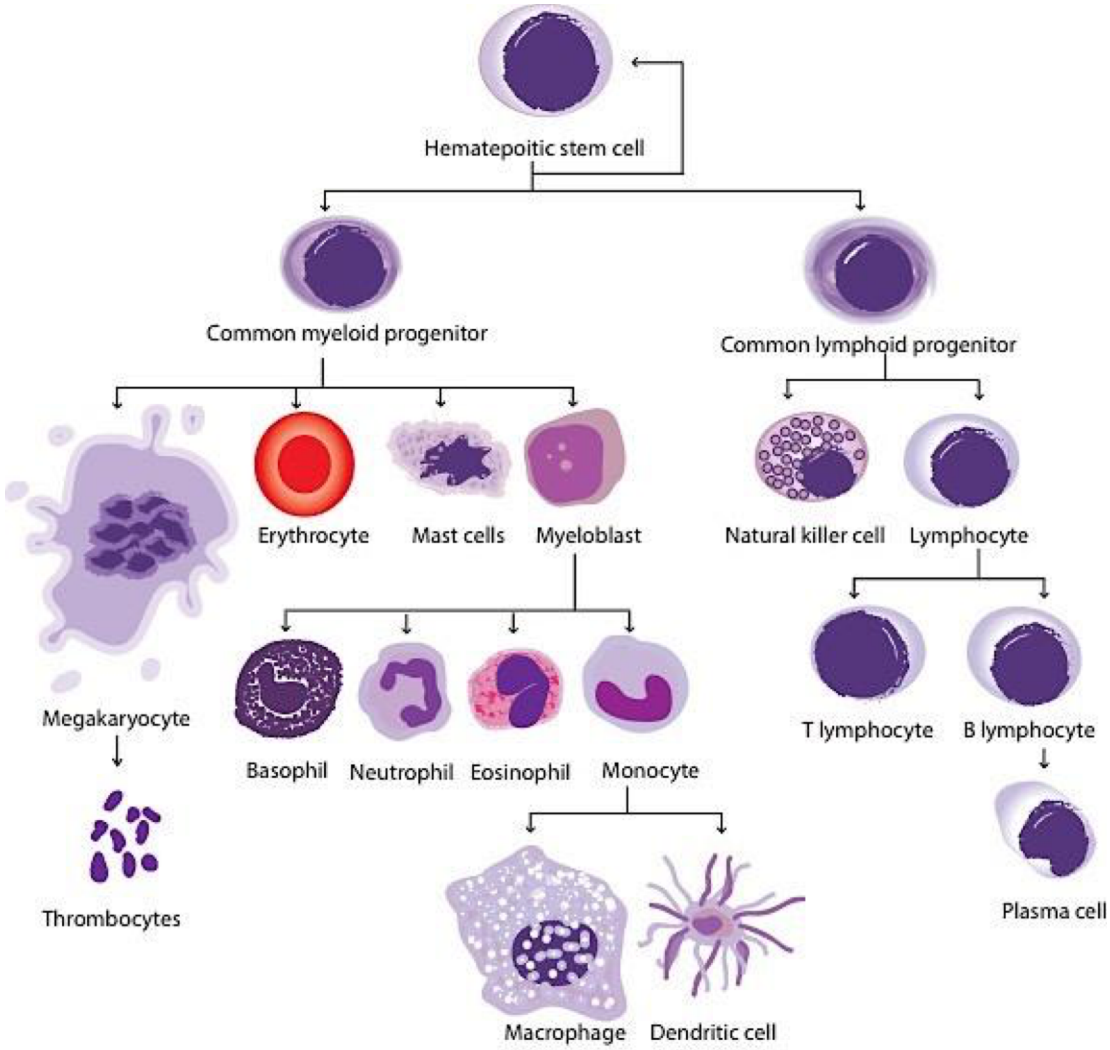

Figure 1. Hematopoiesis: All cellular blood components are derived from hematopoietic stem cells (adapted from OpenStax). The diagram represents the major cell types in hematopoiesis.

killer cells, and dendritic cells make up the cellular components of the innate system that originate from HSCs in the bone marrow (5, 6). Cellular innate immunity is supplemented by its humoral component, which includes complement proteins, C-reactive protein, lipopolysaccharide (LPS) binding proteins and other pentraxins, collectins, and anti-microbial peptides such as defensins. The humoral component proteins circulate in order to identify pathogens and act as an effector mechanism to facilitate clearance of the pathogen (6). The components of the innate immune system prevent pathogen invasion, eliminate the pathogen, and in the event of failure to eliminate the pathogen, the innate immune system activates adaptive immune responses.

1.2 Adaptive immunity

In contrast to innate immunity, adaptive immunity responds more slowly after antigen encounter, but the responses are tailored and specific. In addition, adaptive immunity has the ability to develop antigen-specific memory and can respond rapidly to a second encounter with the same antigen (7). Adaptive immunity is activated through molecular and cellular components of the innate immune response, which are discussed in more detail below. There are two types of adaptive immunity: humoral and cell-mediated. Humoral immunity is primarily mediated by B lymphocytes (B cells) in response to antigens from pathogens that are freely circulating, or outside the infected cells. Cell-mediated immunity is mounted by T lymphocytes (T cells) in response to antigen peptides generated from intracellular and extracellular pathogens by innate immune antigen presenting cells (APC) (8).

1.2.1 Humoral adaptive immunity

The humoral arm of the adaptive immune system is mediated by antibodies secreted by B cells. B cells originate from HSCs and during fetal life, B cells develop in the liver, while during adulthood B cells develop in the bone marrow (8). B cells develop in four differentiation stages: pre-pro-B cells, early pro-B cells, late pro-B cells, and pre-B cells (9). The four precursor B-cells do not express surface immunoglobulin receptors (Ig) (10). Random gene rearrangement occurs in the bone marrow during mature B cell development, which produces a large number of B cells with B cell receptors (BCR) that have different antigenic specificities. To ensure that self-reactive antibodies are not produced, B cells go through clonal deletion, a selection process that eliminates any B cells expressing membrane-bound antibodies that recognize self-components (11). Alternatively, self-reactive B cells may undergo BCR editing, a positive selection process through which new BCRs are formed, resulting in a positive selection of these cells for further development (12)

The majority of B cells are eliminated through deletion in the bone marrow during development and thus only a small number of immature B cells enter the spleen as transitional cells (13). The immature B cells in the spleen receive pro-survival signals and subsequently differentiate into naïve B cells, which start expressing IgM and IgG surface receptors. Based upon the strength of BCR signaling, naïve B cells differentiate into follicular (FO) and marginal zone (MZ) B cells (14). The MZ B cells are resting mature B cells that do not circulate and are located in the splenic white pulp zone. When MZ B cells are activated they develop into short-lived plasma cells; short-lived plasma cells

secrete low-affinity IgM antibodies and do not develop memory B cells. On the other hand, FO B cells circulate between the blood and the spleen. FO B cells are located adjacent to T cell-rich areas in secondary lymphoid organs and are activated through interaction with CD4 T cells. Antigens bind the membrane-bound Ig on the surface of FO B cells. FO B cells process these antigens and present them to CD4 helper T cells; in turn, activated CD4 helper T cells express CD40 ligand (CD40L) and other cytokines necessary to activate FO B cells (15). The activated FO B cells go through clonal expansion and develop into plasma cells that produce and secrete a large amount of high-affinity antibodies. Some of the activated FO B cells form a germinal center within secondary lymphoid organs, where the FO B cells undergo extensive proliferation, Ig class switching, and somatic hypermutation in order to develop memory B cells or long-lived plasma cells (14, 16). Long-lived plasma cells migrate from the germinal center to the bone marrow, continuously producing antibodies that circulate throughout the host to provide long-term protection against secondary exposure to pathogens.

1.2.2 Cell-mediated adaptive immunity

T cells are responsible for cell-mediated adaptive immunity in response to antigen peptides, most often originating from intracellular and extracellular pathogens, that are presented by APCs. T cells express T cell receptors (TCR) that recognize antigens bound to major histocompatibility complex (MHC) molecules on the surface of the APC membrane (Fig. 2). The interaction of the TCR with MHC molecules dictates T lymphocyte development, activation, and differentiation.

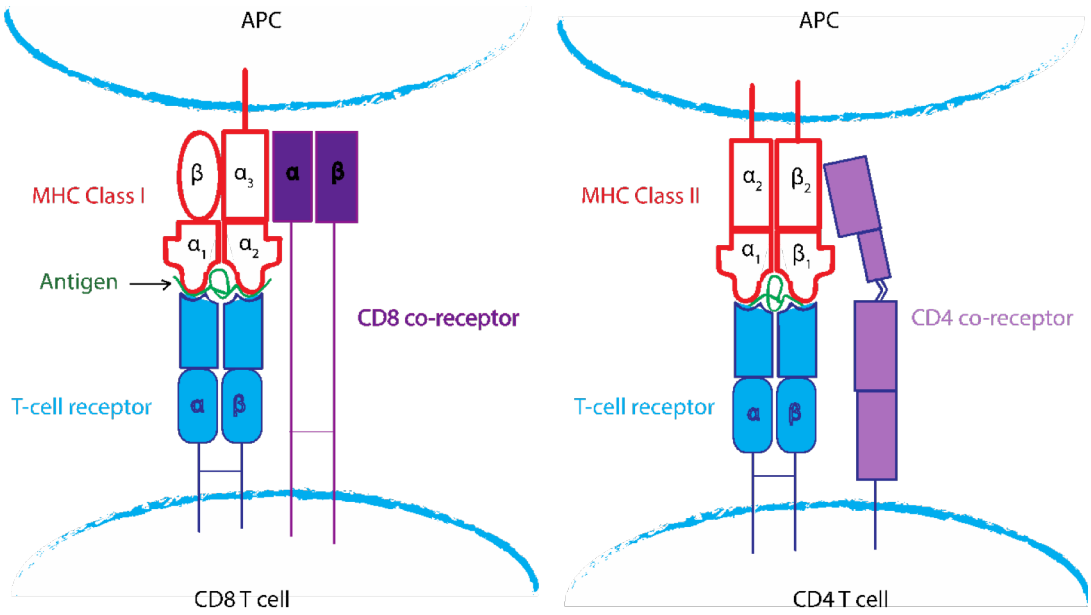

Figure 2. The cartoon depicts TCR-MHC interaction (adapted from The Immune System, Garland Science, 2009). APCs presents peptides originating from intracellular and extracellular pathogens on MHC class I and MHC class II to CD8 and CD4 T cells, respectively

1.2.2.1 T lymphocyte development

T lymphocytes originate from HSCs in the bone marrow and then migrate to the thymus to mature. The thymus is divided into numerous lobules that contain cortex and medulla regions. The thymic stroma provides a suitable environment for T cell development and interacts with and educates developing T cell precursors as they migrate through the cortex (17). T lymphocytes in the thymus go through different stages of differentiation, proliferation, and developmental regulatory mechanisms that eliminate T

lymphocytes that recognize self-antigens or fail to recognize foreign antigens presented by APCs (18). Different stages of T lymphocyte development in the thymus are denoted by a series of changes in TCR gene expression, expression of the TCR complex and the co-receptors CD4 and CD8 (19). As lymphoid progenitor cells enter the thymus through the cortico-medullary junction, they do not express the TCR, CD4, or CD8 co-receptors, thus are named double-negative T cells. The majority of these double-negative T cells will develop into αβ T cells and a minority will develop into γδ T cells. In addition, double-negative T cells can give rise to B and natural killer cells (NK cells), if injected into the blood; however, as they move through the thymic cortex, these double-negative T cells commit to the T cell lineage and lose the ability to give rise to B or NK cells (17, 20). At this stage, the committed T cell precursors express recombination-activating genes (21), which trigger TCRβ then TCRα locus rearrangement. The rearranged TCRβ pairs with TCRα, which together form low levels of TCRs on the cell surface. Subsequently CD4 and CD8 co-receptors are both expressed, and the T cells become highly proliferative double-positive T cells (18, 22).

The transition from double-negative to double-positive T cells takes place in the thymic cortex over the span of about 18 days (23). Double-positive T cells that express fully formed αβ TCRs survey for self-peptides presented by MHC on cortical thymic epithelial cells and subsequently undergo a selection processes (17, 24). In the selection process, T cells that recognize self-peptides with high affinity are eliminated by negative selection, whereas those that recognize self-peptides with low affinity undergo positive selection (25). The remaining double-positive T cells that do not recognize MHC presented self-peptides are deleted by apoptosis in a process called death by neglect (22).

Double-positive cells that have gone through positive selection differentiate into single positive cells, expressing either the CD4 or CD8 co-receptor. Whether the CD4 or CD8 co-receptor expression is maintained depends on the T cell's MHC specificity, which leads to gene expression changes and dictates their potential effector functions (19). Single positive T cells migrate to the medulla where they undergo an additional selection process. The epithelial cells in the medulla (mTEC) express tissue-restricted antigens that are regulated by Autoimmune Regulator genes (AIRE). Single positive T cells spend an average of 2 weeks in the medulla surveying tissue-restricted antigens presented by mTEC, which T cells may encounter in the periphery. T cells that recognize self-antigens in this context are eliminated through negative selection to avoid autoimmunity (23, 26). T cells that survive this selection process are fully mature and egress from the medulla to peripheral tissues (17, 27).

1.2.2.2 Apoptosis

Apoptosis is a process of energy-dependent programmed cell death that relies on coordinated activation of caspases (28). Multicellular organisms use apoptosis as the primary mechanism of programmed cell death during developmental stages and homeostasis throughout their lifetime (29). For example, apoptosis is the primary mechanism for elimination of autoreactive T lymphocytes in development and contracting clonally expanded T lymphocytes following response to antigen to maintain immunological homeostasis (30, 31). In addition to development and homeostasis, apoptosis is also an important mechanism to prevent pathogenesis by removing cells, which are damaged, infected, and potentially malignant (32-36). Apoptosis can be

induced through either intrinsic or extrinsic pathways. The intrinsic pathway is regulated by the balance between pro-apoptotic and anti-apoptotic Bcl-2 family proteins, and the extrinsic pathway is initiated by the ligation of death receptors (DRs) on the cell surface (37). The intrinsic and extrinsic apoptosis pathways converge via the activation of caspases, which are members of the cysteine protease family (38).

The intrinsic apoptotic pathway is regulated by the balance of pro-apoptotic (Bim, Bax, Bak, Puma, Noxa, Bad, Bcl-xS, Bid, Bik) and anti-apoptotic (Bcl-2, Mcl-1, A1, Bcl-xL, Bcl-W) Bcl-2 family proteins (30). The levels of pro- versus anti-apoptotic proteins are crucial for their function due their physical interaction and ability to decide cell fate (39). During an insult, such as stress, hypoxia, oxidative stress, or DNA damage, pro-apoptotic proteins such as Bim, Bad, Puma, and Noxa are upregulated (40). Upon upregulation, these pro-apoptotic proteins create pores in the outer membrane of mitochondria, which releases cytochrome c from the inner member of mitochondria into the cytosol to form a complex of apoptotic protease activating factor 1 (APAF-1) and pro-caspase-9, known as the apoptosome (28). Subsequently, activated pro-caspase-9 activates the downstream effector molecule, caspase-3 (41). Activation of caspase-3 initiates a cascade of events that leads to proteolytic degradation of the cell.

In the extrinsic pathway, apoptosis is triggered by trimerization of DRs such as Tumor Necrosis Factor Receptor (TNFR), Fas, TNFR-1, TNF-related apoptosis-inducing ligand (TRAIL-R1), and TRAIL-R2 upon ligation. Trimerization of DRs induces receptor clustering and recruitment of adaptor proteins, leading to formation of the death-inducing signaling complex (DISC) (41, 42). DISC then recruits initiator caspases, such as pro-caspase-8, which is activated through auto-proteolytic cleavage (41). Finally, the

activated initiator caspases cleave effector caspases such as caspase-3, -6 or -7, resulting in the proteolytic intracellular disintegration of the cell (41).

1.1.1.1.1 Intrinsic apoptosis and T lymphocyte development in the thymus

The elimination of autoreactive lymphocytes during development by apoptosis is called central tolerance. This process is indispensable for the proper development of mature lymphocytes in the thymus, and the deletion of autoreactive T lymphocytes is a critical mechanism to achieve immunological self-tolerance (31). T lymphocyte progenitor cells undergo several developmental and differentiation stages in the thymus to become a mature T lymphocyte. A number of these developmental and differentiation stages rely on survival or death signals that lead to the elimination of autoreactive T lymphocytes via apoptosis (31, 38). T lymphocytes with fully assembled TCRs transition from the double negative (CD4 and CD8 negative) stage to the double positive (CD4 and CD8 positive) stage, where they stay quiescent for 3-4 days and go through the TCR selection process (31). The TCR selection process can result in positive selection of T lymphocytes to become CD4 or CD8 T cells when TCR recognize pMHC with appropriate affinity, elimination of T lymphocytes by negative selection if the interaction between TCR and peptide-MHC (pMHC) is too strong, or elimination of T lymphocytes by neglect if the TCR fails to recognize pMHC. These three fates are regulated by the balance of pro- and anti- apoptotic Bcl-2 family members. For example, the survival of thymocytes in the double positive stage is maintained by the upregulation of anti-apoptotic Bcl-xL prior to TCR selection (43). In addition, the anti-apoptotic Mc1-1

interferes with the pro-apoptotic protein, Bak, thereby promoting thymocytes survival (44). On the other hand, Bim, a pro-apoptotic protein, drives death by neglect and negative selection in thymocytes (45). In addition to Bim, the Nur77 family is also a known effector pathway of eliminating thymocytes during negative selection (46). These data show that the intrinsic pathway of apoptosis is responsible for deletion of thymocytes in response to neglect or negative selection processes during development in the thymus.

1.1.1.1.2 Apoptosis of T lymphocytes during a response

The elimination of autoreactive mature T lymphocytes in the periphery is called peripheral tolerance (31) and occurs, in part, via apoptosis (31, 38). During an immunological response to an antigen, T cells clonally expand to clear the antigen. After the antigen has been cleared, the responding T cells need to be eliminated by apoptosis to prevent self-damage (30). Prior to antigen exposure, there are up to about 200 naïve $CD8^+$ T cells specific to an antigen in a mouse (47). After encountering their cognate antigen, these $CD8^+$ T cells proliferate and expand rapidly within a few days. For example, the $CD8^+$ T cell response to lymphocytic choriomeningitis virus (LCMV) peaks around day 8, producing a population of $CD8^+$ T cells that are both phenotypically and functionally heterogeneous. After the response, 80-90% of these cells will undergo apoptosis during the contraction phase (48, 49). The remaining small fraction survive to become long-lived memory $CD8^+$ T cells, which provide protective immunity. Interestingly, the early contraction phase of $CD8^+$ T cells in response to LCMV is induced by type I interferons associated with elevated activation of caspase-3 and

caspase-8 (50). However, when restimulated through the TCR, these $CD8^+$ T cells undergo activation-induced cell death through autocrine expression of TNF and FasL (51). Mutations in Fas or FasL cause Autoimmune Lymphoproliferative Syndromes (ALPS) in humans (52). Fas-deficient (*Lpr*) and FasL-deficient (*gld*) mice, the mouse model of ALPS, are competent in controlling different viral pathogens, but due to defects in contraction, the accumulation of activated lymphocytes causes severe immunopathology (53-55). On the other hand, TNF, TNFR-1 and TNFR-2-deficient mice do not develop autoimmunity, although $TNF^{-/-}$ mice develop higher numbers of $CD8^+$ memory T cells in response to LCMV (56). These data suggest that TNF and TNFR ligation have a modest role in regulating lymphocyte cell death after viral infection. However, in a cross-presenting self-antigen model, CD8 T cells peripheral tolerance in response to cross-presented self-Ag is achieved through a Bcl-2-sensitive and Bim-dependent intrinsic apoptotic mechanism (57).

Cytokine signaling is important for a robust immune response. IL-2, which is mainly produced by activated T cells, is the most critical cytokine for regulating T lymphocyte activation, expansion, and short-term survival (58). In the case of an infection, IL-2 is reduced after the clearance of the pathogen due to the absence of TCR ligation. Thus, the reduction in the availability of IL-2 triggers intrinsic apoptosis regulated by Bim and related Bcl-2 protein family members leading to the elimination of expanded effector lymphocytes, known as passive cell death or death by neglect (51, 59). Effector T cells from $Bim^{-/-}$ mice are resistant to certain apoptotic stimuli and develop lymphoproliferative disease (59). In addition, Bim and Fas double knockout mice mount higher effector $CD8^+$ T cell responses to LCMV, suggesting a collaboration of Bim and

Fas in controlling lymphocytes responses (60). During LMCV infection in Mcl-$1^{-/-}$ mice, the majority of LCMV-specific T lymphocytes undergo rapid Bax/Bak-dependent cell death (61), highlighting the importance of regulating the balance of pro- and anti-apoptotic Bcl-2 family members in regulating T lymphocyte survival.

Apoptosis is a critical mechanism for elimination of cells during developmental stages, maintenance of homeostasis, and tolerance in T lymphocytes. Deletion of T lymphocytes during central tolerance in the thymus occurs via intrinsic apoptosis pathway, whereas peripheral tolerance in T lymphocytes and their contraction after a response is achieved via both intrinsic and extrinsic apoptosis pathways.

1.1.1.2 T cell activation and differentiation

Naïve CD4 T cells recognize antigens presented on MHC class II complexes, while naïve $CD8^+$ T cells recognize antigens on MHC class I complexes. T cell recognition of their cognate antigens via TCR-MHC interactions leads to T cell activation and differentiation, which plays a crucial role in the regulation of adaptive immune responses. CD4 or CD8 co-receptor association with TCR- pMHC complex is crucial for optimal proximal signaling outcomes (60-63), and the quality of the TCR interactions with pMHC complexes can initiate differential signaling cascades.

The TCR-pMHC interaction activates lymphocyte-specific protein-tyrosine kinase (Lck), a SRC-family kinase, which is associated with the cytoplasmic domain of the CD4 or CD8 co-receptors, and TCR-CD3ζ complex (8). Activated Lck facilitates the binding of SRC-homology 2 (SH2) domains of the SYK-family kinase Zeta-chain-associated protein kinase 70 (ZAP70) to CD3ζ by phosphorylating immunoreceptor tyrosine-based

activation motifs (ITAMs) on the cytoplasmic tail of CD3ζ (62). Activated ZAP70 phosphorylates the linker for activation of T cells protein (63) and other adaptor proteins and enzymes, which results in increasing concentrations of intracellular Ca^{2+}. The increased concentration of intracellular Ca^{2+} leads to nuclear factor of activated T cells (NFAT) transcription factor translocation into the nucleus and activation of mitogen-activated protein kinase (MAPK) pathways. Collectively, these events lead to expression of genes that are vital for the function of mature T cells (64).

When CD4 T cells recognize antigens presented on MHC class II complexes by APCs in the presence of the appropriate environmental cues, they differentiate into various T helper (Th) cells with distinct functions. For example, T follicular helper (Tfh) cells activate B cells to generate antibodies against the same antigen. Other subsets of Th cells, such as Th1, Th2, Th9, and Th17, produce cytokines that stimulate other immune cells to fight infections and diseases (8, 65). $CD4^+$ T cells can also differentiate into T regulatory (Treg) cells that suppress T cell activation and proliferation in order to prevent autoimmunity. $CD8^+$ T cells, on the other hand, when they recognize antigens presented on MHC class I complexes by APCs, they mainly differentiate into cytotoxic lymphocytes (CTLs), also known as killer T cells. CTLs form an immunological synapse with a target cell that displays the specific antigen on MHC class I. Subsequently, CTLs release vesicles containing granzymes and perforins in the immunological synapse and thus trigger apoptosis in the target cell (8).

After the targeted pathogens are cleared, most of the activated T cells die. However, a subset of the activated T cells differentiate into memory T cells, which are able to mount a robust response to a secondary infection within hours, a significantly

shorter time to activation in comparison to activation of a naïve T cell response, which takes days to emerge. Memory T cells are classified based on their location and function. There are many different memory T cells among which the effector, central, and tissue-resident memory T cells are well studied. Effector memory cells circulate the blood and tissue, seeking out and rapidly responding to foreign antigens with their potent effector functions. Central memory cells are able to self-renew and patrol the entire body. In contrast, tissue-resident memory cells are T cells that develop and reside at the original site of infection.

1.1.1.3 $CD8^+$ T cell subsets

Naïve $CD8^+$ T cells are constantly circulating and enter the secondary lymphoid organs in search of specific antigens. Specific molecules expressed on the naïve $CD8^+$ T cell surface enable them to migrate and enter secondary lymphoid organs. Likewise, other molecules expressed on the activated $CD8^+$ T cell surface are involved in conferring specialized $CD8^+$ T cell function and homing to affected tissues (66). Because specific surface molecules indicate functional properties of $CD8^+$ T cells, these surface molecules are used to phenotype and identify $CD8^+$ T cell subsets. Naïve $CD8^+$ T cells express CD62L (L-selectin), which helps them enter the lymph nodes and overcome the shear forces of blood. $CD8^+$ T cells use CD62L to tether to high endothelial venules (67). Then, the CC-chemokine receptor 7 (CCR7), a G-protein coupled chemokine receptor, recognizes CCL21/CCL19 ligands expressed on HEV. CCR7 engagement activates lymphocyte function-associated antigen 1 (LFA1) integrin on $CD8^+$ T cells, which binds the intracellular adhesion molecule 1 (ICAM1) and stops the naïve $CD8^+$ T cell allowing

migration into the lymph node (66, 68). Thus, CD62L and CCR7 are used as markers for identifying naïve $CD8^+$ T cells.

In order to become an effector T cell (T_E), $CD8^+$ T cells need specific cytokine and co-stimulatory signals in addition to TCR-mediated recognition of cognate pMHC complexes. Following TCR-mediated activation, $CD8^+$ T cells transiently upregulate CCR7, which increases retention in the lymph node. Further, CCR7 expression on activated $CD8^+$ T cells is needed for motility in the T cell zone and within lymph nodes, which facilitates activated $CD8^+$ T cell receipt of the necessary cytokine and co-stimulatory signals to enable rapid proliferation (66). For a successful response to a viral infection or invading tumor, effector $CD8^+$ T cells undergo clonal expansion to reach an optimal quantity of up to several million cells (69). Effector $CD8^+$ T cells produce granules containing perforin and granzymes A and B, which lyse infected target cells (69, 70). Macrophages and dendritic cells produce IL-12, which promote effector $CD8^+$ T cell cytotoxicity and induce effector cytokine (IFN-γ) production (70). After T_E are fully armed, they downregulate CD62L and CCR7 in order to egress out of the lymph node and migrate to the site of infection and perform their effector function (68). Migration of T_E cells to the sites of infection is a complex process that depends heavily on local expression of cytokines, chemokines, integrins, selectins, as well as the expression of different markers on the T_E cell surface (71). After the response, T_E cell populations contract and a portion of them typically transition into long-lived memory T cells.

CD45RA and CD45RO are variants of CD45 and are generally used to subtype naïve T cells and memory T cells, respectively. Memory T cells can be further subtyped

into central memory (T_{CM}) and effector memory (T_{EM}) (72) cells based upon their homing markers (73). Toward the end of the initial immune response, T_E transition into T_{CM} and thus re-express CD62L and CCR7, which enables them to recirculate through the secondary lymphoid organs. T_{CM} cells are able to secret a high amount of IL-2, self-renew, and they have the potential to become T_E upon re-encountering the cognate antigen (74, 75). On the other hand, T_{EM} cells do not express CD62L and CCR7, reside in the peripheral non-lymphoid tissues, and have T_E-like function and are ready to respond to infection. T_{EM} express some co-stimulatory, activation, and/or pro-survival markers, such as CD28, CD127, PD-1 and CD122 (73-75). T_{EM} cells respond first in the peripheral tissues in the case of pathogen invasion, while T_{CM} cells must proliferate and differentiate into T_E cells upon recognition of cognate antigen in order to mount a robust response. The ability of T_{EM} and T_{CM} cells to occupy different locations and the difference in their timing of cytolytic functions help in shaping the overall memory T cell repertoire (71, 73).

1.1.1.3.1 IL-2-IL-2 receptor signaling

Cytokines are a group of small proteins involved in cellular differentiation, proliferation, and survival (76, 77). Type 1 cytokines (IL-2, IL-12, IFN-γ, etc.) generate a strong cellular immune response and Type 2 cytokines (IL-4, IL-5, IL-13, etc.) produce a strong humoral immune response. Both types of cytokines can act in an autocrine, paracrine, or endocrine manner (78). The common cytokine receptor gamma chain (γc) family plays a crucial role in $CD8^+$ T cell development and differentiation (79-81). The γc cytokine family consists of cytokines whose receptors contain the γc subunit in their

structure (76) and includes interleukin-2 (IL-2), IL-4, IL-7, IL-9, IL-15, and IL-21. Because of the common γc subunit, γc family cytokines transduce overlapping signals through JAK-STAT pathway. However, the differential activation of Signal Transducers and Activators of Transcription protein (STAT) pathways is responsible for the distinct effects triggered by each of the γc cytokines (82). IL-2 and the IL-2 receptor are well studied and will be described here as an example to describe the γc cytokine and γc receptor interaction. The high-affinity IL-2 receptor (IL-2R) is a trimeric complex of IL-2Rα, IL-2Rβ, and common γc. However, IL-2Rα alone does bind IL-2 with low affinity, while the dimeric complex of IL-2Rβ and γc binds IL-2 with intermediate affinity. IL-2 is one of the first cytokines secreted by T cells following TCR stimulation and has multifaceted effects on T cells. IL-2 is known to induce proliferation, survival, and sustains T cell expansion (81, 83).

Most of the biological functions of IL-2 are mediated through the trimeric high-affinity IL-2R. Because the IL-2R does not have an intrinsic kinase domain or other enzymatic activity, it was previously assumed to couple with cytosolic GTPases and kinases. Initial studies of IL-2 signaling pathways suggested that IL-2 signal transduction in T cells occurred via the SRC family kinases, Lck and Tyrosine-protein kinase Fyn (Fyn) (84, 85). However, recently it was shown that SRC family kinases, independent of IL-2R engagement, have high constitutive activity in T cells (86). Further, the finding that the IL-2R uses Janus family kinase (JAK) members for signal transduction was a major breakthrough in understanding IL-2R function. IL-2 stimulation was shown to activate JAK1 and JAK3 via phosphorylation of their tyrosine residues. Additional studies demonstrated the binding of JAK1 to IL-2Rβ at a serine-rich region and binding

of JAK3 to IL-2Rγ at the carboxyl-terminal region (87). Subsequently, JAK1 and JAK3 activation leads to phosphorylation of tyrosine residues on the IL-2Rβ chain, which in turn recruits STAT5A and STAT5B transcription factors via their SH2 domains and phosphorylates their tyrosine residues (86). The phosphorylated STAT5 proteins dissociate from the IL-2Rβ subunit and form dimers through their SH2 domains. The dimerization of STAT5 proteins induces their transcriptional activation and translocation to the nucleus. In the nucleus, STAT5 dimers bind to the gamma interferon-activated sequence (GAS) DNA site to induce transcription. Induction of STAT5-mediated transcriptional programs via IL-2 is crucial to the biological actions of IL-2 (88-90). The importance of IL-2 activated STAT5-mediated transcriptional programs for IL-2 biological action is evident in murine gene knockout studies. STAT5-deficient mice lose the ability to develop Treg cells or induce proliferation of activated peripheral T cells, highlighting the key role of STAT5 in IL-2 signal transduction (67, 91). Some of the essential lineage-defining transcription factors, such as forkhead box P3 (FoxP3), T-box transcription factor (T-bet), and GATA binding protein 3 (Gata3) are STAT5 targets. Moreover, IL-2-activated STAT5 can bind and induce IL-2Rα, IL-12Rβ2, and IL-4Rα genes to sustain IL-2 signaling and promote the differentiation of T cells by other cytokines (86). STAT5 also binds and negatively regulates other genes. For example, STAT5 binds to the IL-17α-IL17F locus, leading to suppression of STAT3-mediated transcription of the IL-17 gene and Th17 differentiation (92). Another repressive activity of IL-2 is the induction of the microRNA miR-182, which binds and inhibits the forkhead box O1 (FOXO1) transcription factor. FOXO1 blocks cell cycle progression in resting T

cells and thus, inhibition of FOXO1 by IL-2-induced miR-182 leads to clonal expansion of activated helper T cells (93).

Besides STAT5-mediated transcriptional activation, IL-2 signaling also has broader effects on other signaling pathways relevant to T cell biology. IL-2 binding to the IL-2R recruits and phosphorylates the Src homology 2 domain containing (22) adaptor protein (94). The phosphorylated SHC protein binds growth factor receptor-bound protein 2 (GRB2) adaptor protein, via its SH2 domain, which binds Ras guinine nucleotide exchange protein (95) through its SH3 domain (96). The SHC-GRB2-SOS complex triggers the exchange of guanosine diphosphate (GDP) to guanosine triphosphate (GTP) on Ras. These events allow the accumulation of active, GTP-bound Ras, which leads to activation of the Raf-ERK-MAP kinase pathway.

Mammalian target of rapamycin (mTOR) is another important serine/threonine kinase that conducts IL-2 signaling (97). mTOR is part of the mTORC1 (mTOR, RAPTOR, and mLST8) and mTORC2 (mTOR, RICTOR, and mLST8) complexes (98). IL-2 induces and maintains activated mTORC1 to control IL-2-induced metabolic and transcriptional processes in T_E cells via the transcriptional factor, hypoxia inducible factor 1 subunit alpha (HIF1A). HIF1A is involved in some mTORC1-regulated genes such as glucose transporters, glycolysis, pyruvate metabolism, and perforin. The mTORC1-HIF1A pathway is critical for repression of CD62L, CCR7, and sphingosine-1-phosphate receptor 1 (S1P1) gene expression (99). The loss of mTORC1 in T_E cells leads to reduced glucose transporters, glycolytic enzymes expression, and decreases the rate of glycolysis with intact oxidative phosphorylation pathways (99, 100). In addition, mTORC1 plays an important role in controlling the expression of perforin, granzymes,

and IFN-γ (100). The phosphoinositol 3-kinase (PI 3-K)-akt-p70 S6 kinase signaling pathway, which promotes cell growth and survival, is also activated by IL-2 binding IL-2R (89, 101).

1.1.1.3.2 OX40-OX40 receptor signaling

In addition to recognition of cognate pMHC complexes on APCs, naïve T cells require a costimulatory signal to generate an optimal response. This costimulatory signal transduction both amplifies and strengthens the primary outcome of the TCR signal that leads to clonal expansion, differentiation, and survival. In the absence of a costimulatory signal, T cells undergo tolerance, which is important for thymic and peripheral tolerance. CD28 is a well-characterized T cell co-stimulatory molecule that is constitutively expressed on the surface of naïve T cells. When CD28 binds its ligands, B7.1 and B7.2, it lowers the threshold for TCR ligation and drives T cell expansion, proliferation, differentiation, and survival (102, 103). While CD28-B7 signaling is crucial for T cell activation, it is not sufficient to sustain an optimal T cell response (104).

Tumor necrosis factor receptor (TNFR), immunoglobulin, integrin, and C-type lectins are the four families of molecules that play crucial roles in immune synapses and work as signaling adaptors, cytoskeletal components, receptors, and regulators of lipid distribution to orchestrate immune responses. The costimulatory members of the TNFR family contribute to signaling in the T cell synapse (105, 106). T lymphocytes express an array of TNFR family co-stimulatory molecules (106). Moreover, TNFR co-stimulatory molecules are differentially expressed depending on the state of the cells. For example, the CD27 co-stimulatory molecule is constitutively expressed on T cells. In contrast,

other co-stimulatory molecules, including OX40 (CD134), 4-1BB (CD137), and GITR (CD357), are typically expressed following T cell activation. The ligands for the TNFR co-stimulatory molecules are type II transmembrane proteins that are expressed by APCs (107, 108). TNFR ligands form trimers, and subsequent multimerization of the trimer with their respective TNFR results in multi-protein complexes that induce the downstream signaling cascade. TNFR family members have TNF receptor associated factor (TRAF) binding domains on their cytoplasmic tails that recruit TRAFs upon ligand-receptor engagement (109). There are different TRAF adaptors that interact with different members of the TNFR family. For example, TRAF1, TRAF2, and TRAF5 have been shown to interact with the cytoplasmic tails of 4-1BB, OX40, and GITR co-stimulatory receptors (110).

T lymphocyte activation is required for OX40 expression on the cell surface (111-113). Interestingly, in addition to TCR ligation, CD28 and/or other cytokine receptors are also required for optimal expression of OX40 on the T cell surface (104). CD28-B7 signaling transduction leads to IL-2Rα expression and IL-2 production (114, 115), and IL-2-IL-2R ligation induces OX40 expression (116). In turn, OX40-mediated co-stimulation leads to IL-2 production and IL-2Ra expression (63, 117, 118). While the exact mechanism of CD28-B7 signaling contribution to OX40-mediated co-stimulation is yet to be elucidated, it is known that IL-2 and OX40 regulate each other.

OX40 is differentially expressed on lymphocyte subsets. For example, OX40 expression appears on the surface of $CD8^+$ T cells 24 hours after activation and peaks within 72 hours, while it is constitutively expressed on naturally occurring Tregs ($FoxP3^+$ CD4 T cells) (119, 120). OX40 ligand (OX40L) is a type II transmembrane receptor, and

it is expressed as a trimer on stimulated APCs (121-123). Upon OX40 ligation, TRAF molecules are recruited to the intracellular domain of OX40. Activated TRAF2 and TRAF3 in turn activate canonical and non-canonical nuclear factor kappa-light-chain-enhancer of activated B cells (NF-kB) pathways, which are key for survival (124, 125).

1.2 Tumor Immunology

One of the first hypotheses of tumor immunology, which arose at the beginning of the 20th century, suggested that the host immune system may eliminate neoplastic cells, thus preventing tumor formation. This hypothesis was not tested experimentally at the time, but it led scientists to the theory of immune surveillance against tumor cells (126). Later, Lewis Thomas postulated that the immune system eliminates tumors through the recognition of neoantigens expressed by a newly arising tumor. This theory of immune stimulation by tumor neoantigens was supported by the observation that C3H mice implanted with tumors derived from other mice of the same strain develop immunity against those tumors, which led to spontaneous tumor regression (127). The spontaneous tumor regression was suggested to be due to a tumor mutation that occurred during repeated transplantation over long period of time, which led to expression of a neoantigen. Foley later showed that C3H-He mouse anti-tumor immunity was induced following ligation (strangulation of the tumor) and atrophy of methylcholanthrene-induced sarcomas from the same inbred strain against first or second transplantation, minimizing the chance of mutations in the tumor due repeated passages (128). Sir Frank Mac Farlane Burnet subsequently hypothesized the theory of immune surveillance, which states that neoantigen expression by developing tumors elicits an effective immune

response that leads to regression and complete elimination of the tumor before appearance of any clinical signs (126).

Burnet's theory of immune surveillance has been supported experimentally by animal models and observations in humans. However, tumor development in patients with apparently normal immune systems suggests that tumors can escape immune surveillance. Thus, Dr. Robert D. Schreiber formulated the concept of the three "Es" of cancer immunoediting: elimination, equilibrium, and escape (129, 130). In the elimination phase of immunoediting the immune system recognizes tumors as abnormal cells and kills it with natural killer cells (NK), CD4+ T cells, and $CD8^+$ T cells (131). In the equilibrium phase of immunoediting, which is the longest phase of the three Es, the immune system can exert a potent response that is enough to contain tumor cells, but not enough to completely eliminate all tumor cells (129). The equilibrium phase eventually leads to rapidly mutating tumor cells that can escape the immune system; this leads to the escape phase of immunoediting. In the escape phase, the tumor evades the immune system through loss of tumor antigens, increase of pro-survival genes, and/or the development of an immunosuppressive tumor microenvironment (TME) (129). Alteration of the TME by tumor cells is one of the ways tumors escape immune cells, which leads to tumor progression and metastasis. The concepts of immunosurveillance and immunoediting have been instrumental in understanding the function of anti-tumor immunity and in investigating new mechanisms to boost immune responses against tumors.

The TME includes the tumor cells, stromal cells, and infiltrating immune cells. One feature of the TME is that malignant tumor cells can hijack non-malignant cells

within the TME to make them take on pro-tumor functions (such as M2 macrophage polarization) (132). In addition, the TME may include many different signaling molecules that promote tumor growth, angiogenesis, and metastasis, including pro-tumor growth factors (epidermal growth factor (EGF), colony stimulating factor 1(CSF-1), fibroblasts growth factor (FGF), heparin-binding EGF (HB-EGF), neuregulin (NRG), transforming growth factor (TGF), vascular endothelial growth factor (VEGF)) and chemokines/chemokine receptor (C, CC, CXC, CX3C chemokine families and receptors) depending on the tumor type (133, 134). The TME has gained considerable attention in the field of cancer immunotherapy in the past decade and efforts to find new targets in TME continues.

1.2.1 Anti-tumor immunotherapy

Tumor regression or disappearance was first reported during an infection or febrile episodes in the early 18th century. More than a century later, the phenomena of tumor regression coinciding with a bacterial infection or febrile episodes was proven by the founding fathers of immunotherapy, William Coley and Lloyd Old (126, 135). Meanwhile, a better understanding of the immune system and discoveries about cellular and humoral immunity intensified the investigation of an immune-driven anti-tumor response. For example, the discovery of T lymphocytes and their key role in anti-tumor responses grabbed the attention of immunologists. With the more recent discoveries of checkpoint inhibitors and costimulatory receptors on T lymphocytes and immunomodulatory antibodies, cancer immunotherapy has joined surgery, cytotoxic chemotherapy, radiation, and targeted therapy to become the fifth pillar of cancer therapy

(135). It has been suggested that immunotherapy will be the leading cancer treatment for all cancers within a decade due to its ability to drive a response against cancers that do not respond to chemotherapy or radiation therapies, ability to improve anti-tumor response in combination with other therapies, and the generation of durable responses with potentially long-term tumor-specific immunity (136).

There are several different types of cancer immunotherapies available for cancer patients (126). One of the cancer immunotherapies approaches is vaccine therapy, which can induce immune responses against tumor cells. Cancer vaccines are designed to induce the adaptive immune system to recognize, eliminate, and provide long-term protection against tumors. IL-2 therapy is another cancer immunotherapy approach, which induces T cell survival and sustains effector function. Other approaches are adoptive T cell and B cell therapies or antibodies that block immune checkpoints (checkpoint blockade) or, conversely, stimulate immune costimulatory receptors (137). Currently, immunotherapies that are US Food and Drug Administration (FDA) approved include chimeric antigen receptor (CAR) T and B cell therapy and monoclonal antibodies (mAbs) against cytotoxic T-lymphocyte-associated protein 4 (CTLA-4) (anti-CTLA-4), programed cell death-1 (PD-1) (anti-PD-1), and programed death-ligand 1 (PD-L1) (anti-PD-L1). CTLA-4, PD-1, and PD-L1 are all checkpoint inhibitors. Costimulators, such as OX40 and 4-1BB, on the other hand, are currently under investigation and have yet to be approved by the FDA. Here, I will briefly explore the role of CTLA-4 and PD-1 checkpoint inhibitors and recombinant IL-2 in anti-tumor response as well as the recent advancements in OX40 and 4-1BB-specific therapies.

1.2.1.1 Recombinant IL-2

Before the discovery of T lymphocytes, adoptive transfer of lymph nodes cells was shown to confer anti-tumor immunity (138). This study highlighted the key role of lymphocytes in rejection of the transplanted tumors. With the discovery of T lymphocytes, the idea of growing and expanding T lymphocytes *in vitro* and then transferring them into tumor-bearing hosts arose. However, immunologists struggled with sustaining T lymphocytes survival and growth *in vitro*. A decade after the discovery of T lymphocytes, IL-2, a T cell growth factor, was the key discovery that allowed for sustained survival and growth of T lymphocytes *in vitro* (139). Subsequent studies suggested that not only could IL-2 sustain T cells *in vitro*, but its administration could mediate T cell survival and sustain T cell function *in vivo* in order to mount and support a robust response against tumors. The first clinical trial testing the efficacy of IL-2 therapy used IL-2 purified from a Jurkat T cell tumor line. In this trial, the administration of IL-2 to patients with advanced cancer caused dose-related toxicity but no anti-tumor activity. The failure of this clinical trial was attributed to the dosage of IL-2, which was too low to generate *in vivo* activity (140). However, Jurkat T cells could not produce enough IL-2 to enable higher doses, thus, scientists needed a better system to generate a large amount of IL-2. Engineering *E. coli* to produce recombinant IL-2 (rIL-2) solved this issue, as they became able to produce large amounts of rIL-2, which made evaluating the efficacy of high-dose IL-2 *in vivo* possible (141, 142). While, as expected, the high dosage of rIL-2 yielded improved anti-tumor results in comparison to low dose rIL-2, unfortunately, there was severe IL-2-related toxicity in animal models (143). Nevertheless, the anti-tumor activity of rIL-2 in animal models was enough to propel rIL-2 in to human studies.

A dose escalation study of rIL-2 (6-60x10^4 IU/kg) in patients with advanced metastatic cancer yielded encouraging results. Among the 25 patients in the study, 11 patients had more than 50% regression in tumor volume. One patient with metastatic melanoma had complete tumor regression and nine patients had partial responses (144). The toxicities due to the rIL-2 therapy were transient and alleviated after the rIL-2 treatment ended. In another high-dose rIL-2 clinical trial at the National Cancer Institute, out of 157 patients with advanced cancer, 59 patients were treated with 60-72x10^4 IU/kg rIL-2 (145). Among those, 46 patients were evaluable: one patient had a complete response (total regression of all cancer), five had a partial response (> %50 tumor reduction), and one had a minor response (%25-%50 tumor reduction). Most of the patients responding to rIL-2 in these clinical trials had metastatic melanoma or metastatic renal cell cancer, therefore melanoma and renal cancer became the focus of rIL-2-specific clinical trials. Subsequent single- and multi-institutional studies led to the FDA approval of a high-dose bolus of rIL-2 in 1992 for the treatment of patients with metastatic renal cancer. 6 years later, the FDA approved rIL-2 for the treatment of patients with metastatic melanoma. Although transient, toxicities due to high-dose rIL-2 treatment are still of great concern, as four rIL-2-related deaths were reported in the National Cancer Institute clinical trial (145).

After learning about the principles of administration and management of toxicities from previous high-dose rIL-2 clinical trials, the dosage of rIL-2 was changed. In a subsequent clinical trial of rIL-2, patients with metastatic cancers were treated with fewer doses of the high-dose bolus rIL-2 in the first cycle of the therapy, 7 compared to the 13 doses initially used, without any decrease in the response rates, but with substantial

decreases in toxicities (2). Improvements in the administration of rIL-2 and reduction in related toxicities led to a decrease in treatment-related deaths from 4% to less than 1% (146). More recently, the use of rIL-2 in patients with metastatic melanoma has expanded to include combinations with adoptive cell therapy, chemotherapy, and radiation (146).

1.2.1.2 Immune checkpoint blockade

T cells have the capacity to selectively recognize tumor-derived antigens and orchestrate diverse immune responses to eliminate tumor cells. The quantity and quality of T cell responses to an antigen are regulated by fine-tuned costimulatory and inhibitory signals (immune checkpoints) (147, 148). In a healthy situation, immune checkpoints are crucial for preventing autoimmunity and protecting normal cells. However, immune checkpoints can be exploited by tumors by engaging the immune checkpoint proteins on T cells in order to suppress the anti-tumor immune response. To the delight of immunologists, blocking immune checkpoints with antibodies results in enhanced anti-tumor responses that have vastly improved cancer therapy (149).

Different immune checkpoints regulate immune functions through different mechanisms. For example, CTLA-4 and PD-1 immune checkpoints regulate immunity at different stages of the response. CTLA-4 downregulates the strength of T cell activation by disrupting CD28/CD86 interaction by binding to CD86 with higher affinity than CD28 (150). Interaction of CD28 on T cells with its ligand, CD86, expressed on the APC, plays a critical role in enhancing and sustaining T cell responses initiated through TCR engagement. CTLA-4 can also initiate a signal transduction cascade that results in the dephosphorylation of TCR-associated kinases (Fyn, Lck, and ZAP-70) or their substrates

(SH2, MAPK, and Ras) (150). The engagement of PD-1 on T cells by its ligand, PD-L1, also results in the suppression of T cell activity, but through a different intracellular signaling pathway. PD-1/PD-L1 signaling inhibits PI3K/AKT signaling, resulting in inhibition of effector T-cell differentiation and function (151). The anti-tumor response of $CD8^+$ T cells infiltrating the tumor is driven by interferon-γ (IFN-γ), which also induces expression of PD-L1 in tumor cells (152). PD-L1 expressed by tumor cells binds PD-1 on the tumor infiltrating $CD8^+$ T cells, suppresses the anti-tumor immune response, restricts T cell effector function within TME, and drives T cells to exhaustion. Thus, blocking the interaction between PD-1 and PD-L1 is effective in reversing T cell exhaustion and results in T cells regaining the effector function needed to eliminate cancer cells (149, 153, 154).

Multiple immune checkpoints, in addition to aPD1 and aCTLA-4, and their inhibitors are entering the clinic or are currently under investigation, including lymphocyte activation gene 3 (LAG-3), T cell membrane protein 3 (TIM-3), B and T lymphocyte attenuator (BTLA), T cell immunoreceptor with Ig and ITIM domains (TIGIT), and V-domain Ig suppressor of T cell activation (VISTA) (149, 155). Because CTLA-4 and PD-1 antagonist therapies are FDA-approved, I will briefly explore them as examples of the improvement in clinical outcomes that can occur following immune checkpoint blockade. Anti-CTLA-4 mAb therapy was first used for treating melanoma. The increased efficacy of anti-CTLA-4 mAb (ipilimumab) in combination with a chemotherapy agent (dacarbazine) versus chemo alone was shown in a phase III clinical trial in untreated metastatic melanoma patients (156). There was higher overall survival (11.2 months) in the group receiving ipilimumab plus dacarbazine compared to overall

survival (9.1 months) in the group receiving dacarbazine plus placebo. Another phase III clinical trial of anti-CTLA-4 mAb administered in combination with a glycoprotein 100 vaccine (gp100) or anti-CTLA-4 mAb alone resulted in significantly increased long-term overall survival in patients with stage III and IV metastatic melanoma compared to patients treated with gp100 alone (95). With the subsequent approval of PD-1 antagonists, nivolumab and pembrolizumab, PD-1 antagonists became a clinical breakthrough in melanoma immunotherapy. Nivolumab improved 1-year overall survival in treatment-naive patients with serine/threonine-protein kinase (BRAF) wild-type melanoma to 72.9% compared to 42.1% in the dacarbazine-treated arm in a phase III clinical trial (157). Pembrolizumab was also evaluated in advanced melanoma patients in comparison to anti-CTLA-4. Pembrolizumab patients had 15.9% (every 3 weeks treatment) and 10.2% (every 2 weeks treatment) higher 1-year overall survival compared to patients treated with anti-CTLA-4 (158). In addition to melanoma, immune checkpoint antagonists also have shown efficacy in non-small cell lung cancer, hypermutated gastrointestinal cancers, renal cell cancers, as well as other histologies (159, 160). mAbs against immune checkpoints have been in the clinic for several years, as both monotherapy and combination therapies in advanced cancers (161). The PD-1-blocking antibody pembrolizumab was the first immune checkpoint therapy that was granted FDA approval for microsatellite instability-high (MSI-hi) tumors regardless of tumor type or origin (162). However, there are still about 50% to 60% of patients that do not respond to immune checkpoint antagonists, referred to as primary resistance, and a subset of patients that initially respond, but subsequently relapse and develop resistance to therapy, referred

to as acquired resistance (163). Primary and acquired resistance are poorly understood and these phenomena are currently under investigation.

1.2.1.3 Immune costimulatory agonists

T cell costimulatory receptors are essential for mounting a robust T cell response to an antigen. Despite strong evidence supporting the agonist stimulation of costimulatory receptors driving productive anti-cancer immunity and their role in mediating anti-cancer immune responses (164-166), no costimulatory agonists are, as of yet, approved by the FDA. Unlike co-inhibitory receptors' role in the anti-tumor response, costimulatory receptors' function in cancer immune surveillance depends on the timing and duration of co-stimulatory receptor induction following TCR stimulation and the expression of co-inhibitory receptors on T cells (167). In addition, unlike antagonist antibodies against co-inhibitory receptors, designing and predicting potential activity of agonist antibodies for costimulatory receptors is complex and mostly characterized functionally by using cell-based and *in vivo* models (168, 169). These challenges have made it difficult to design the desired agonist antibodies, which have the ability to bind and stimulate costimulatory receptors in a way that would mimic the activity of a native ligand. However, there has been substantial advances in the past decade in improving costimulatory agonist activity, and I will cover the advancement of anti-OX40 and anti-4-1BB mAbs, as specific examples of T cell agonists capable of inducing anti-tumor immune responses.

1.2.1.3.1 OX40

The OX40 agonist antibody (clone OX86) was the first agonist antibody against OX40 used in preclinical mouse models and has become the most predominantly used clone to date (169, 170). OX86 exhibited exciting and promising immune stimulatory and anti-tumor activity in the preclinical studies, which led to the development of a murine anti-human mAb OX40 agonist antibody by the Earle A. Chiles Institute (171). The preclinical activity of surrogate OX40 agonist antibodies in murine tumor models led six different pharmaceutical companies to develop OX40 agonist antibodies that entered clinical trials in a short period of time (167, 172). Anti-OX40 mAbs entered clinical trials in patients with solid tumors for the first time in 2006 with promising results (171, 173). Forty percent of the 30 patients treated with an OX40 agonist in one clinical trial had regression of at least one metastatic lesion after only one dose. OX40 treatment induced the expansion of effector $CD4^+$ and $CD8^+$ T cells, without inducing the expansion of Treg either in the blood or the tumor. Moreover, two out of three patients had tumor-specific $CD8^+$ T cells that were shown to produce IFN-γ in response to autologous tumor cell lines *in vitro* (173). Anti-OX40 was later licensed to MedImmune/AstraZeneca, which opened several Phase 1 clinical trials to investigate OX40 agonists (NCT02318394, NCT02205333, and NCT02221960). However, in these cases, no objective clinical responses were observed.

Preclinical studies have shown anti-tumor activity of OX40 agonists when given in combination with other agents, such as immune checkpoint antibodies, targeted inhibitors, and cancer vaccines (172). In a murine ID8 ovarian cancer model, anti-OX40 or PD-1 mAb treatment alone did not have therapeutic effects. However, combined

treatment with concurrent anti-OX40/PD-1 mAbs significantly inhibited tumor growth and cured 60% of the mice (174). In another study, concurrent therapy of anti-OX40 and anti-PD-L1 conferred antitumor immunity in murine sarcoma (CT26) and carcinoma (MCA205) models (175). Interestingly, in the MMTV-PyMT breast cancer model, combination of anti-PD-1 with an OX40 agonist in the presence of a vaccine resulted in inhibition of OX40 agonist antitumor potential by anti-PD-1 (176). In the MMTV-PyMT model, treatment with PD-1 blockade and OX40 agonist concurrently did not reduce tumor growth, whereas sequential treatment with an OX40 agonist followed by PD-1 blockade significantly increased tumor growth inhibition and survival outcomes compared to control groups (177). These studies raise the question of how to optimally combine the many new immunotherapy agents being developed, which remains a major question in cancer research. Addressing this question requires a deeper understanding of the therapeutic mechanism of different drugs, which is critical to achieve maximum therapeutic benefits in combinatorial therapies.

1.2.1.3.2 4‑1BB

4-1BB (CD137) expression on $CD4^+$ and $CD8^+$ T cells increases early following activation, and its expression is transient (178). 4-1BB ligation induces downstream signaling pathways that lead to increased proliferation, survival, and effector functions (179-181). Agonist activation of 4-1BB became attractive for cancer therapy due strong evidence for its ability to induce anti-tumor activity, which is mediated primarily by cytotoxic T cells and NK cells in preclinical mouse models, either alone or in combination with other agents (180, 182, 183). Urelumab (BMS-663513) and

utomilumab (PF-05082566) are currently the only two 4-1BB agonist antibodies being tested clinically for cancer therapy. Urelumab is a fully human IgG4 4-1BB agonist antibody that entered human clinical trials in 2005 (NCT00309023). However, due to hepatotoxicity related to doses at or higher than 1 mg/kg, the ongoing clinical trials were discontinued. Preclinical studies of 4-1BB agonists in mice also showed hepatotoxicity that was deemed to be caused by increased accumulation of activated $CD8^+$ T cells (184). A subsequent clinical trial of urelumab at doses bellow 1 mg/kg demonstrated some disease stabilization and immune activation (NCT01471210). Combination studies of urelumab with other agents, including nivolumab (anti-PD-1), in multiple cancer types are ongoing. Utomilumab, the second 4-1BB agonist antibody, is fully human IgG2, has not shown dose-related toxicity in humans, and has an excellent safety profile in preclinical models (185). In addition, utomilumab has shown signs of promising clinical activity in patients with solid tumors in advanced stages. In a combination study of utomilumab and pembrolizumab, 26% of patients had a complete or partial response (186). This study provides strong rational to further explore the anti-tumor activity of 4-1BB agonists in combination with PD-1 or PD-L1 checkpoint blockade therapy. A second integration of 4-1BB signaling in immunotherapy has been the integration of 4-1BB's intracellular signaling domain into CAR T cells, named second generation CARs. The addition of 4–1BB signaling domains in second generation CARs is thought to prevent anergy and promote T cell proliferation and memory (187). This integration has greatly improved the clinical activity and durable responses of CAR autologous T cell therapies in leukemia (188) and led to FDA approval.

Chapter 2: The role of Galectin-3 in modulating tumor growth and immunosuppression within the tumor microenvironment

2 Abstract

The efficacy of cancer immunotherapy is limited, in part, by the multitude of immunosuppressive mechanisms present within the TME. Galectin-3 (Gal-3) is a lectin that contributes to TME immunosuppression and regulates diverse functions including cellular homeostasis and cancer biology. Increased Gal-3 expression during cancer progression augments tumor growth, invasiveness, metastatic potential, and immune suppression, which highlights the potential use of Gal-3 as a therapeutic target capable of modulating anti-tumor immunity. Here, we discuss the mechanisms by which Gal-3 regulates lymphocytes, the role of Gal-3 in lung and prostate tumors, and the contribution of Gal-3 to TME immunosuppression.

2.1 Introduction

The immune system is designed to protect the host against disease and possesses numerous mechanisms that tightly regulate its activity to prevent autoimmune reactions against normal, healthy host cells. However, these same regulatory mechanisms may be hijacked by cancerous cells, thereby allowing them to escape detection and attack by the immune system. This often occurs in the TME, which is a complex ecosystem involving innumerable interactions between immune cells, cancer cells, stromal cells, and the extracellular matrix, and can support tumor proliferation, survival, and metastasis, and is highly immunosuppressive (189-191). The TME achieves immunosuppression through a myriad of different ways; for example, tumor-associated macrophages, cancer-associated fibroblasts, and tumor cells can all secrete suppressive cytokines and chemokines, and there can be metabolic competition over consumption of nutrients by tumor cells, or a shortage of oxygen. Other immunosuppressive mechanisms include the production of inhibitory metabolites, migration failure due to rigid extracellular matrix, poor antigen presentation, chronic TCR signaling, and inhibitory receptor expression by tumor cells and stromal cells (192). An additional important regulatory mechanism at play in the TME occurs through the glycoprotein Gal-3. Gal-3 binds the TCR in the immunological synapse on the cell surface, thereby restricting TCR movement, potentiating TCR downregulation, and suppressing early activation of T cells through the TCR signaling pathway (193, 194).

Gal-3 is a structurally unique glycoprotein that has been studied extensively in different disease contexts including fibrosis, inflammation, and cancer. Gal-3 is a member of the lectin family, of which 14 mammalian galectins have been identified.

Mammalian galectins have binding specificity to ß-glycoside structures and are classified into three groups based on their conserved carbohydrate-recognition-binding domain (CRDs) structures: prototypes, tandem repeat, and chimera groups (195). Galectin-1, -2, -5, -7, -10, -11, -13, and -14 are members of the prototype galectin group that contain only one CRD. Members of the tandem repeat group (galectin-4, -6, -8, -9, and -12) contain two distinct CRDs connected by a non-conserved 70 amino acid linker sequence that enables each galectin to bind two carbohydrate epitopes. The chimera galectin group contains only one member, Gal-3, which contains one CRD like the prototype group, but the CRD in Gal-3 is connected to a unique N-terminal domain of about 120 amino acids that are rich in proline and glycine (196). Gal-3, with only one CRD, can form homo-dimers and oligomers through its N-terminal domain depending on the concentration and availability of the ligands. Further, the oligomeric structure of Gal-3 contributes to its function, (197) as the oligomeric form of Gal-3 allows Gal-3 to perform biological functions not performed by all other galectins (198, 199). The oligomeric forms of Gal-3 only form in the extracellular space (**Fig. 3**), where Gal-3 oligomers can bind substrates through its CRD domain and induce intracellular signal transduction through clustering surface proteins, cell-cell interactions, or cell to extracellular matrix (**Fig. 3**) (200). Furthermore, Gal-3 function depends not only on its oligomeric state in the extracellular space but also on its subcellular location, where Gal-3 monomers can be found either in the cytoplasm or nucleus (see ref. 9 for additional details of the subcellular location of Gal-3 and its function). There is no known difference in the generation of extracellular versus intracellular Gal-3. The signal that determines the subcellular localization and the mechanism of extracellular Gal-3 secretion are not clear. In the intracellular space, Gal-3

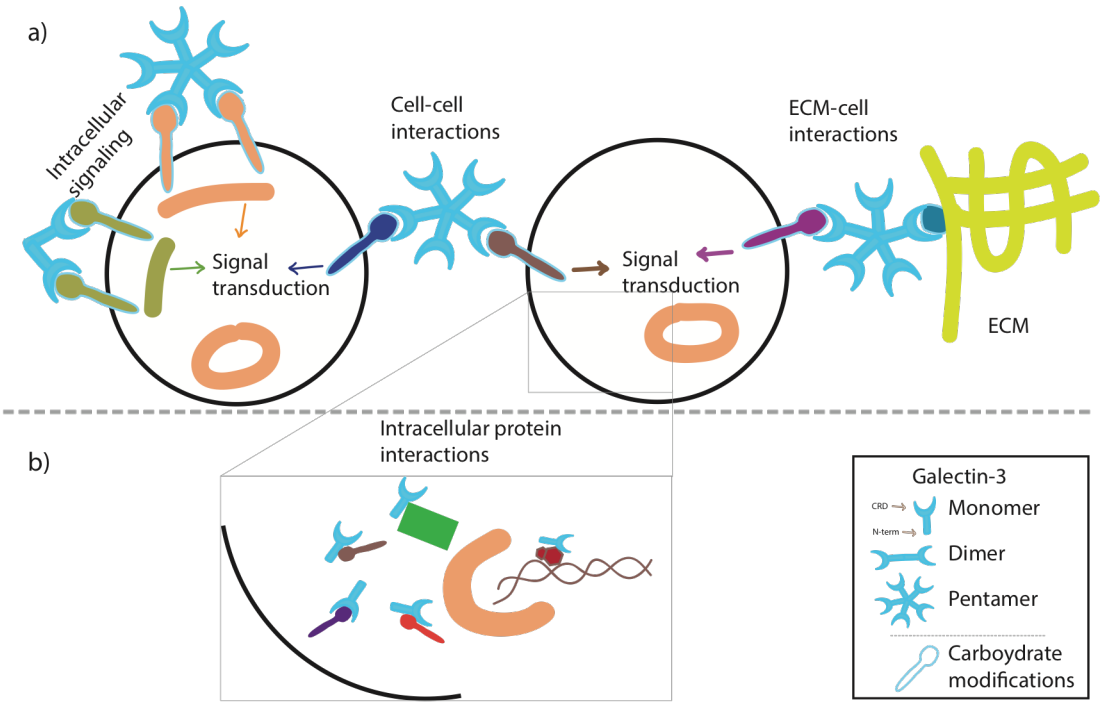

Figure 3. Gal-3 binds substrates through different mechanisms depending on its cellular location. a) In the extracellular space, Gal-3 binds to its substrate through CRD-specific carbohydrate modifications on the substrate. Gal-3 binding to these substrates can induce surface protein interactions, cell-cell and cell to extracellular matrix interactions, which can all lead to initiation of downstream signaling. **b)** In the intracellular space, Gal-3 binds to its substrates through direct protein-protein interactions between Gal-3 and the substrate.

binds substrates through protein-protein interactions, for example, intracellular Gal-3 binds Bcl-2 to inhibit apoptosis (197, 201, 202).

On a cellular level, Gal-3 expression is dynamic during mouse development. The earliest Gal-3 protein is detected in the cells of trophectoderm of blastocyst (203), and then a few days later in gestation Gal-3 is exclusively found in the notochord cells (204). In later stages of development, Gal-3 protein is found in the cartilage of vertebrae, ribs and facial bones, the suprabasal layer of epidermis, the endodermal lining of the bladder,

larynx, and esophagus. The liver and lungs, as well as the mineralizing part of the bones and some other organs, have a punctate Gal-3 distribution that is associated with macrophages and/or related cell types such as osteoclasts (203). In adult mice, Gal-3 is mainly restricted to epithelial and myeloid cells. Within these cell types, Gal-3 can be either localized in the nucleus, cytoplasm, plasma membrane or secreted into extracellular space, however the primary location is in the cytoplasm.

The cellular presence of Gal-3 in humans is similar to what is observed in mice. During the first trimester of human embryogenesis, Gal-3 is found in epithelia such as the skin, epithelial lining of the digestive and respiratory tract, urothelium and excretory tubes of the kidney, myocardial cells, peripheral and pre-ossifying hypertrophic chondrocytes, as well as in the notochord and liver (205). Notably, Gal-3 protein is not found in lymphoid tissues and naïve lymphocytes do not express Gal-3; however, sufficient stimuli (both mitogen and IL-2) can induce lymphocytes to produce intracellular Gal-3, which is not secreted into the extracellular space (206). Gal-3 protein is also not found in cells of the central nervous system. According to the Human Protein Atlas project, in adults, the majority of epithelial cells and variety of normal tissue types contain both cytoplasmic and nuclear Gal-3 protein (**Fig. 4**) (1). The same study showed little or no Gal-3 in hepatocytes, neuronal cells, and most lymphoid cells along with microglia and astrocytes (1).

The presence of Gal-3 across most adult tissue types illustrates the necessity of Gal-3 in basic biology. However, increased levels of Gal-3 in the tumor and TME in several cancer types suggests a contribution to immunosuppression and a role in

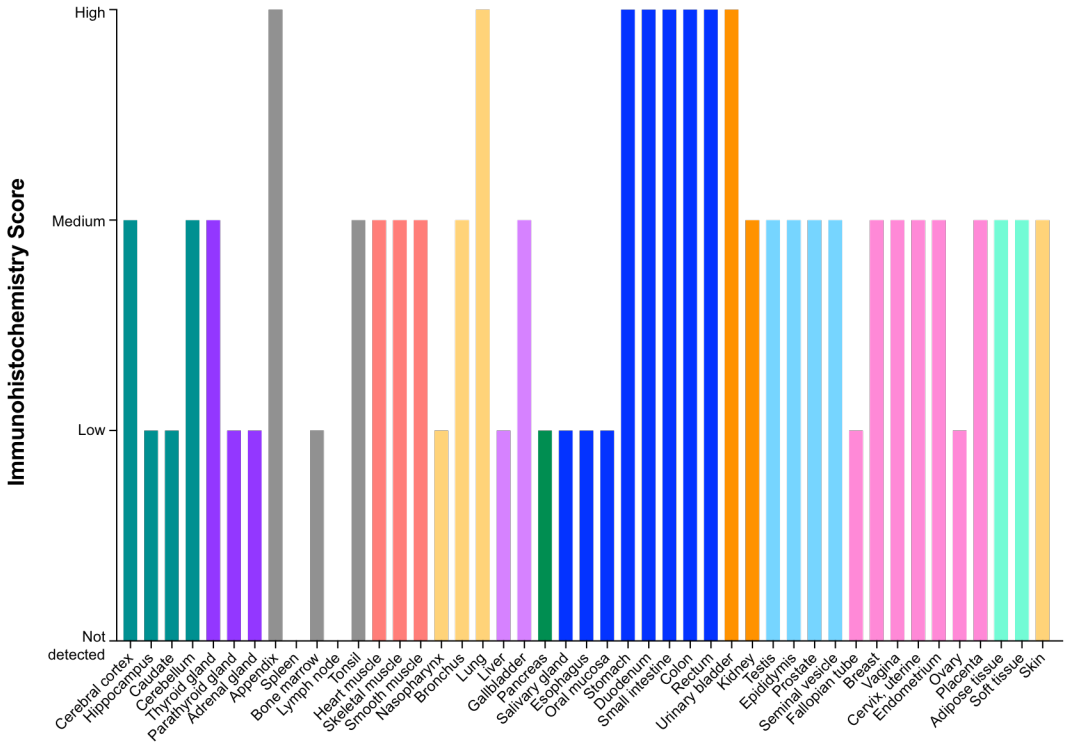

Figure 4. Gal-3 protein expression levels in different human tissue. Each color represents an organ system and its sub-tissues. All images of immunohistochemistry are manually annotated considering staining intensity, fraction of stained cells, and subcellular localization using fixed guidelines for classification (adapted from The Human Protein Atlas) (1). Within these tissue types, Gal-3 can be localized in the nucleus, cytoplasm, plasma membrane or secreted into the extracellular space, however the primary location is in the cytoplasm.

promoting tumor growth. Given the critical role the TME plays in regulating tumor progression and metastasis, recent studies have focused on new therapeutic strategies that will turn the TME from an immunosuppressive to immunostimulatory. Cancer immunotherapies such as checkpoint blockade, T cell agonists, and adoptive cell therapy have been successful at producing effective antitumor responses within the TME. However, these immunotherapies are often not sufficient to overcome the complex

immunosuppressive nature of the TME. Given this impediment in improving cancer immunotherapy, understanding the glycoprotein interactions within the TME, such as the immunosuppressive effects of Gal-3, will help us to overcome the challenges of immunosuppression. This review focuses on how Gal-3 affects immune cells, how Gal-3 contributes to immunosuppression in lung and prostate tumors (tumor types selected due to the differential expression of Gal-3 in these tumors compared to other solid tumors) and within the TME, and how targeting Gal-3 has evolved in cancer immunotherapy.

2.2 Galectin-3 in immune cells

Gal-3 is known to influence immune cells and can negatively regulate their function in pathological settings. Here, we focus on the effects of Gal-3 specifically on lymphocytes and macrophages because of their critical contribution to anti-tumor responses in the TME.

2.2.1 Gal-3 effects on lymphocytes

Due to the expression of Gal-3 in normal tissue and its participation in a vast range of functions, it has been challenging to investigate the role of Gal-3 in lymphocytes *in vivo;* however, for decades, researchers have studied the role of Gal-3 in mediating lymphocyte suppression *in vitro*. Further, extracellular and intracellular Gal-3 can have disparate effects on lymphocyte function, which complicates the understanding of Gal-3 function. Extracellular Gal-3 secreted by tumor or normal cells regulates several important lymphocyte functions such as apoptosis, activation, TCR signaling, migration, adhesion, and IL-5 production. Notably, the cellular location of Gal-3 determines whether

it has apoptotic or anti-apoptotic effects on T cells—extracellular Gal-3 induces apoptosis, while intracellular Gal-3 inhibits apoptosis. Extracellular Gal-3 induces apoptosis in human thymocytes and T cells by directly binding the glycoprotein receptors CD45 and CD71 (207). In contrast, overexpression of Gal-3 within the intracellular compartment of Jurkat T cells inhibited apoptosis induced by anti-Fas antibody and staurosporine (201). Intracellular Gal-3 is also involved in promoting cell growth and enhancing TCR signaling (201, 208). Furthermore, Gal-3 knockout CD4 T cells exhibited increased TCR expression and higher IFN-γ secretion compared to wild-type CD4 T cells (193).

The role of Gal-3 specifically within $CD8^+$ T cells is a topic of intense interest due to the vital role $CD8^+$ T cells play in immunotherapy. Despite this, little is known about the effects of either extracellular or intracellular Gal-3 on $CD8^+$ T cell function. In one experiment, extracellular Gal-3 had a suppressive effect on $CD8^+$ T cells as a Gal-3-deficient melanoma tumor cell line or its supernatant cultured with tumor-reactive $CD8^+$ T cells induced a significant expansion and increase in IFN-γ levels in the $CD8^+$ T cells compared to co-cultures with Gal-3-expressing tumor cell lines or supernatant (209, 210). In human tumor-derived $CD8^+$ T cells, Gal-3 expression has been associated with the loss of TCR and CD8 marker localization at the immunological synapse and subsequent loss of effector function (211, 212). A recent study showed that extracellular Gal-3 binds to LAG-3 on $CD8^+$ T cells and possibly suppresses $CD8^+$ T cell function (213). However, in most studies the effect of Gal-3 on $CD8^+$ T cells was shown in total splenocytes and/or in the presence of $CD4^+$ T cells, thus these data may not reflect direct effects of Gal-3 on $CD8^+$ T cells.

2.2.2 Galectin-3 effects on macrophages

Macrophages play an important role in host defense and maintenance of tissue homeostasis. Macrophages are a functionally heterogeneous cell population and depending upon the micro-environmental stimuli they can polarize into two main groups, M1 and M2. M1 are classically activated macrophages whose activating stimuli are IFN-γ and LPS. M2 are alternatively activated immunosuppressive macrophages, which include the subtypes M2a (exposure to IL-4 or IL-13) and M2c (exposure to IL-10 or glucocorticoids) (214). Gal-3 is highly expressed and secreted by macrophages themselves, which suggests a role for Gal-3 in the innate physiology of these cells (215-217).

Classical M1 macrophage activation with LPS inhibits Gal-3 expression and release, whereas alternative macrophage activation by IL-4/IL-13 leads to the accelerated biosynthesis and secretion of Gal-3, (218, 219) suggesting that Gal-3 may be a specific and highly up-regulated marker of M2-type macrophages (220). IL-4 mediates M2 macrophage activation and subsequently activates increased Gal-3 expression as well as other phenotypic M2 activation markers. Gal-3 then becomes part of a feedback loop for driving M2 macrophage activation by binding to CD98 or CD98 and β1 integrin complex, which leads to PI3K activation and thus M2 activation. This IL-4-driven M2 macrophage activation is blocked by an extracellular Gal-3 carbohydrate binding inhibitor, bis-(3-deoxy-3-(3-methoxybenz- amido)-D-galactopyranosyl) sulfane, and is also inhibited by the deletion of Gal-3, CD98, or inhibition of PI3K using small interfering RNA (siRNA) (218). Thus, Gal-3 can turn classical M1 macrophages into alternative M2 macrophages, a source of additional Gal-3 in the TME.

2.3 Galectin-3 contribution to immunosuppression

Several studies have reported that Gal-3 expression increases during cancer progression and this expression results in detrimental outcomes such as increased tumor progression, invasiveness, and metastatic potential (198, 221-223). Interestingly, Gal-3 affects more cancer types than other galectins (Table 1) (222). The common function of Gal-3 in many different cancer types is reviewed elsewhere (197, 198); this review will focus exclusively on Gal-3 expression in prostate and lung cancer due to their unique Gal-3 expression profile.

Table 1. Summary of the effect of Galectin-3 on specific cancers[a]

Cancer Type	Gal-3 Expression	Consequences of Gal-3
Breast	increased expression	helps evade immune surveillance and killing of active T cells
Prostate	**decreased expression over disease progression**	**regulates metastatic cascade**
Cervical	increased expression	resistance to chemotherapy
Lung	**increased expression in NSCLC**	**involved in regulating metastasis to lung**
Gastric	increased expression	enhances gastric cell motility and mediates metastasis
Melanoma	increased expression	increased growth, progression, angiogenesis, and metastasis
Renal cell cancer	increased expression	anti-apoptotic, resistance to cytotoxic treatment
Bladder	increased expression	increases malignant potential
Pituitary	increased expression	cell proliferation and tumor progression
Thyroid	increased expression	increased progression of differentiated thyroid cancer
Pheochromocytoma	increased expression	predicts benign vs. malignant potential
Glioma	increased expression	activated in microglia and macrophages the glioma progresses

[a] adapted from Ebrahim et al. Galectins in solid malignancies

2.3.1 Galectin-3 expression and function in prostate cancer

In other cancer types, Gal-3 expression increases throughout disease progression, (224) whereas Gal-3 expression in prostate cancer is notably different. Gal-3 is strongly expressed in the early stages of prostate cancer, but this expression gradually decreases over disease progression and is completely lost in advanced stage prostate cancer (224-226). Due to this gradient of expression over disease progression, Gal-3 expression (in prostate cancer vs. benign tissues) may be useful in predicting biochemical recurrence (225, 227).

In prostate cancer, Gal-3 regulates two coordinated steps of the metastatic cascade: the metastatic cells adhering to the microvascular endothelium (heterotypic adhesion) and the metastatic cells aggregating through interactions of tumor-associated Thomsen-Friedenreich glycoantigen with Gal-3 (homotypic aggregation) (223). Knockdown of Gal-3 using siRNA in human prostate cancer PC3 cells reduces tumor growth, cell proliferation, cell migration, colony formation, and invasion (228). Another study using the human prostate cancer PC3 cell line showed that Gal-3 knockdown results in a perturbed cell-cycle progression, including cell-cycle arrest at the G1 phase, up-regulation of nuclear p21, and hypo-phosphorylation of the retinoblastoma tumor suppressor protein (pRb). Up-regulation of nuclear p21 and hypo-phosphorylation of pRb leads to cell cycle arrest, suggesting a regulatory role for Gal-3 in cell-cycle progression (222). Gal-3 is also reported to be involved in osteoclastogenesis through binding myosin-2A (229).

In addition to different oligomeric forms, Gal-3 can also take on a cleaved form after cleavage by matrix metalloproteinases (MMP)-2/-9. In mouse models of breast and

prostate cancers this cleavage is associated with angiogenesis, tumor growth, and resistance to apoptosis (230). Further, the levels of cleaved Gal-3 have been shown to increase with metastasis (228), suggesting that the loss of Gal-3 expression during disease progression in prostate cancer may reflect cleavage of Gal-3 on the cell surface. Once cleaved, the Gal-3 CRD binds with higher affinity to its carbohydrate ligand, but loses it is ability to multimerize through its N-terminal domain, thus abrogating any Gal-3 biological function that depends on its dimer or pentamer formation (231). For example, intact Gal-3 promotes osteoclastogenesis through localization with myosin-2A, a suppressor of osteoclast differentiation. In contrast, the prostate bone metastases expressing cleaved Gal-3 can still bind to myosin-2A, but only partially reduce osteoclast differentiation because cleaved Gal-3 cannot form multimers (229). Further investigation is necessary to elucidate the relationship between the loss of Gal-3 expression and Gal-3 cleavage in advanced prostate cancer.

2.3.2 Galectin-3 expression and function in lung cancer

The majority of studies investigating Gal-3 in lung cancer have suggested Gal-3 involvement in tumor initiation, metastasis, and migration (221). Gal-3 expression varies among different types of lung cancer. For example, small cell lung cancer (SCLC) expresses Gal-3 at very low levels or not at all, while non-small cell lung cancer (NSCLC) expresses high levels of Gal-3 (232). Lung spheres of cancer stem cells derived from a NSCLC cell line (H1299) express relatively high levels of Gal-3 over serial passages compared to monolayer cells. Gal-3 knockdown in these NSCLC cell line-derived spheres decreased stemness-related genes, suggesting a co-factor role for Gal-3

by interacting with β-catenin to increase the transcriptional activity of downstream stemness-related genes. In addition, after Gal-3 knockdown the cell line lost its ability to initiate tumors and had decreased aggressiveness, clonogenicity, and chemoresistance to cisplatin or paclitaxel (233). Furthermore, Gal-3 knockout resulted in attenuation of lung carcinogenesis. These experiments suggest a regulatory role for Gal-3 in carcinogenesis-related B-cell receptors, ERK/MAPK, and peroxisome proliferator-activated receptor (PPAR) signaling pathways. Furthermore, the 4-(methylnitrosamino)-1-(3-pyridyle)-1-butanone (NNK)-induced incidence of lung tumors were significantly lower in Gal-3 knockout mice compared to their Gal-3 positive counterparts (21).

Gal-3 is expressed on the endothelium of all the major compartments of the normal lung, and the presence of Gal-3 in normal lung tissue is thought to be a homing factor for lung metastasis because it provides a location for cells to adhere as they spread throughout the tissue (234). For example, endothelium membrane-bound Gal-3 binds high affinity ligands poly-N-acetyllactosamine (polyLacNAc) on N-oligosaccharides on melanoma cells, thus providing adhesion for melanoma cells to metastasize into the lung. Manipulating Gal-3 expression, or expression of Gal-3 substrates in the lung after the onset of a primary tumor elsewhere, could be a means of controlling metastasis to lung. For example, down-regulation of the Gal-3 binding substrate polyLacNAc in melanoma cells resulted in a loss of adhesion, spreading, MMP-9 secretion, and motility of Gal-3 expressing cells. Due to the loss of these properties, melanoma cells also lost the ability to metastasize to the lung (234). Because of the connection between Gal-3 expression and metastasis, Gal-3 has been explored for its use as a biomarker to predict metastasis in lung cancer, but the results have been mixed. Some studies demonstrated that high levels

of Gal-3 and osteopontin in the serum and high expression of Gal-3 and osteopontin mRNA in NSCLC are associated with increased risk of developing metastasis and could be used as an index for evaluating undetectable NSCLC (235). However, other studies concluded that the expression and binding capacity of Gal-3 does not correlate with the staging of lung cancer and is therefore unfavorable as a prognostic marker (236). Gal-3 involvement in metastasis to the lung makes Gal-3 a potential therapeutic target in order to eliminate homing of tumor metastasis into the lung.

2.3.3 Galectin-3 mediated immunosuppression in the TME

The TME consists of many different cell types including leukocytes, stroma, and neoplastic cells along with associated growth factors and chemokines. The functions of many of these TME components can be altered by the tumor to promote tumor proliferation and survival. For example, tumors promote immune suppression by inhibiting T cell activation, polarizing pro-tumor macrophages, and turning normal fibroblasts into cancer associated fibroblasts (237). Alteration of immune cells within the TME is one of the ways tumors escape immune control, which allows tumor progression and metastasis.

Gal-3 plays a crucial role in promoting tumor-driven immune suppression. In mixed lymphocyte cultures of T cells derived from peripheral blood mixed with autologous tumor cells, inhibition of tumor-expressed Gal-3 led to the expansion of high numbers of tumor-reactive T cells (209), suggesting that Gal-3 suppresses expansion of tumor-reactive T cells. Furthermore, Gal-3 secreted by tumor cells has been shown to alter macrophage polarization from M1 (anti-tumor macrophage) to M2 (pro-tumor

macrophage), trigger $CD8^+$ T cell apoptosis, and restrict TCR clustering, all of which contribute to immunosuppression and facilitate tumor escape (**Fig. 5**).

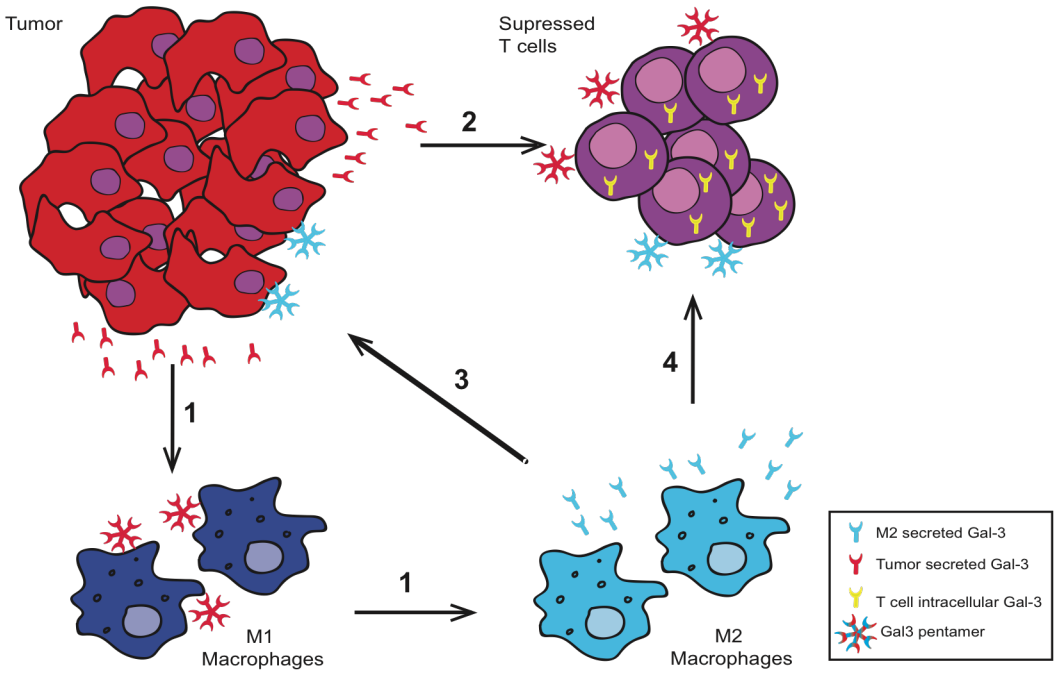

Figure 5. Impact of Gal-3 within the TME. Gal-3 is secreted by the tumor cells as monomers, which can form pentamers and bind substrates. The arrows indicate the influence of extracellular Gal-3 on various cell subsets. Gal-3 secreted by tumor cells: 1) polarizes M1 macrophages to M2 macrophages and 2) suppresses CD4 and/or CD8 T cells. Gal-3 secreted by M2 macrophages: 3) binds tumor cells to promote tumor progression/metastasis and 4) suppresses T cells.

2.3.4 Targeting Galectin-3 in immunotherapy

Due to the extensive role played by the TME in promoting tumor progression and metastasis, modulating the TME to decrease immunosuppression and increase immune activation has gained considerable attention in the field of cancer immunotherapy. The overwhelming evidence of Gal-3 involvement in boosting tumor growth, metastasis, and immune suppression has made Gal-3 an exciting target for cancer immunotherapy. The inhibition of Gal-3 in solid tumors in combination with T cell checkpoint blockade or T cell agonists has potential to augment anti-tumor immunity and improve tumor regression. In pre-clinical studies, our group has shown that treatment with a Gal-3 inhibitor, GR-MD-02, promotes antigen specific T cell expansion *in vivo*. In addition, GR-MD-02 combined with a stimulatory (agonist) anti-OX40 monoclonal antibody (mAb) improved survival in the MCA-205 sarcoma, 4T1 mammary carcinoma models, and TRAMP-C1 prostate cancer models (238). GR-MD-02 combined with anti-OX40 also reduced lung metastases in the 4T1 model (238). Furthermore, combination of GR-MD-02 with CTLA-4 or PD-1 checkpoint inhibitors has robust anti-tumor effects in multiple murine tumor models (239). This pre-clinical data provided the rationale for evaluating GR-MD-02 plus immunotherapy for patients with advanced cancer. GR-MD-02 was entered into two separate phase 1 clinical trials in combination with ipilimumab, a CTLA-4 inhibitor, or pembrolizumab, a PD-1 inhibitor, in patients with metastatic melanoma (anti-CTLA-4 or anti-PD-1), head and neck squamous cell carcinoma (anti-PD-1), and NSCLC (anti-PD-1) (NCT02575404; NCT02117362).

Another Gal-3 inhibitor, GCS-100, was used to treat elderly patients with relapsed chronic lymphocytic leukemia (CLL) in a phase II clinical trial, which resulted

in partial responses in 6 out of 24 patients (240). In a phase I clinical trial for treating refectory solid tumors, GCS-100 stabilized the disease in 16 of 24 patients (241). Since the completion of these clinical trials, GCS-100 has not been used by any other cancer-specific clinical trials. However, recently GCS-100 was examined in preclinical mouse models. Mice bearing P815 tumors (mastocytoma tumor model) that were vaccinated and treated with GCS-100 exhibited 50% survival compared to controls treated with either GCS-100 or the vaccine, which all succumbed due to the tumors (212). A recent preclinical study also showed that GCS-100 was efficacious in limiting disease progression and increasing survival of KRAS mutant NSCLC and pancreatic cancers and a KRAS-derived spontaneous cancer models (242). In the light of this new pre-clinical data, GCS-100 may have a stronger anti-tumor response when used in combination therapy. These studies provide evidence for the potential efficacy of Gal-3 inhibition in combination with checkpoint blockade or T cell agonist immunotherapy for the treatment of cancer.

2.4 Conclusion

The uniquely structured lectin Gal-3 is expressed in most cell types in adults. The structure of Gal-3 allows it to oligomerize, which confers distinctive Gal-3 functions in situations of both homeostasis and pathological processes, such as cancer. Gal-3 expression typically increases during cancer progression, and this expression results in both enhanced suppression of the immune response and other detrimental outcomes including increased tumor progression, invasiveness, and metastatic potential. Recent data suggests that inhibiting Gal-3 in combination with established immunotherapy has

the potential to both alleviate immune suppression and decrease tumor growth. Given these promising preliminary results, additional studies are warranted to further investigate how Gal-3 contributes to tumor progression and the mechanisms by which Gal-3 inhibition combined with checkpoint blockade or T cell agonists augment cancer immunotherapy.

Chapter 3: Intracellular Galectin-3 is essential for OX40-mediated memory $CD8^+$ T cell development

3 Abstract

$CD8^+$ T cells are critical mediators of adaptive immunity and enhancing their function can promote robust responses against invading pathogens and neoplastic cells. In addition to TCR stimulation, the provision of co-stimulation through ligation of TNFR family members, such as OX40, provides essential signals driving T cell differentiation, survival, and memory in part through enhanced interleukin-2 (IL-2)/IL-2 receptor (IL-2R) signaling. Interestingly, TCR stimulation in the presence of IL-2 upregulates intracellular expression of the beta-galactoside binding protein, Galectin-3 (Gal-3). Gal-3 has been shown to regulate Th1/Th2 polarization of $CD4^+$ T cells, however, the extent to which Gal-3 regulates the OX40/IL-2 signaling axis and $CD8^+$ T cell proliferation, effector function, and/or survival is unknown. Here, we demonstrate that Gal-3-deficient $CD8^+$ T cells exhibited no defects in early (36 hrs) activation or proliferation following TCR stimulation. In contrast, Gal-$3^{-/-}$ $CD8^+$ T cells exhibited decreased survival and a reduced capacity to develop into memory cells following stimulation with cognate antigen plus agonist anti-OX40 mAb or IL-2 *in vivo*. Decreased survival of Gal-$3^{-/-}$ T cells was associated with increased apoptosis and occurred in a cell-intrinsic manner. Together, these data implicate intracellular Gal-3 as a critical mediator of OX40-mediated $CD8^+$ T cell survival and memory formation following antigen exposure.

3.1 Introduction

$CD8^+$ T cells are critical mediators of the adaptive immune response and they play an important role in protecting against invading pathogens and tumors. After TCR stimulation, $CD8^+$ T cells go through clonal expansion and in the presence of appropriate co-stimulatory molecules and cytokines, polarize into multiple specialized subsets (83, 243). A majority of activated $CD8^+$ T cells undergo apoptotic cell death, while a minority differentiate into memory cells capable of mounting a robust recall response (244). One of the critical components driving T cell differentiation, survival, and memory is the presence of TNFR-mediated co-stimulation (105, 106). Specifically, ligation of the TNFR OX40 (CD134) by OX40L plays a crucial role in promoting the expansion and survival of effector and memory $CD8^+$ T cells (72, 119, 245-247).

OX40-OX40L signaling activates canonical and non-canonical NF-kB signaling pathways to promote T cell survival (124, 125) and OX40-OX40L ligation enhances IL-2/IL-2R signaling by inducing interleukin-2 (IL-2) production and IL-2Rα (CD25) expression (104). This IL-2/IL-2R signaling is essential for OX40-mediated differentiation of $CD8^+$ T cells (248, 249). IL-2 is one of the first cytokines secreted by T cells following TCR stimulation and has multifaceted effects on T cells including inducing proliferation, promoting survival, and sustaining T cell expansion (81, 83). The high-affinity IL-2R consists of a trimeric complex of the IL-2Rα (CD25), IL-2Rβ (CD122), and common γc (CD132) subunits. IL-2 binds the IL-2Rα alone with low affinity, while the dimeric IL-2Rβ/γc complex binds IL-2 with intermediate affinity. Interestingly, TCR stimulation in the presence of IL-2 upregulates intracellular expression of Gal-3. However, what role Gal-3 plays in the OX40/IL-2 signaling axis or

whether it contributes to $CD8^+$ T cell proliferation, effector function, and survival is unknown (208, 250).

Gal-3 is one of 15 known mammalian galectins that are β-galactoside-binding lectins characterized by structural similarities in their C-terminal carbohydrate-recognition domains. Of these, Gal-3 is the only chimeric lectin and its substrate binding and function depends on its subcellular location. Extracellular Gal-3 form multimers through its N-terminus upon binding to glycoproteins in the extracellular space. However, intracellular Gal-3 facilitates protein-protein interactions via its non-lectin binding N-terminus and interacts with a variety of proteins important in preventing apoptosis and promoting cell growth. Recent work also revealed that Gal-3 enhances TCR signaling in $CD4^+$ T cells through protein-protein interactions. The pro-survival effects of Gal-3 are derived, in part, from the significant structural similarity between Gal-3 and the anti-apoptotic protein, Bcl-2. The pro-survival activity of Bcl-2 is driven by a highly conserved amino acid sequence in the BH1 domain, the NWGR sequence (201). Gal-3 also contains the NWGR sequence and, moreover, Gal-3 has been shown to have anti-apoptotic activity, as Gal-3 overexpression within the intracellular compartment of Jurkat T cells inhibits apoptosis induced by Fas ligation and staurosporine (201). Additionally, *in vitro* studies have shown that Gal-3-deficient $CD4^+$ T cells secrete more IFN-γ and IL-4 compared to wild-type (WT) cells and that Gal-3 potentiates TCR down-regulation in $CD4^+$ T cells following TCR engagement (193). However, the extent to which intracellular Gal-3 regulates $CD8^+$ T cell responses is unknown.

Here, we report that Gal-$3^{-/-}$ $CD8^+$ T cells have no defect in early activation *in vitro* or *in vivo*. However, Gal-$3^{-/-}$ $CD8^+$ T cells exhibit decreased survival and a defect in

transition to memory cells following antigenic challenge in the presence of an OX40 agonist or IL-2 stimulation *in vivo*. Together, these data implicate Gal-3 as a critical mediator of OX40 and IL-2-induced $CD8^+$ T cell survival and memory formation.

3.2 Results

3.2.1 OX40 costimulation maintains Gal-3 mRNA expression in $CD8^+$ T cells

T lymphocytes that have been activated with mitogen and a secondary signal, such as IL-2, express Gal-3 at significantly higher levels than T lymphocytes that have been activated with either mitogen or IL-2 alone (206, 208). Because high levels of Gal-3 expression require both IL-2 and T cell activation and because OX40 and IL-2 signaling co-regulate each other in $CD8^+$ T cells (63, 116-118), we asked whether OX40 co-stimulation was sufficient to induce Gal-3 expression. We investigated Gal-3 mRNA expression in antigen (Ag)-specific $CD8^+$ T cells following TCR stimulation in the presence of agonist anti-OX40 (aOX40) mAb therapy. Purified OT-I $CD8^+$ T cells were adoptively transferred into wild-type (WT) mice, and then mice were vaccinated with soluble ovalbumin (OVA) plus control IgG or aOX40 mAb (67). The donor $CD8^+$ T cells were isolated from lymph nodes on days 4, 6, and 8 post-treatment and processed for mRNA analysis (Fig. 6A). Minimal Gal-3 mRNA expression was detected in naïve OT-I or endogenous $CD8^+$ T cells, consistent with a lack of Gal-3 expression in quiescent cells (Fig. 6B). In contrast, on day 4 stimulated $CD8^+$ T cells exhibited high levels of Gal-3 expression that decreased over time. Interestingly, agonist aOX40 therapy was sufficient

to sustain high levels of Gal-3 expression 6 to 8 days post-treatment (Fig. 6B). These data demonstrated that OX40 signaling sustains Gal-3 expression in Ag-specific $CD8^+$ T cells.

We then asked whether there was any difference in the initial activation status of WT versus Gal-$3^{-/-}$ $CD8^+$ T cells *in vivo* or *in vitro*, focusing on expression of CD25 and the OX40 receptor because these are upregulated shortly after TCR stimulation. WT and Gal-$3^{-/-}$ $CD8^+$ OT-I T cells were adoptively transferred into WT hosts and stimulated with OVA (as in Fig. 6B), and then we evaluated OX40 and CD25 expression on the donor $CD8^+$ T cells from lymph nodes (LN) 36 hours post-vaccination. There was no difference in the percent of cells expressing OX40 or CD25 expression between WT and Gal-$3^{-/-}$ $CD8^+$ T cells (Fig. 6C). We also examined OX40 and CD25 expression on WT and Gal-$3^{-/-}$ OT-I T cells stimulated with OVA peptide *in vitro*. Similar to our *in vivo* findings, there was no difference in the percent of cells expressing OX40 or CD25 between WT and Gal-$3^{-/-}$ T cells *in vitro* (Fig. 7). Taken together, these data demonstrate that Gal-$3^{-/-}$ OT-I T cells do not have a defect in their initial response to TCR stimulation *in vivo* or *in vitro*.

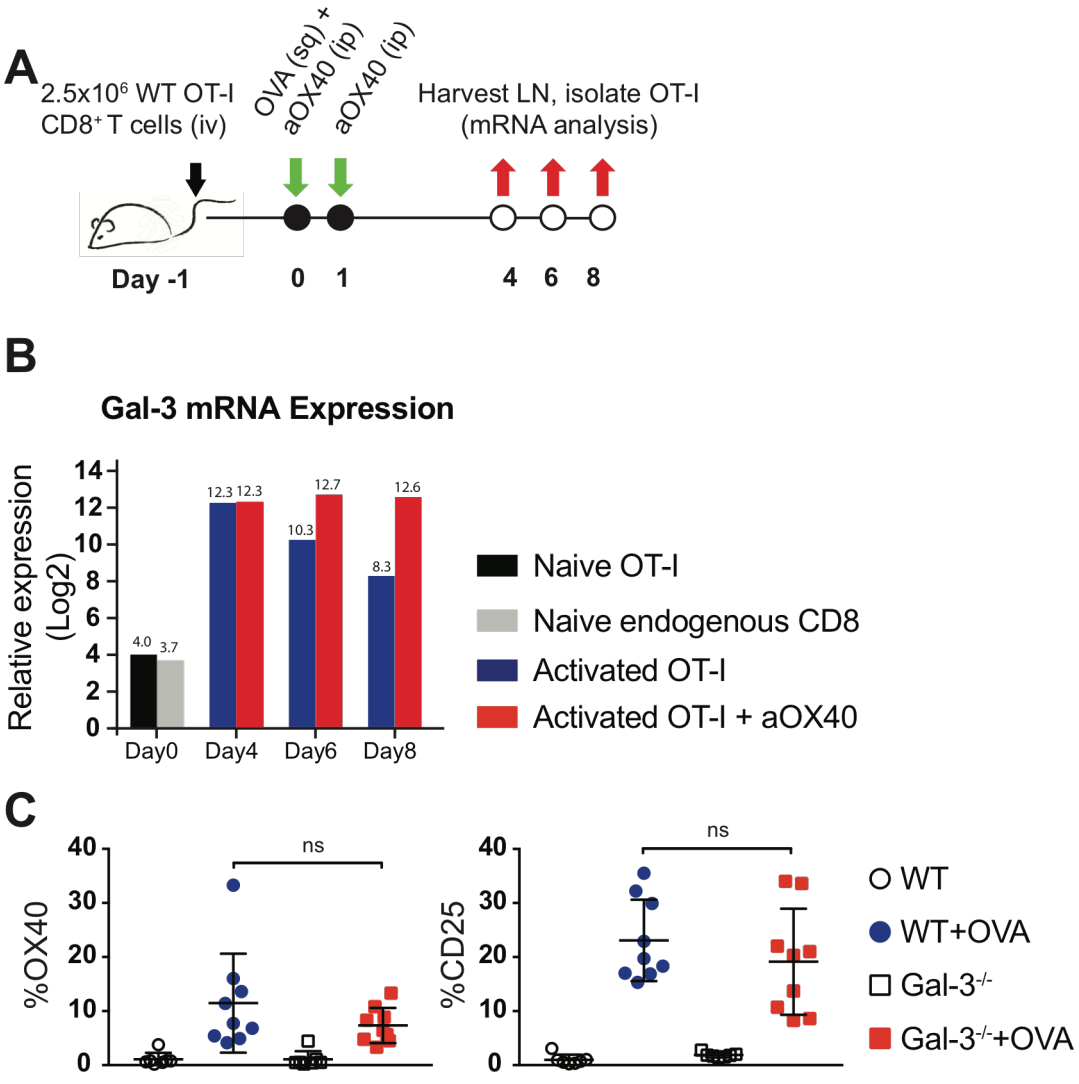

Figure 6. OX40 agonist treatment maintains Gal-3 mRNA expression in CD8$^+$ T cells. A) Experimental scheme for determining Gal-3 mRNA expression in OT-I CD8$^+$ T cells *in vivo*. **B)** 2.5x10^6 WT OT-I T cells were adoptively transferred into WT mice and then stimulated with soluble OVA protein (day 0) along with control (rat IgG) or aOX40 (day 0, 1). At the indicated time points, donor OT-I T cells were harvested and the relative expression of Gal-3 mRNA was determined. **C)** 2x10^6 CFSE-labeled WT or Gal-3$^{-/-}$ OT-I T cells were adoptively transferred into WT mice and then stimulated as in (B). Thirty-six hours later, the expression of OX40 and CD25 WT or Gal-3$^{-/-}$ OT-I T cells isolated from the lymph nodes was determined. Graphs represent the mean+/-SD from 2 independent experiments (n=4-5/ group). *P<0.05, **P<0.01, ***P<0.001, ****P<0.0001

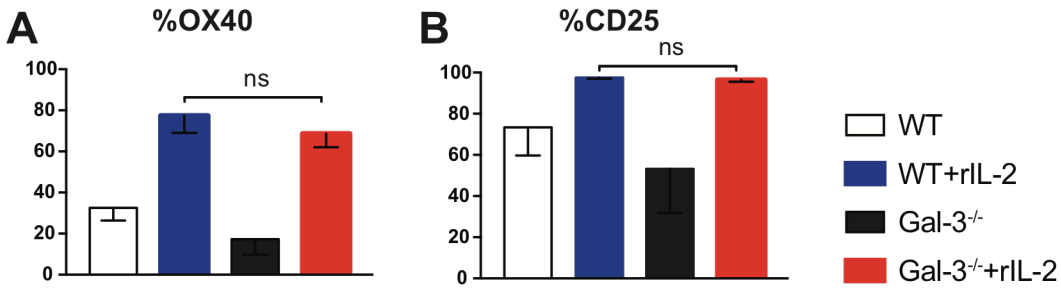

Figure 7. Expression of OX40 and CD25 in WT and Gal-3$^{-/-}$ CD8^{+} T cells. WT or Gal-3$^{-/-}$ OT-I CD8^{+} T cells were stimulated with irradiated SIINFEKL peptide-pulsed APCs (DC2.4 cells). After 24 hours, cells were washed and re-cultured with media or 100ng rhIL-2 and then 48 hours later, OX40 and CD25 expression were determined. Graphs represent the mean+/-SD from 2 independent experiments (n=4/ group). *P<0.05, **P<0.01, ***P<0.001, ****P<0.0001

3.2.2 Gal-3 is essential for OX40-mediated CD8^{+} T cell survival

OX40 signaling plays an important role in regulating CD8^{+} T cell expansion and survival and we observed that aOX40 therapy drives sustained expression of Gal-3 (Fig. 6B), suggesting that Gal-3 may regulate the downstream effects of OX40 signaling. To test whether Gal-3 contributes to OX40-mediated CD8^{+} T cell differentiation and survival, WT or Gal3$^{-/-}$ OT-I T cells were adoptively transferred into WT recipients and then stimulated with cognate antigen along with control IgG or agonist aOX40 mAb. Subsequently, we determined the Ag-specific CD8^{+} T cell response at 7, 14, and 29 days post-treatment (Fig. 8A). Anti-OX40 therapy induced an equally potent expansion of WT and Gal-3$^{-/-}$ CD8^{+} T cells as compared to controls on day 7 post-treatment; however, by 14 and 29 days post-stimulation, Gal-3$^{-/-}$ CD8^{+} T cells were significantly reduced in comparison to WT cells (Fig. 8B and Fig. 9). This defect was not due to a reduction in

proliferation as there was no difference in Ki-67 expression (a marker of cellular proliferation) between WT and Gal-3$^{-/-}$ T cells across all time points (Fig. 8C).

Because we did not detect a difference in proliferation, we hypothesized that the lack of Gal3$^{-/-}$ CD8^{+} T cell survival could be a deficiency in the development of and/or transition to memory cells, which starts occurring approximately 1 week post-stimulation. During this phase of the T cell response, a proportion of short-lived terminal effector T cells (T_E) die off and effector memory cells (72) and long-lived central memory cells (T_{CM}) start to accumulate, resulting in a reduction in T_E cells (251). These cells can be identified based upon their differential expression of CD62L and KLRG-1 1 (T_E/T_{EM}: CD62L^{lo}/KLRG1^{+} and T_{CM}: CD62L^{+}/KLRG1^{-}) (252, 253). To determine if there were differences in the proportion of T_E/T_{EM} and/or T_{CM}, we determined the expression of CD62L and KLRG-1 in WT and Gal-3$^{-/-}$ CD8^{+} T cells. On day 7, aOX40 therapy induced equivalent levels of KLRG-1 in WT and Gal-3$^{-/-}$ T cells in comparison to IgG-treated controls (Fig. 8D); however, increased KLRG-1 expression was uniquely maintained in Gal-3$^{-/-}$ T cells by day 14 as compared to WT T cells (Fig. 8D). There were no significant differences in CD62L expression between WT and Gal-3$^{-/-}$ T cells across the time course, although the Gal-3$^{-/-}$ CD8^{+} T cells treated with aOX40 trended towards a lower frequency of CD62L^{+} compared to aOX40-stimulated WT cells (Fig. 8D).

Thus, aOX40 treatment drives KLRG-1 expression in Gal-3$^{-/-}$ T cells, resulting in a significantly higher frequency of T_E/T_{EM} cells and a corresponding lower frequency of T_{CM} cells compared to their aOX40-treated WT counterparts on day 14 (Fig. 8E). The increase in T_E/T_{EM} was present as early as day 7 and maintained until day 29 (Fig. 10).

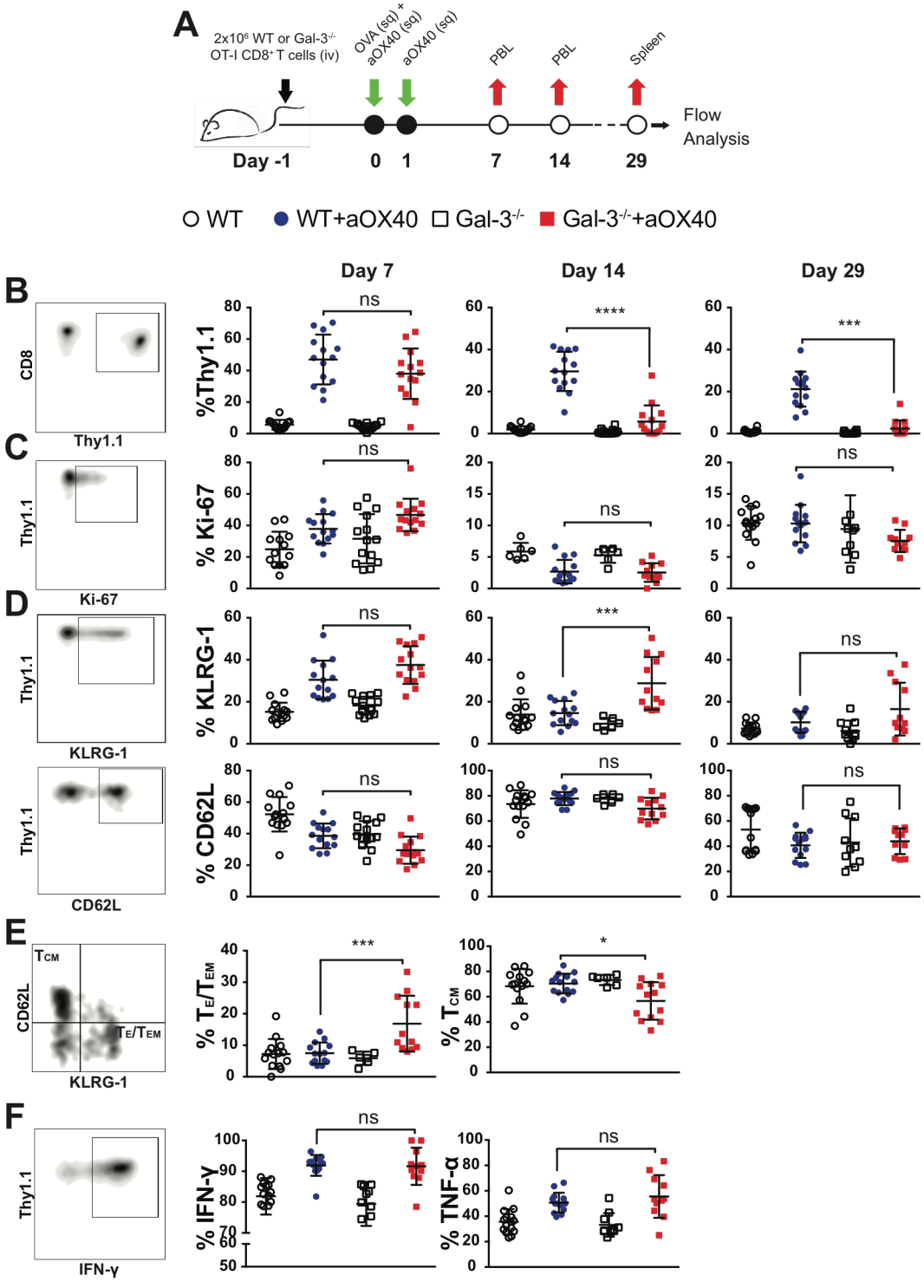
A
2x10⁶ WT or Gal-3⁻/⁻ OT-I CD8⁺ T cells (iv)
OVA (sq) + aOX40 (sq)
aOX40 (sq)
PBL
PBL
Spleen
Flow Analysis
Day -1
0
1
7
14
29
WT
WT+aOX40
Gal-3⁻/⁻
Gal-3⁻/⁻+aOX40
Day 7
Day 14
Day 29
B
CD8
Thy1.1
%Thy1.1
C
Thy1.1
Ki-67
% Ki-67
D
Thy1.1
KLRG-1
% KLRG-1
Thy1.1
CD62L
% CD62L
E
TCM
TE/TEM
CD62L
KLRG-1
% TE/TEM
% TCM
F
Thy1.1
IFN-γ
% IFN-γ
% TNF-α
ns
****
***
*

Figure 8. Gal-3 deficient $CD8^+$ T cells exhibit reduced survival following aOX40 therapy. A) Experimental schema. WT or Gal-$3^{-/-}$ $CD8^+$ OT-I T cells were adoptively transferred into WT mice and stimulated as in Fig. 1. The frequency of adoptively transferred cells was determined in the peripheral blood (days 7 and 14) and spleen (day 29) by flow cytometry. **B-F)** Graphs depict the frequency of **B)** donor ($Thy1.1^+$) cells of total $CD8^+$ T cells, **C)** Ki-67^+ $Thy1.1^+$ of total $Thy1.1^+$ cells, **D)** KLRG-1^+ $Thy1.1^+$ or $CD62L^+$ $Thy1.1^+$ of total $Thy1.1^+$ cells, and **E)** T_E/T_{EM} and T_{CM} cells within the donor OT-I T cell population on day 14. **F)** On day 29, splenocytes were harvested and stimulated with cognate Ag (SIINFEKL peptide). Graphs depict the frequency of IFN-γ^+ or and TNF-α^+ $Thy1.1^+$ of total $Thy1.1^+$ $CD8^+$ T cells. Graphs represent the mean+/-SD from 2 independent experiments (n=7/ group). *P<0.05, **P<0.01, ***P<0.001, ****P<0.0001

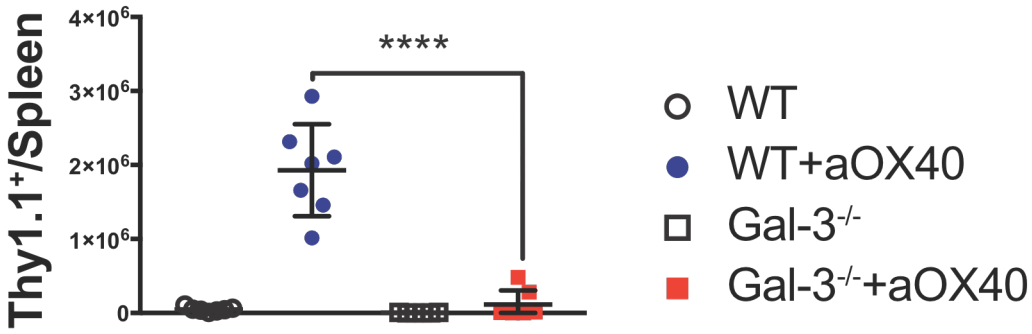

Figure 9. Number of isolated adoptively transferred OT-I CD8$^+$ T cells. Total number of isolated adoptively transferred OT-I CD8$^+$ T cells on day 29 per spleen.

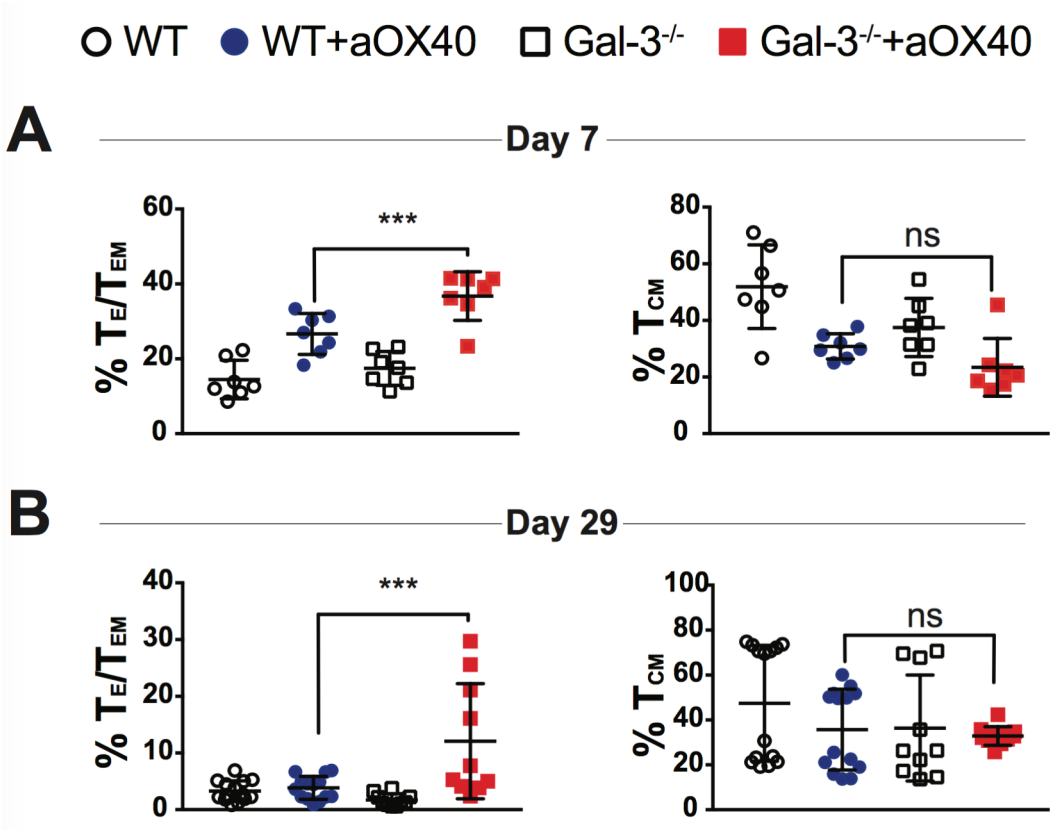

Figure 10. T_E/T_{EM} and T_{CM} cells within the donor CD8$^+$ T cell population. A) Frequency of T_E/T_{EM} and T_{CM} cells within the donor Thy1.1$^+$ OT-I T cell population on day 7. **B)** Frequency of T_E, T_{EM} and T_{CM} cells within the donor Thy1.1$^+$ OT-I T cell population on day 29. Graphs represent the mean+/-SD from 2 independent experiments (n=7/ group). *P<0.05, **P<0.01, ***P<0.001, ****P<0.0001

These data suggested that the survival benefits of aOX40 therapy are abrogated in Gal-3$^{-/-}$ CD8^{+} T cells and that Gal-3$^{-/-}$ CD8^{+} T cells exhibit a defect in the generation of central memory cells. Next, we asked whether Gal-3$^{-/-}$ CD8^{+} T cells retain their effector function, in addition to their reduction in survival. We evaluated the extent of effector cytokine production in the adoptively transferred CD8^{+} T cells isolated from spleens on day 29. These data revealed no differences in IFN-γ or TNF-α cytokine production between Gal-3$^{-/-}$ and WT CD8^{+} T cells following restimulation *in vitro* (Fig. 8F).

Subsequently, we asked whether the defect in Gal-3$^{-/-}$ CD8^{+} T cell survival occurred through a cell intrinsic or extrinsic mechanism. Thy$^{1.1/1.2}$ WT and Thy$^{1.1/1.1}$ Gal-3$^{-/-}$ CD8^{+} T cells were co-transferred into Thy$^{1.2/1.2}$ WT mice, stimulated with antigen plus aOX40 therapy, and then donor T cell responses were monitored over time (Fig. 11A). These data revealed that the Gal-3$^{-/-}$ CD8^{+} T cells treated with aOX40 had reduced survival compared to the WT cells, supporting our findings from the single transfer model and suggesting that the reduced survival of Gal-3$^{-/-}$ CD8^{+} T cells is cell intrinsic (Fig. 11B). Additional co-transfer studies revealed similar differences with respect to CD62L and KLRG-1 expression, including an increase in the extent of T_E/T_{EM} CD8^{+} T cells, between WT and Gal-3$^{-/-}$ co-transferred CD8^{+} T cells treated with aOX40 (Fig. 11C). Taken together, these data demonstrate that aOX40-treated Gal-3$^{-/-}$ CD8^{+} T cells are not defective in early activation, differentiation, or proliferation, but exhibit cell-intrinsic defects in survival and a skewed differentiation that favors effector and effector memory cell generation with a concomitant decrease in the proportion of central memory cells.

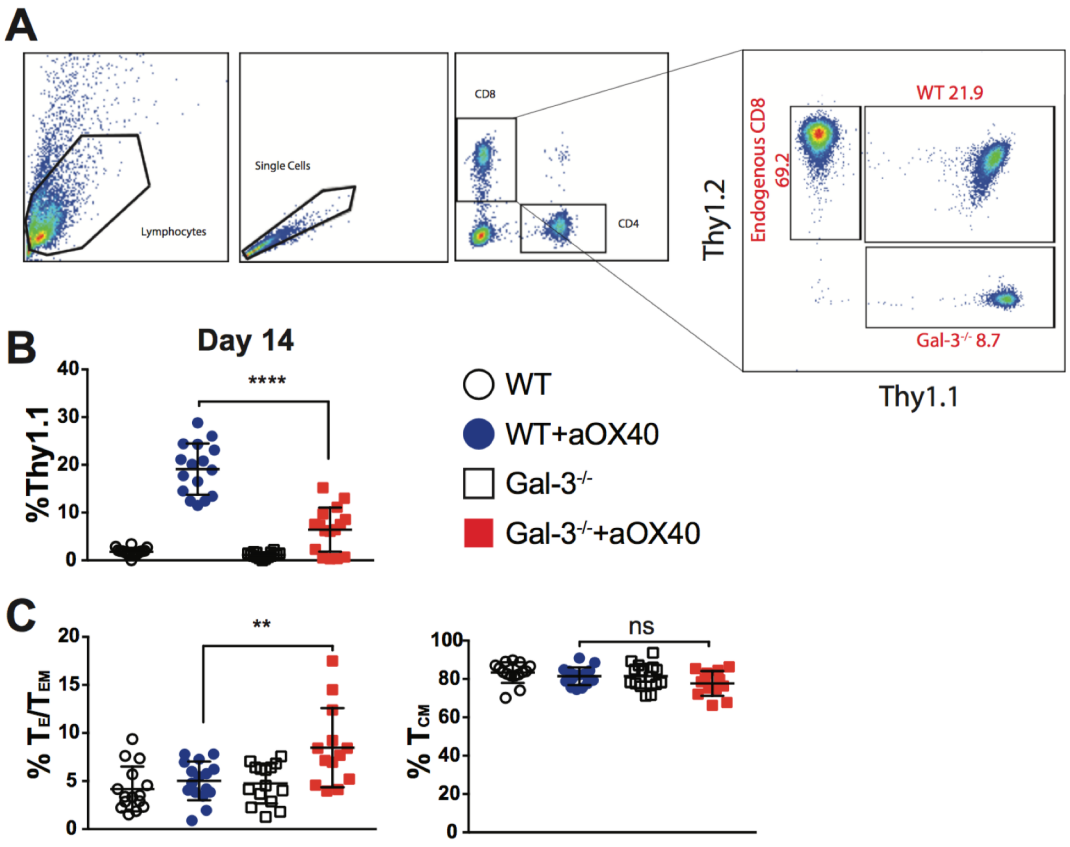

Figure 11. Defect in Gal-3-deficient CD8$^+$ T cell survival is cell intrinsic. 2x10^6 Thy1$^{.1/1.2}$ WT or Thy$^{1.1/1.1}$ Gal-3$^{-/-}$ OT-I CD8$^+$ T cells were co-transferred into Thy$^{1.2/1.2}$ WT mice and then stimulated with OVA plus control (rat IgG) or aOX40 mAb. The frequency of adoptively transferred OT-I T cells was determined in the PBL (days 7 and 14) and spleen (day 29) by flow cytometry. **A)** Gating strategy for determining the frequency of adoptively transferred cells WT OT-I (Thy$^{1.1}$/Thy$^{1.2}$), Gal-3$^{-/-}$ OT-I (Thy$^{1.1}$ /Thy$^{1.1}$), and endogenous (Thy$^{1.2}$/Thy$^{1.2}$) CD8$^+$ T cells. **B)** Frequency of adoptively transferred WT and Gal-3$^{-/-}$ OT-I T cells. **C)** Frequency of T_E, T_{EM} and T_{CM} donor OT-I T cells on day 14. Graphs represent the mean+/-SD from 2 independent experiments (n=8/group). *P<0.05, **P<0.01, ***P<0.001, ****P<0.0001

Furthermore, we also examined the impact of Gal-3 on $CD8^+$ T cell survival following infection with a non-virulent strain of *Listeria monocytogenes* expressing ovalbumin (*Lm-ActA*-OVA). WT or $Gal3^{-/-}$ OT-I T cells were adoptively transferred into WT recipients and then infected with *Lm-ActA*-OVA along with control IgG or agonist aOX40 mAb. The Ag-specific OT-I T cell response was determined at 7, 14, and 29 days post-treatment (Fig. 12A). Anti-OX40 therapy induced an equally potent expansion of WT and Gal-$3^{-/-}$ OT-I T cells as compared to controls on day 7 post-treatment; however, by 14 and 29 days post-stimulation, Gal-$3^{-/-}$ OT-I T cells were significantly reduced in comparison to WT cells (Fig. 12B). On day 29, the recipient mice were rechallenged with *Lm-ActA*-OVA to assess the recall response. The rechallenged Gal-$3^{-/-}$ $CD8^+$ T cells treated with aOX40 had significantly reduced

expansion compared to aOX40-treated WT OT-I T cells (Fig. 12C). However, there was no significant difference in pre- vs. post-challenge expansion (fold-change) between WT and Gal-$3^{-/-}$ $CD8^+$ cells (Fig. 13) or IFN-γ and TNF-α expression (Fig. 12C). Together, these data suggest that the surviving Gal-$3^{-/-}$ $CD8^+$ T cells treated with aOX40 can form long-term memory and, upon rechallenge, these cells can undergo secondary expansion and retain their effector function.

We also determined the impact of Gal-3 on $CD8^+$ T cell-mediated anti-tumor immunity in a B16-OVA (melanoma) tumor model. B16-OVA tumors were implanted in the flank of WT mice and then two weeks later, WT or $Gal3^{-/-}$ OT-I $CD8^+$ T cells were adoptively transferred into tumor-bearing recipients and then treated with control IgG or agonist aOX40 mAb (Fig. 12D). Tumor-bearing mice treated with Gal-$3^{-/-}$ $CD8^+$ T cells plus aOX40 exhibited significantly reduced survival as compared to WT $CD8^+$ T cells +

aOX40 (Fig. 12E). Together, these data demonstrate the critical role of intracellular Gal-3 in regulating aOX40-treated $CD8^+$ T cell responses in the context of an infection (*Lm-ActA*-OVA) or tumor (B16-OVA) therapy.

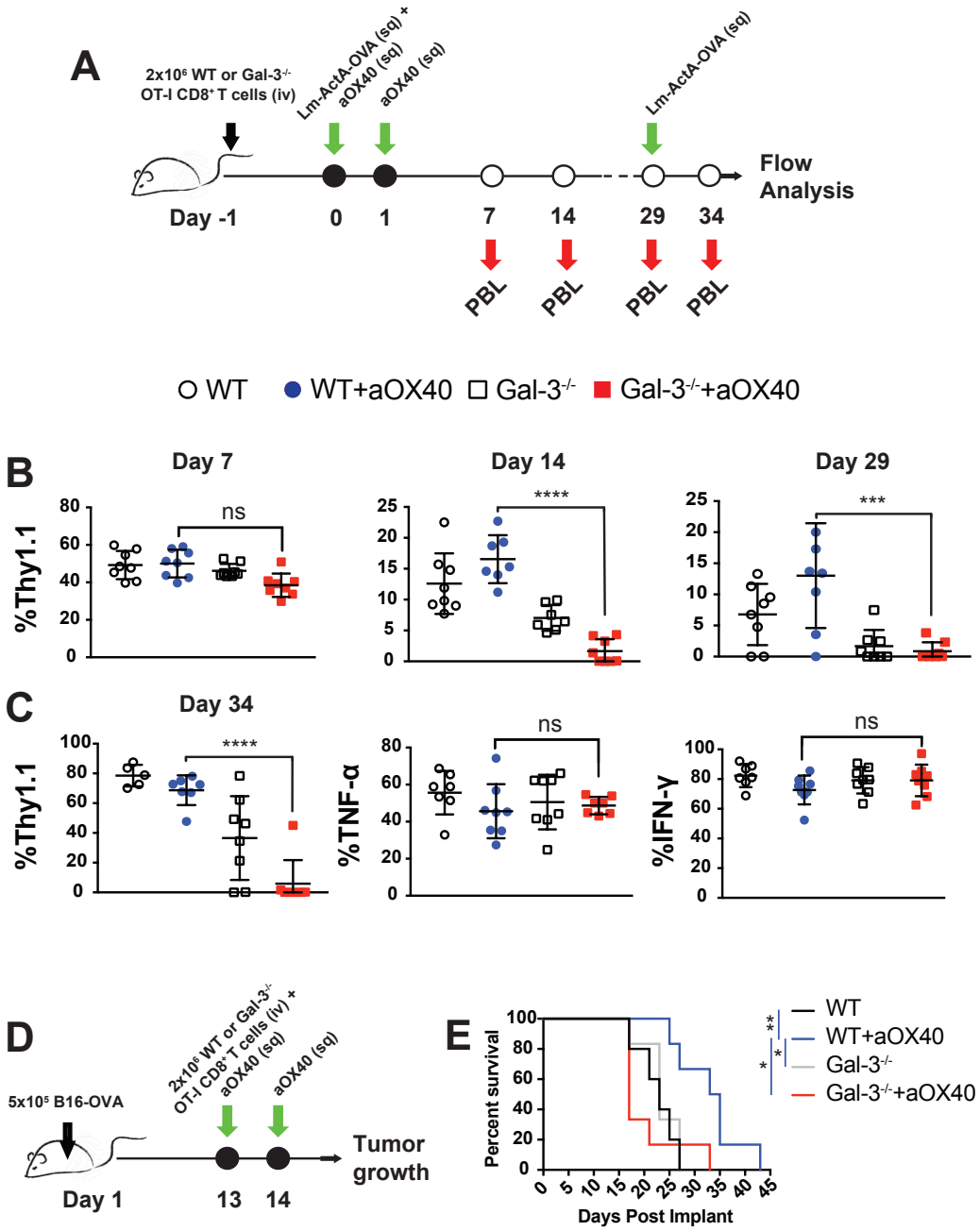
A
2x10⁶ WT or Gal-3-/- OT-I CD8+ T cells (iv)
Lm-ActA-OVA (sq) + aOX40 (sq)
aOX40 (sq)
Lm-ActA-OVA (sq)
Flow Analysis
Day -1
0
1
7
14
29
34
PBL
WT
WT+aOX40
Gal-3-/-
Gal-3-/-+aOX40
B
Day 7
Day 14
Day 29
%Thy1.1
ns
****
***
C
Day 34
%Thy1.1
%TNF-α
%IFN-γ
****
ns
ns
D
5x10⁵ B16-OVA
2x10⁶ WT or Gal-3-/- OT-I CD8+ T cells (iv) + aOX40 (sq)
aOX40 (sq)
Tumor growth
Day 1
13
14
E
Percent survival
Days Post Implant
WT
WT+aOX40
Gal-3-/-
Gal-3-/-+aOX40
**
*
*

Figure 12. The relevance of Gal-3 in aOX40-treated CD8$^+$ T cell responses to vaccination and anti-tumor immunity. A) Experimental schema. WT or Gal-3$^{-/-}$ OT-I CD8$^+$ T cells were adoptively transferred into WT mice and stimulated with 10x10^6 *Lm-ActA*-OVA along with aOX40 agonist on day 0 and another dose of aOX40 agonist the next day. The frequency of adoptively transferred cells was determined in the peripheral blood (days 7, 14, and 29) by flow cytometry. The mice were rechallenged with 10x10^6 *Lm-ActA*-OVA on day 29 and the frequency of adoptively transferred cells was determined in the peripheral blood five days after the rechallenge. **B)** Frequency of adoptively transferred WT and Gal-3$^{-/-}$ OT-I T cells. **C)** Frequency of adoptively transferred WT and Gal-3$^{-/-}$ OT-I T cells after rechallenge and the expression of IFN-γ and TNF-α. **D)** Experimental schema for tumor model. 5x10^6 B16-OVA cells were implanted in the flank of WT mice. WT or Gal-3$^{-/-}$ OT-I T cells were adoptively transferred into B16-OVA tumor-bearing mice along with aOX40 agonist on day 13 and another dose of aOX40 agonist the next day. Tumor growth was measured every two days. **E)** Kaplan-Meier survival curve for B16-OVA tumor-bearing mice following treatment with WT or Gal-3$^{-/-}$ OT-I T cells plus control IgG or agonist aOX40 mAb. (n=5-7/group). *P<0.05, **P<0.01, ***P<0.001, ****P<0.0001

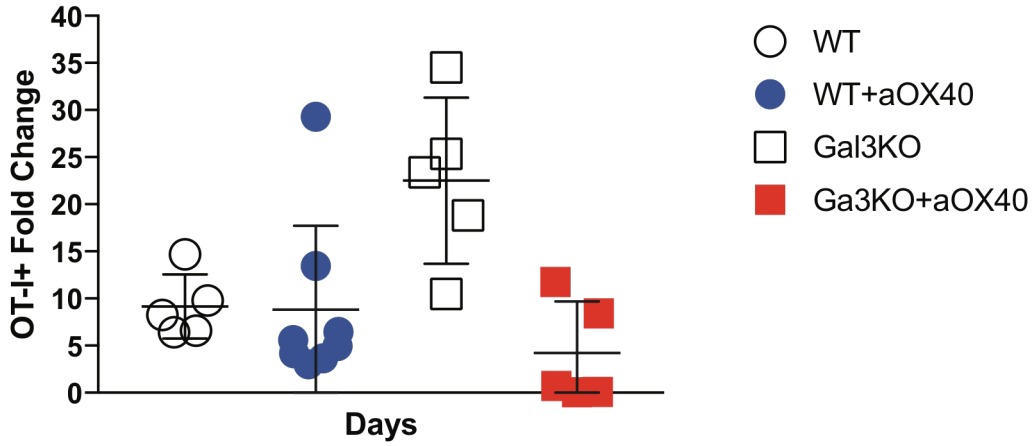

Figure13. Pre- vs. post-challenge expansion (fold-change) between WT and Gal-3$^{-/-}$ OT-I T cells. Fold change in expansion of adoptively transferred OT-I CD8^{+} T cells post-challenge (day34) normalized to pre-challenge (day 29).

3.2.3 Gal-3 is essential for IL-2-mediated $CD8^+$ T cell survival

Because OX40 ligation augments $CD8^+$ T cell expansion and survival in part through an IL-2-dependent mechanism (104, 119, 124), we asked whether $Gal3^{-/-}$ $CD8^+$ T cells would exhibit a similar defect in survival and formation of central memory cells following IL-2-specific stimulation *in vivo,* independent of enhanced OX40 ligation. To test this, WT or $Gal3^{-/-}$ $CD8^+$ T cells were adoptively transferred into WT mice and then activated with antigen plus IL-2-complexes (IL-2c). IL-2c are made by mixing recombinant IL-2 (rIL-2) with an anti-IL-2 mAb (clone S4B6) that preferentially binds to the IL-2Rβ chain with a half-life of 22-24 hours, thereby stimulating effector T cells (254, 255). Treatment with IL-2c has the added benefit of limiting the expansion of regulatory $FoxP3^+CD4^+$ T cells (T_{reg}) and is less toxic compared to rIL-2 (255). We saw IL-2-induced expansion of $CD8^+$ T cells on day 7, but we observed a significant reduction in Gal-$3^{-/-}$ $CD8^+$ T cell survival compared to WT cells by days 14 and 29, similar to our observations following aOX40 treatment (Fig. 14A). There was no difference in proliferation (Ki-67 expression) between WT and Gal-$3^{-/-}$ $CD8^+$ T cells treated with IL-2c (Fig. 14B). Interestingly, we did not observe significant differences in the frequency of T_E/T_{EM}, or T_{CM} cells in Gal-3-/- CD8+ T cells treated with IL-2c as compared to WT cells (Fig. 14C), which may reflect differences in systemic inflammation following IL-2c therapy as compared to OX40 stimulation. All groups exhibited similar levels of IFN-γ and TNF-α production on day 29, indicating that there was no defect in effector function in the absence of Gal-3 (Fig. 14D). Together, these data demonstrate that Gal-$3^{-/-}$ $CD8^+$ T cells are not defective in early proliferation and

generation of memory following treatment with IL-2c, but exhibit reduced survival compared to their WT counterparts.

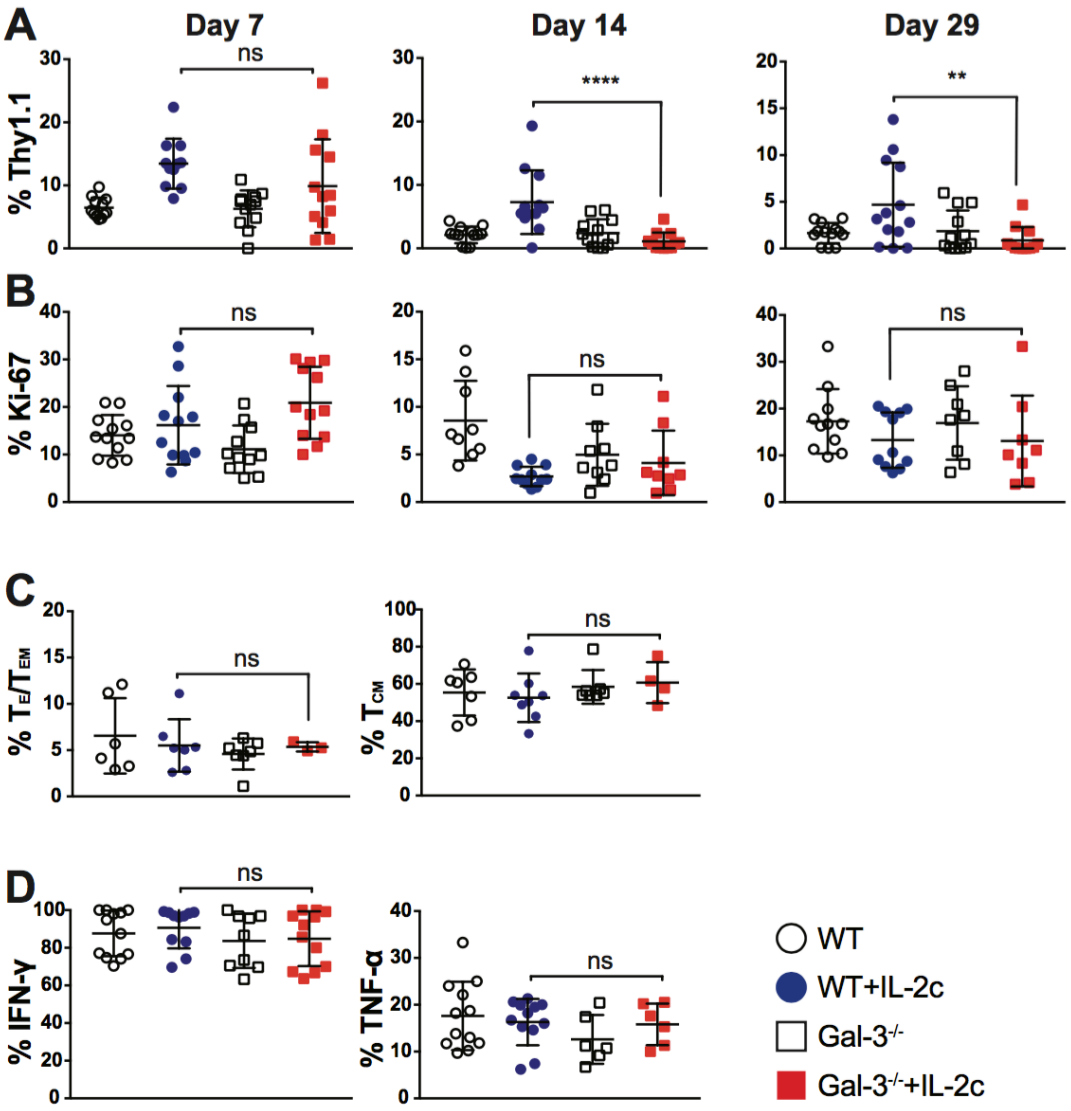

Figure 14. Gal-3 is essential for IL-2-mediated CD8$^+$ T cell survival. 2x10^6 WT or Gal-3$^{-/-}$ OT-I T cells were adoptively transferred into WT hosts and stimulated with OVA+/-IL-2c. IL-2c was given every day for three days. The frequency of adoptively transferred OT-I T cells was determined in the PBL (days 7 and 14) and spleen (day 29) by flow cytometry. **A-C)** Graphs depict the frequency of **A)** donor (Thy1.1$^+$) cells of total CD8$^+$ T cells, **B)** Ki-67$^+$ Thy1.1$^+$ of total Thy1.1$^+$ cells, **C)** T_E, T_{EM} and T_{CM} cells within the donor OT-I T cell population on day 14. **D)** On day 29, splenocytes were harvested and stimulated with cognate Ag. Graphs depict the frequency of IFN-γ^+ or TNF-α^+ Thy1.1$^+$ of total Thy1.1$^+$ OT-I T cells. Graphs represent the mean+/-SD from 2 independent experiments (n=6-7/ group) *P<0.05, **P<0.01, ***P<0.001, ****P<0.0001

3.2.4 Gal-3-deficient $CD8^+$ T cells undergo increased apoptosis in vitro and in vivo in comparison to WT $CD8^+$ T cells

Because Gal-$3^{-/-}$ $CD8^+$ T cells exhibited reduced survival in comparison to WT cells (Fig. 8B and 14A), we asked whether their lower frequency was due to increased apoptosis. T cell apoptosis was determined by measuring Annexin V expression, a widely used marker for detecting apoptotic cells *in vitro* and *in vivo* based upon its ability to bind phosphatidylserine expressed on the surface of dying cells. WT or Gal-$3^{-/-}$ OT-I T cells were stimulated with OVA *in vitro* in the presence or absence of rIL-2 and then the extent of Annexin V expression was determined. We observed a significant increase in Annexin V^+ Gal-$3^{-/-}$ T cells *in vitro* as compared to WT cells, regardless of the presence of IL-2 (Fig. 15A). Similarly, Annexin V expression was significantly increased in Gal-$3^{-/-}$ $CD8^+$ T cells isolated from lymph nodes following stimulation with antigen plus IL-2 *in vivo* (Fig. 15B). Furthermore, we looked at Annexin V expression in different subsets (T_E/T_{EM}, and T_{CM}) of donor OT-I T cells in the spleen on day 14. Interestingly, there was a significant increase in Annexin V within the T_E/T_{EM} subset of Gal-$3^{-/-}$ T cells treated with aOX40 agonist compared to their WT counterparts (Fig. 15C). Together, these data suggest that Gal-$3^{-/-}$ $CD8^+$ T cells are more susceptible to apoptotic cell death in comparison to WT $CD8^+$ T cells.

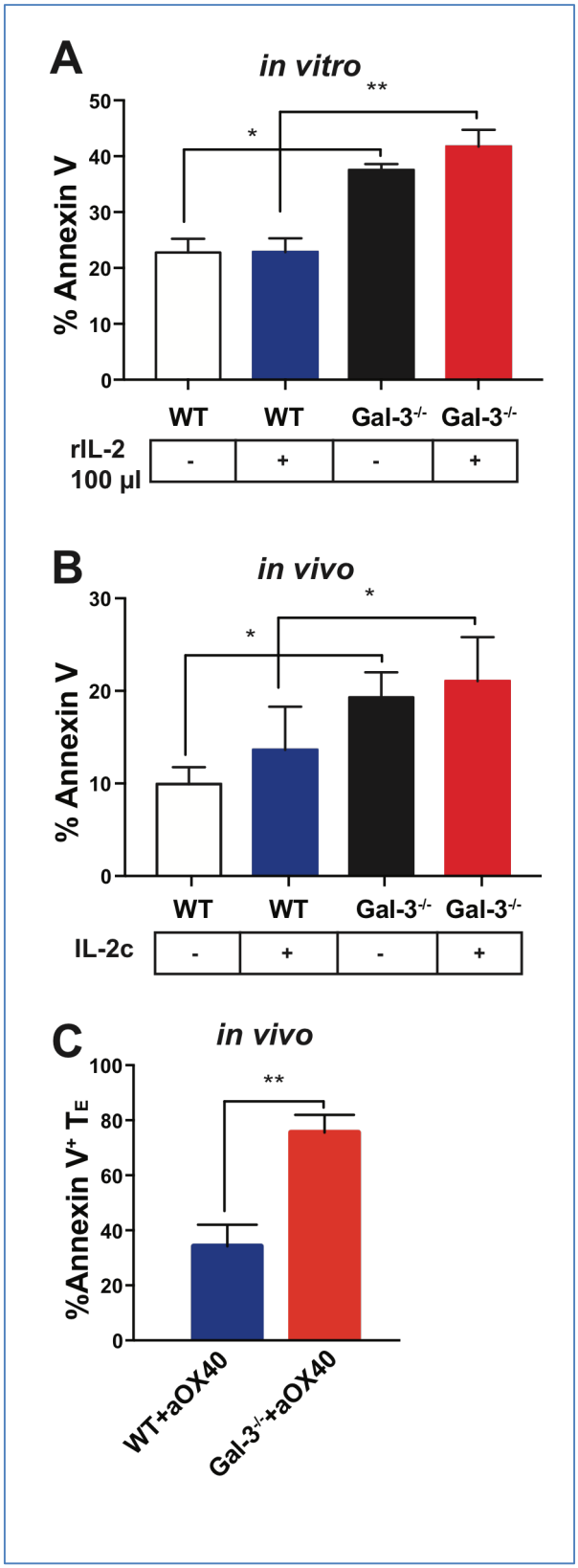

Figure 15. Gal-3-deficient CD8$^+$ T cells exhibit increased apoptosis *in vitro* and *in vivo*. A) 3x10^5 WT or Gal-3$^{-/-}$ OT-I CD8$^+$ T cells were stimulated with 5x10^4 irradiated SIINFEKL peptide-pulsed APCs (DC2.4 cells). Twenty-four hours later, cells were incubated +/- 100ng rhIL-2 for 48 hours. The frequency of Annexin V$^+$ CD8$^+$ T cells was determined by flow cytometry. **B)** 2x10^6 WT or Gal-3$^{-/-}$ OT-I T cells were adoptively transferred into WT mice and then stimulated with soluble OVA (day 0) +/- IL-2c (days 0-2). On day 7, the frequency of Annexin V$^+$ donor OT-I T cells in the LN was determined by flow cytometry. **C)** On day 14, the frequency of Annexin V$^+$ donor OT-I T cells stimulated with soluble OVA (day 0) + aOX40 (days 0-1) in the spleen was determined by flow cytometry. Graphs for *in vitro* experiments represent the mean+/-SD from 2 independent experiments and *in vivo* experiment (n=4/ group) *P<0.05, **P<0.01, ***P<0.001, ****P<0.0001

3.2.5 Erdr1 is upregulated in Gal-3-deficient $CD8^+$ T cells

To further investigate the mechanism of increased apoptosis in Gal-$3^{-/-}$ $CD8^+$ T cells, we evaluated the expression of Erythroid differentiation regulator 1 (Erdr1). Erdr1 is a secreted autocrine factor that induces apoptosis in T cells (256). Overexpression of Erdr1 in $CD4^+$ T cells results in a concomitant downregulation of Gal-3 expression (256), which suggests a possible connection between Gal-3 and Erdr1-induced apoptosis. Thus, we used a flow cytometry based method to determine whether *Erdr1* mRNA expression is altered in Gal-$3^{-/-}$ $CD8^+$ T cells. We used *dapB*, a *Bacillus subtilis* reductase gene, as a negative control, and *ActB*, the beta-actin gene, as a positive control. We found that *Erdr1* expression was significantly higher in *in vitro* stimulated Gal-$3^{-/-}$ $CD8^+$ T cells compared to WT cells (Fig. 16A and B). In addition, we looked at the extent of *Erdr1* mRNA expression in adoptively transferred WT or Gal-$3^{-/-}$ $CD8^+$ T cells treated *in vivo* with or without aOX40 agonist and observed increased *Erdr1* mRNA expression in the Gal-$3^{-/-}$ $CD8^+$ T cells compared to WT cells (Figs. 16C and D). Although agonist aOX40 therapy significantly decreased *Erdr1* expression in WT $CD8^+$ T cells, aOX40 treatment was not sufficient to reduce *Erdr1* expression in Gal-$3^{-/-}$ $CD8^+$ T cells (Figs. 16C and D). The increased expression of *Erdr1* in Gal-$3^{-/-}$ $CD8^+$ T cells supports the increased apoptosis in Gal-$3^{-/-}$ $CD8^+$ cells compared to WT cells *in vitro* and *in vivo* (Figs. 15A and B). It should be noted that these data support a correlation between the increased expression of *Erdr1* and increased apoptosis in Gal-$3^{-/-}$ $CD8^+$ T cells. The extent to which *Erdr1* directly induces increased cell death in Gal-$3^{-/-}$ $CD8^+$ T cells remains unclear and is currently under investigation.

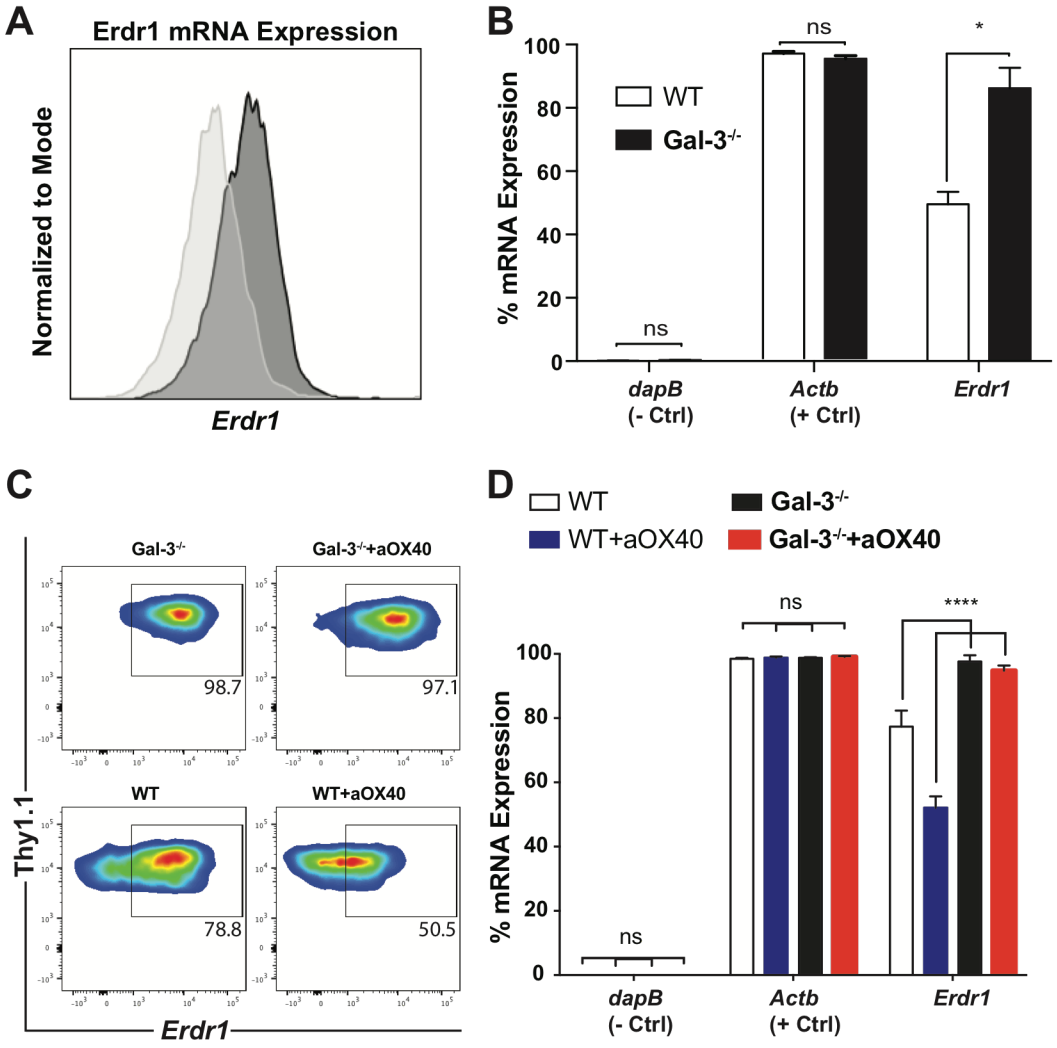

Figure 16. Erdr1 is upregulated in Gal-3-deficient CD8$^+$ T cells. 3x10^5 WT or Gal-3$^{-/-}$ OT-I CD8$^+$ T cells were stimulated with 5x10^4 irradiated SIINFEKL peptide-pulsed APCs (DC2.4 cells). Forty-eight hours later, cells were washed and re-cultured for another 48 hours in media. Cells were then analyzed by PrimeFlow assay. Bacillus subtilis *dapB* (negative control), IFN-γ or *Actb* (positive control), and *Erdr1* mRNA expression was determined. **A)** The histogram represents *Erdr1* expression in WT (2) and Gal-3$^{-/-}$ (red) OT-I T cells. **B)** Bar graphs represent total mRNA expression of *dapB, Actb*, and *Erdr1*. **C)** The flow plots are representatives of in vivo expression of Erdr1 from different experimental groups and controls. **D)** The bar graphs are the summary of *dapB, Actb* and *Erdr1* mRNA expression *in vivo* using PrimeFlow assay. Graphs represent the mean+/-SD from 2 independent *in vitro* experiments. *In vivo* experiments (n=4). *P<0.05, **P<0.01, ***P<0.001, ****P<0.0001

3.3 Discussion

OX40-OX40L signaling induces the expansion and survival of memory $CD8^+$ T cells (72, 119, 245-247) and here we show that intracellular Gal-3 contributes to agonist aOX40-induced $CD8^+$ T cell survival and memory formation. Gal-$3^{-/-}$ $CD8^+$ T cells receiving aOX40 therapy underwent a similar expansion as WT cells 1 week post-stimulation, and we did not observe any differences in proliferation or effector differentiation of the Gal-$3^{-/-}$ $CD8^+$ T cells during this initial response (Fig. 8). However, we did observe significantly reduced survival of Gal-$3^{-/-}$ $CD8^+$ T cells treated with aOX40 by days 14 and 29. as well as significantly reduced survival of aOX40-treated Gal-$3^{-/-}$ $CD8^+$ T cells following *Lm-ActA*-OVA infection (Fig. 12B), suggesting a crucial role for Gal-3 in regulating OX40-induced $CD8^+$ T cell survival. In addition, a significantly higher percentage of Gal-$3^{-/-}$ $CD8^+$ T cells remained in an effector or effector memory phenotype by day 14 post-aOX40 therapy, indicating a key role for intracellular Gal-3 in facilitating the development of central memory $CD8^+$ T cells (Fig. 8E). Although only a fraction of Gal-$3^{-/-}$ $CD8^+$ T cells survive by day 29 (Fig. 8B), the remaining cells did not exhibit any defects in the production of effector cytokines including IFN-γ and TNF-α (Fig. 8F), indicating that these cells had no defect in the acquisition of effector function.

Different groups have shown a critical role for OX40 in mediating memory $CD8^+$ T cell formation following infections with *Lm*-OVA or vaccinia virus (245, 252). Engagement of the OX40 signaling pathway leads to expression of anti-apoptotic proteins that help the T cells survive long-term and transition into memory cells (124, 257-259). OX40 is also known to maintain Protein kinase B (PKB, also known as Akt)

activity, which has an essential role in regulating T cell longevity (259). Interestingly, Gal-3 has been shown to upregulate Akt phosphorylation (260). Similarly, we show that OX40 ligation sustains Gal-3 mRNA expression over time (Fig. 6B) and in the absence of Gal-3, OX40 signaling does not induce the long-term survival of $CD8^+$ T cells. In light of these studies, one explanation for our observation of defective survival in OX40-stimulated Gal-$3^{-/-}$ $CD8^+$ T cells is perhaps the critical role of Gal-3 in regulating Akt phosorylation following OX40 ligation, which mediates the formation of memory $CD8^+$ T cells and supports their long-term survival. Whether there is such a defect in the phosphorylation of Akt or other related family members in Gal-$3^{-/-}$ $CD8^+$ T cells after aOX40 therapy is currently under investigation.

Agonist aOX40 stimulation of $CD8^+$ T cells *in vivo* induces IL-2Rα expression and IL-2 production (63, 117, 118). In turn, IL-2/IL-2R signaling creates a positive feedback loop that sustains IL-2 secretion and IL-2R expression. Thus, the mechanisms driving OX40-mediated survival would likely include those elicited via IL-2/Gal-3 signaling as OX40 stimulation induces IL-2/IL-2R-dependent signaling in $CD8^+$ T cells. Therefore, to identify whether the phenotype we observed in Gal-$3^{-/-}$ $CD8^+$ T following aOX40 therapy is independent of IL-2, we tested whether Gal-$3^{-/-}$ $CD8^+$ T cells exhibited any defects following IL-2 stimulation. Similar to the results obtained with aOX40 therapy, Gal-$3^{-/-}$ $CD8^+$ T cells stimulated with antigen in the presence of IL-2c did not exhibit any defect in their initial expansion or differentiation (day 7) as compared to WT cells (Fig. 14A). However, we observed a significant decrease in the survival of Gal-$3^{-/-}$ $CD8^+$ T cells treated with IL-2c later in response (days 14-29) (Fig. 14A).

In contrast to aOX40 therapy, there was no difference in the frequency of T_E/T_{EM} and T_{CM} cells following IL-2c treatment. One explanation for the difference in the T_E/T_{EM} and T_{CM} cell subsets between the aOX40 and IL-2c-treated models may be differences in the inflammatory mileu between these models and the differing roles of aOX40 and IL-2 in regulating the long-term survival and differention of $CD8^+$ T cells *in vivo*. Different studies have shown that IL-2/IL-2R signaling is important for initial T cell activation and short-term survival, but it is not responsible for *in vivo* generation and maintenance of memory $CD8^+$ T cell (259, 261). Therefore, it is not surprising that we do not see differences in the frequencies of T_E/T_{EM}, and T_{CM} cells following IL-2c treatment. Further analysis revealed no defect in IFN-γ or TNF-α production by the Gal-$3^{-/-}$ $CD8^+$ T cells and that Gal-3 regulated $CD8^+$ T cell survival through a cell-intrinsic mechanism (Figs. 11B and 14D). Thus, while Gal-3 was necessary to support T cell survival following IL-2-stimulation, it did not affect their effector function or proportion of each memory subset.

Gal-3 shares significant structural properties with the anti-apoptotic protein, Bcl-2. Specifically, Gal-3 has a NWGR motif, which is a highly conserved amino acid sequence in the BH1 domain of the BCL-2 gene and is responsible for the anti-apoptotic activity of Bcl-2 proteins (201). Intracellular Gal-3 inhibits induced Fas-dependent apoptosis in Jurkat T cells (201). In addition, Gal-3 can suppress apoptosis through the induction of the phosphatidylinositol 3-kinase (PI3K)/Akt pathway, which inhibits caspase-9 and caspase-3 activation (197). Indeed, Gal-$3^{-/-}$ $CD8^+$ T cells were significantly more apoptotic *in vitro* and *in vivo* (Fig. 15A and 15B). The increased apoptosis of Gal-$3^{-/-}$ $CD8^+$ T cells was also associated with their failure to generate central memory cells

(Fig. 11C). We were able to determine the extent of Annexin V expression among the $T_{E,}$ T_{EM} and T_{CM} T cells subsets and observed significantly higher apoptosis in the effector subsets of Gal-$3^{-/-}$ $CD8^{+}$ T cells treated with aOX40 compared to the effector subset (day 14). Thus, Gal-$3^{-/-}$ $CD8^{+}$ T cells experience increased cell death due to skewing towards a short-lived effector cell phenotype. However, whether reduced long-term survival of Gal-$3^{-/-}$ $CD8^{+}$ T cells is due to increased cell death of the effector cell phenotype or if they are simply unable to develop into central memory cells following aOX40 therapy is unclear. Single cell gene expression profiling assays may be useful in elucidating the underlying mechanisms regulating the deficiencies in the generation of memory Gal-$3^{-/-}$ $CD8^{+}$ T cells.

Contrary to intracellular Gal-3's ability to inhibit Fas-dependent apoptosis, ERDR1 has been shown to induce T cell apoptosis via a Fas-dependent pathway (256). The common interaction of Gal-3 and Erdr1 with Fas-dependent apoptosis and the reciprocal expression of Gal-3 and Erdr1 mRNA in T cells suggests that there is also a regulatory connection between Gal-3 and Erdr1. We observed a significant increase in Erdr1 mRNA expression in Gal-$3^{-/-}$ $CD8^{+}$ T cells, suggesting that higher levels of Erdr1 in Gal-$3^{-/-}$ $CD8^{+}$ T cells triggers apoptosis. However, we were unable to detect any difference in Fas expression between WT and Gal-$3^{-/-}$ $CD8^{+}$ T cells (data not shown). Thus, it remains to be determined whether a Erdr1-Fas-related pathway is the primary mechanism of increased cell death in Gal-$3^{-/-}$ $CD8^{+}$ T cells.

The interaction of OX40 with OX40L results in activation of canonical and non-canonical NF-kB pathways that are key for survival (124, 125, 262). Furthermore, multiple studies have shown that NF-kB regulates Gal-3 expression *in vitro* (197, 263),

suggesting an important role for Gal-3 in regulating cell survival (221). Interestingly, inactivity of NF-kB in OX40-deficient T cells leads to poor expansion and survival (262), which closely emulates the Gal-$3^{-/-}$ $CD8^+$ T cell phenotype of reduced long-term survival. Future experiments are warranted to evaluate the activity of NF-kB in Gal-$3^{-/-}$ $CD8^+$ T cells and if constitutive activation of NF-kB in Gal-$3^{-/-}$ $CD8^+$ T cells would rescue the phenotype.

In light of our findings, we propose a mechanism that illuminates the role of Gal-3 in regulating agonist aOX40 and IL-2c-induced $CD8^+$ T cell survival *in vivo* (Fig. 17). Agonist aOX40 and/or IL-2c co-stimulation induces Gal-3 expression in $CD8^+$ T cells and Gal-3 and Erdr1 mRNA expression are inversely correlated. Therefore, in WT $CD8^+$ T cells, aOX40 or IL-2c-mediated co-stimulation induces Gal-3, which subsequently down-regulates Erdr1 expression to decrease apoptosis, potentially through a Fas-dependent pathway. However, in the absence of Gal-3, OX40 and/or IL-2c co-stimulation upregulates Erdr1 expression thereby increasing apoptosis of Gal-$3^{-/-}$ $CD8^+$ T cells. This study highlights the vital function of intracellular Gal-3 in regulating the long-term survival of $CD8^+$ T cells following aOX40 or IL-2 therapy and suggests that modulation of intracellular Gal-3 may enhance the development and/or persistence of Ag-specific $CD8^+$ T cells.

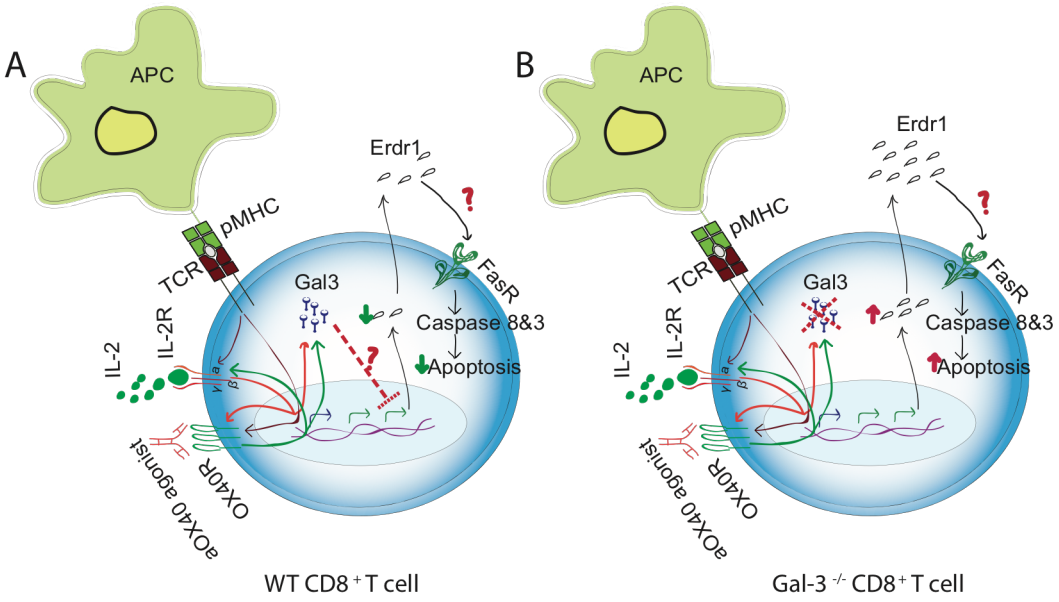

Figure 17. Potential mechanism of Gal-3-mediated regulation of aOX40 agonist and IL-2c-induced CD8$^+$ T cell survival *in vivo*. A) Anti-OX40 and/or IL-2c co-stimulation induces Gal-3 expression in CD8$^+$ T cells, which is inversely correlated with Erdr1 mRNA expression, thus decreasing apoptosis. **B)** In the absence of Gal-3, aOX40 and/or IL-2c co-stimulation upregulates Erdr1 expression, leading to increased apoptosis.

3.4 Materials and Methods

3.4.1 Mice

Wild-type C57BL/6 and OT-I transgenic (264) mice were purchased from Jackson Labs (Bar Harbor, ME). Gal-$3^{-/-}$ C57BL/6 mice were kindly provided by Dr. Fu-Tong Liu (UC Davis, Davis, CA). OT-I Thy$1.1^{+/+}$ mice were crossed to Gal-$3^{-/-}$ mice to generate Gal-$3^{-/-}$ OT-I Thy$1.1^{+/+}$ mice. OT-I Thy$1.1^{+/+}$, OT-I Thy$1.1^{+/-}$ and Gal-$3^{-/-}$ OT-I Thy$1.1^{+/+}$ mice were bred in our facility. All mice were maintained under specific pathogen-free conditions in the Providence Cancer Institute animal facility. Experimental procedures were performed according to the National Institutes of Health Guide for the Care and Use of Laboratory Animals.

3.4.2 Lymphocyte isolation and analysis

Lymph nodes and spleens were harvested and processed to obtain single cell suspensions. ACK lysing buffer (Lonza, Walkersville, MD) was added for 5 min at room temperature (RT) to lyse red blood cells. Cells were then rinsed with complete media (RPMI 1640 medium containing 10% FBS supplemented with 1 M HEPES, 1% non-essential amino acids, 1% sodium pyruvate (all from Lonza), 1% pen-strep glutamine (ThermoFisher, Carlsbad, CA), and 0.5% 2-Mercaptoethanol (Sigma, St. Louis, MO). Murine peripheral blood lymphocytes were collected via the submandibular vein into tubes containing 20 µl heparin (Hospira, Lake Forest, IL), 1 ml of flow cytometry wash buffer (0.5% FBS, 0.5 mM EDTA, and 0.02% NaN_3 in PBS) was added, cells were mixed, and then 700 µl of Ficoll-Paque (GE Healthcare, Piscataway, NJ) was added prior

to centrifugation. After centrifugation, lymphocytes were collected from the interface and then washed with flow cytometry buffer prior to staining.

3.4.3 Adoptive transfer and activation of OT-I T cells in vivo

Single cell suspensions were prepared from the spleens of OT-I Thy1.1$^{+/+}$, OT-I Thy1.1$^{+/-}$, and Gal-3$^{-/-}$ OT-I Thy1.1$^{+/+}$ TCR Tg mice. Mice were treated with 200 μg (ip) anti-CD4 (clone GK1.5; Bio-x-Cell, West Lebanon, NH) and then naïve OT-I T cells were purified (isolated from spleen; ~98% purity) by negative selection using the Dynal mouse CD8^{+} T cell isolation kit (ThermoFisher) and 2 × 10^{6} were injected (iv) in 200 μl of PBS into recipient mice. Recipient mice received 500 μg of soluble ovalbumin (Sigma), and 50 μg anti-OX40 (aOX40; clone OX86; Bio-x-Cell) or control rat IgG Ab (Sigma) (sq). Mice received an additional dose (50 μg) of aOX40 or control Ab one day later.

3.4.4 T cell activation *in vitro*

Single cell suspensions were prepared from the spleens of OT-I Thy1.1$^{+/+}$ and Gal-3$^{-/-}$ OT-I Thy1.1$^{+/+}$ mice and CD8^{+} T cells were purified using the Dynal mouse CD8^{+} T cell negative isolation kit (Invitrogen). 1 × 10^{6} (or 5 × 10^{5}) cells/well were seeded in 24 or 96-well plates, respectively, and then stimulated with OVA peptide (SIINFEKL)-pulsed irradiated (3,000 rads) DC2.4 cells (5 × 10^{3} cells/well in 96-well plates). Twenty-four hours later activated OT-I T cells were harvested and live cells were enriched over a Ficoll-paque gradient prior to re-seeding in 10% cRPMI (5 × 10^{5} cells/ml) +/- 100 μl hrIL-2 for 24 - 72 hours.

3.4.5 Flow cytometry

Cells were stained for 30 min at 4°C with: Thy1.1 PE, Thy1.1 eFluor 450, Viability Dye eFluor 780, Thy1.2 APC, Thy1.2 eFluor 450, IFN-γ APC, (eBioscience), OX40 PE, CD4 Brilliant Violet 605, CD8 Brilliant Violet 785, KLRG-1 PE-Dazzle, CD25 eFluor 488, CD25 Alexa Fluor 700, Thy1.2 PE, TNF-α PE-Cy7, Lag-3 Alexa Fluor 700, CD62L Alexa Fluor 700 (BioLegend), Ki-67 FITC (BD Biosciences), PD-1 PE-Cy7 (Invitrogen), and/or Tim-3 PE (R&D systems). For intracellular staining, cells were fixed and permeabilized with the FoxP3 Staining Buffer Set (eBioscience) according to the manufacturer's instructions. Cells were analyzed with an LSR II flow cytometer using FACSDiva software (BD Biosciences) and analyzed by FlowJo software (v10.4).

3.4.6 Intracellular mRNA detection

Erdr1 mRNA expression was measured with the PrimeFlow RNA Assay (ThermoFisher), using ViewRNA probes following the manufacturer's instructions. Positive and negative controls (Actb and dapB) were included in each assay.

3.4.7 mRNA Analysis

Naïve OT-I T cells were adoptively transferred into wild-type mice and then activated with soluble OVA and anti-OX40 or rat IgG Ab. Four days later, lymph nodes were harvested and donor OT-I T cells purified by magnetic bead separation using an AutoMACS (Miltenyi Biotec). Total RNA from the donor OT-I T cells was harvested

using RNeasy (Qiagen, Valencia, CA), according to the manufacturer's instructions. Prior to submission to the Oregon Health & Science University Gene Microarray Shared Resource core facility (Portland, Oregon), the purity and quantity of the RNA was assessed by NanoDrop ND-1000 (Thermo Scientific, Wilmington, DE). The quality and quantity of RNA samples was further analyzed on the Bioanalyzer platform (Agilent, Santa Clara, CA). Labeled target cDNA was prepared from total RNA samples using the Ambion Message Amp Premier protocol (3'IVT assay). Each sample target was hybridized to a Mouse 430 2.0 Gene Chip array (Affymetrix, Santa Clara, CA). Image processing and expression analysis were performed using Affymetrix Gene Chip Command Console (AGCC) v. 3.1.1 and Affymetrix Expression Console v.1.1 software, respectively. Data from all biological replicates and conditions was imported into the Affymetrix Expression Console and normalized (RMA), annotated and exported to CSV files, which were then processed in Excel. Raw expression data is represented on a log2 scale.

3.4.8 Reagents

Recombinant murine IL-2 was purchased from eBioscience and anti-mIL-2 mAb (clone S4B6) was obtained from Bio-X-Cell. IL-2/anti-IL-2 mAb complexes (IL-2c) were generated by mixing 2 μg IL-2 with 8 μg anti-IL-2 mAb for 20 min at 37°C and then mice received injections of IL-2c in 200 μl PBS (ip or sq) for 3 days.

3.4.9 Statistical analysis

Statistical significance was determined by unpaired Student's t-test (for comparison between 2 groups) or one-way ANOVA (for comparison among >2 groups) using Prism software (GraphPad, San Diego, CA); a P value of <0.05 was considered significant.

Chapter 4: Immunohistochemistry in immunotherapy

1 Introduction

Recently, immunotherapy has taken the center stage in the search to find better therapies for cancer. Immunotherapy is the treatment of disease by activating or suppressing the patient's own immune system. An immune system that recognizes neoplastic cells can eradicate those cells by different processes that involve the innate and/or adaptive arms of the immune system. When successful, immunotherapy restores the patient's antitumor immune response, leading to long-term remission and even cures in a subset of patients. In contrast, traditional cancer therapies including surgery, chemotherapy, radiotherapy, and endocrine therapy often induce initial responses in patients with metastatic disease, but the disease typically recurs and most patients will die from their cancer (265, 266). Despite the advancement and great success of cancer immunotherapy, especially immune checkpoint blockade, more than half of cancer patients do not respond to immunotherapy (163). In order to administer the appropriate immunotherapy to achieve optimal anti-tumor responses and potentially predict treatment outcome of (responder vs. non-responder), profiling the cancer patient's immune system status needs to be incorporated into the current strategies to classify cancer. Currently, malignant tumors are classified by the TNM system: tumor burden (T), the presence of cancer cells in draining and regional lymph nodes (N), and evidence for distant metastases (M) (267). The TNM system is solely based on the tumor cells and does not take into account the potential contribution of the immune system. However, a closer look at histopathology analysis has revealed the presence of immune cells in the center of the tumor (CT), the invasive margin (IM), and tertiary lymphoid structures adjacent to the tumor to a various degree (268, 269). Identifying the status of the immune system and

predictive markers in the TME in patients are likely the keys for effective immunotherapies. Numerous studies have reported the importance of immune biomarkers in order to classify tumors such that we can better predict prognosis and response to therapy. Thus, an international consortium initiated a tremendous effort to incorporate immune scoring to a TNM-classification system in routine diagnostic and prognostic classification of tumors, to be named TNM-I (TNM-Immune) (270).

Traditionally, the haematoxylin and eosin (H&E) staining method is used to determine TNM classification and can be also used to determine basic immune cell infiltration based on their morphology. The H&E dye combination can highlight the significant features of cells and tissues under low microscopic magnifications and has been used for more than a century as the gold standard of histology. Haematoxylin stains basophilic structures in the cell (nucleus, rough endoplasmic reticulum, and ribosomes) and eosin stains eosinophilic cellular organelles and extracellular matrix. The difference in the spectrum, intensity, and texture of colors of nuclei, cytoplasm, and granules observed in H&E stained cells can determine different basic cell types that have distinct morphological attributes (271). However, evaluating and distinguishing different subsets of immune cells is not possible using the H&E staining method. In order to distinguish and evaluate immune cells with specific markers, researchers use antibodies against specific immune markers in a process called immunohistochemistry (IHC) (272, 273). IHC is widely used to understand the distribution and localization of biomarkers and differentially expressed proteins in different parts of a tissue and cells. Chromogenic IHC, a commonly used IHC technique, utilizes enzyme-catalyzed deposition of chromogens at the site of the antigen (Table 2). Single staining standard chromogenic

IHC with specific high-affinity antibodies provides a high signal:noise ratio and enables detection of immune cells subsets based upon various markers (272). Chromogenic IHC is used for predicting prognosis of cancer patients based on immune cells present in the TME (immunoscore), as well as for immunophenotyping the TME and assessing the anti-tumor response pre- and post-therapy. Although chromogenic IHC allows for up to double marker staining (274), immunophenotyping the TME requires a larger panel of relevant markers. Immunophenotyping using standard IHC entails doing single staining on serial section of tissues, which is typically a huge limitation due to tissue availability. To extract colocalization information of different markers, single marker stained serial sections need to be reconstructed. This can be laborious and technically challenging.

Researchers have overcome the standard IHC limitations by developing multiplex IHC (mIHC), which allows for staining of multiple markers on the same section. Thus, mIHC makes it possible to assess the spatial relationships between these different cell types within the heterogeneous TME. Thus, mIHC provides important prognostic and predictive information. For example, a recent meta-analysis study of 10 different tumor types in 8135 patients showed that mIHC had significantly higher diagnostic accuracy than PD-L1 IHC, tumor mutational burden, or gene expression profiling in prediction clinical response to anti-PD-1/PD-L1 therapy (275). mIHC can also provide colocalization and spatial orientation of target biomarkers, which allows for accurate analysis of the target biomarker's subcellular location and relative proximity to other biomarkers (276). In a quantitative spatial profiling of PD-1/PD-L1 interaction and HLA-DR/IDO-1 in predicting anti-PD-1 therapy outcome in metastatic melanoma study showed that PD-1/PD-L1 interaction score and/or IDO-1/HLA-DR coexpression was

strongly associated with anti-PD-1 response, whereas, individual biomarkesrs (PD-1, PD-L1, IDO-1, HLA-DR) were not associated with response or survival (277). Due to these benefits, mIHC enables improved analysis and immunophenoyping, and thus, furthered our understanding of the TME. Several different types of mIHC have been developed in the recent years including brightfield and fluorescent multiplexing, which are the two main methods of mIHC. Here, I will briefly cover the brightfield multiplexing method and will explore the fluorescent multiplexing method of mIHC in depth.

Table 2: Selected chromogen products for brightfield mIHC

Chromogen	Catalytic agent	Deposition color	Stability
3,3′-diaminiobenzidine (DAB)	Horseradish peroxidase (HRP)	Brown	Insoluble
Nickel enhanced DAB (DAB-Ni)	HRP	Black	Insoluble
3-amino-9-ethylcarbazole (AEC)	HRP	Red	Susceptible to organic solvents
Vector VIP	HRP	Purple	Insoluble
Nitro blue tetrazolium/5-bromo-4-chloro-3-indolyl-phosphate (NBT/BCIP)	Alkaline phosphatase (AP)	Deep blue	Soluble in water
Vulcan Fast Red	AP	Red	Insoluble
Vector Black	AP	Black	Insoluble
Nova Red	HRP	Deep red	Insoluble
3,3'5,5'-tetramethylbenzidine (TMB)	HRP	Blue	Insoluble

1.1 Multiplex IHC

1.1.1 Brightfield multiplex IHC

The brightfield mIHC on formalin-fixed paraffin-embedded (FFPE) tissues uses chromogenic deposition of several different chromogens and enzyme pairs as well as a counterstaining dye that enhances brightfield mIHC (Table 2) (278). The brightfield chromogenic mIHC method uses both direct and indirect detection strategies. In the direct detection strategy, antigens are detected by primary antibodies from the same or different species that are directly labeled with different chromogens (Table 2) (276), whereas, in the indirect detection strategy, antigens are detected with two or more layers of antibodies, generally a primary antibody against the antigen of interest, and a secondary antibody against the Fc region of the primary antibody. In some cases, with indirect detection, the secondary antibody can be conjugated to different chromogens. In other cases, the Avidin–Biotin Complex (ABC) and the Labeled Streptavidin–Biotin (LSAB) staining methods are used for detection. The main advantage of indirect staining over direct staining is the amplification of signals (276), however, indirect staining increases the possibility of non-specific staining, where the secondary antibody binds to the tissue in the absence of the primary antibody.

Some of the disadvantages of the direct detection method include: low sensitivity for low abundance targets, high concentration of conjugated primary antibodies is required, and the risk of alteration of antibody activity by direct labeling process. To solve the cross-reactivity between primary antibodies, antibodies are inactivated through manual microwave heating, which could increase the risk of tissue damage or complete loss of tissue and producing heterogeneous results (279). To circumvent the limited

number of available antibodies from different hosts, the multiplexed immunohistochemical consecutive staining on single slide (MICSSS) approach was developed for FFPE samples by repetitive staining cycle of immunoperoxidase labeling, image scanning, then chemical stripping of the chromogenic substrates (280).

1.1.2 Fluorescent multiplex IHC

In fluorescent mIHC, the secondary antibody is conjugated to a fluorophore rather than to a chromogen. Fluorescent mIHC depends on the individual fluorophores' excitation by one wavelength and emission at a longer, unique wavelength. Fluorescent mIHC is primarily done using the indirect labeling method, typically the fluorophore is conjugated to the secondary antibody. As with chromogenic staining, indirect labeling allows amplification of the fluorophore signal through either multiple secondary antibodies binding to a single primary antibody or through robust amplification approaches (278). While fluorescence 2-plex mIHC in FFPE tissues and quantum dot (nanocrystals with narrower emission peaks compared to fluorophores) 4-plex mIHC are relatively common (281, 282), there are still fundamental challenges in successfully performing mIHC. There are several fluorophores available for mIHC (Table 3), however their use in mIHC requires certain microscopes that are capable of proper visualization such as a bright light source, paired excitation, and an emission filter that is set specific to the fluorophores used. In addition, fluorescent mIHC faces the challenge of co-localization of different fluorophores, which causes colors to mix and requires analysis software to un-mix the colors.

Table 3: TSA Fluorophore Excitation and Emission

Fluorophore	Excitation Wavelength [nm]	Emission Wavelength [nm]
DAPI	358	461
Opal 520	494	525
Opal 540	523	536
Opal 570	550	570
Opal 620	588	616
Opal 650	627	650
Coumarin	402	443
FITC	494	517
Cyanine 3	550	570
Cyanine 3.5	581	596
Cyanine 5	648	667
Cyanine 5.5	673	692

1.1.3 Challenges of multiplex IHC

Brightfield and fluorescent mIHC both face significant challenges. In brightfield mIHC, chromogenic/enzyme pairs are sufficient to distinguish different cell types, however, they are insufficient for assessing cells' subtypes or different targets within cells by localization (274). Another limitation of brightfield chromogenic mIHC is the lack of availability of antibodies that are raised in many different host species. If different antibodies raised in the same species are used against different antigens on the same tissue section, then it requires removal/inactivation of antibodies between each labeling cycle to avoid cross-reactivity between primary antibodies, which cannot be done in brightfield chromogenic mIHC (283). The issue of a limited number of available antibodies from different hosts for in brightfield mIHC was resolved with MICSSS approach (280). However, MICSSS is labor-intensive, prone to tissue degradation, and requires prolonged time for yielding results, which is not suitable for a routine clinical setting (278, 284).

The origin of antibody species is also an issue in indirect labeling in fluorescent mIHC. Indirect labeling only allows one species of primary for each target of interest and is recognized by a specific secondary antibody conjugated with a specific fluorophore, which limits the multiplexing to a limited number of targets (278). This is a significant issue for protocols using more than one antibody from the same species. In addition to the limited availability of fluorophores that do not completely overlap, the fluorophores that are far enough from each other (spectrally) requires deconvolution of the multispectral images (MSI).

High noise to signal ratio (background) due to cross reactivity or nonspecific binding of antibodies is another challenge in mIHC. However, high background could be resolved by using antibodies with high specificity and affinity for its target, proper titration of the primary antibody, and/or sufficiently blocking to prevent nonspecific binding.

1.1.4 Tyramide signal amplification system

A relatively recent detection strategy, tyramide signal amplification (TSA), can circumvent the main challenges in fluorescent mIHC mentioned above (285). I will explore the TSA system, the methodology of using the TSA system to develop a 7-plex mIHC in human FFPE and zinc-fixed paraffin-embedded mouse tissues, image analysis, and mIHC advantages and limitations. The TSA system depends on tyramide, an organic phenol, bound to a fluorophore. When tyramide is in the presence of a catalyst, such as horseradish peroxidase (HRP), it becomes activated and covalently binds electron-rich regions, such as tyrosine residues, present in proteins. In the TSA system, HRP conjugated to a secondary antibody catalyzes the deposition of tyramide-fluorophore molecules at the site of the antigen (285, 286). Because the deposited tyramide conjugated to a fluorophore is inactive and bound covalently to tyrosine residues, this allows for removal of the primary/secondary antibody complex, which leaves the fluorescence signal associated with the target protein (286) and makes it possible to use antibodies from the same species in serial staining in mIHC. This alleviates one of the most challenging technical aspects of mIHC. The removal of primary/secondary complex also minimizes potential cross-reactivity between antibodies. In addition, using a polymer

of HRP-conjugated secondary antibody generates high density for tyramide labeling and it is the reason for the exceptionally enhanced sensitivity of the TSA system. Moreover, the TSA system enhances the signal to noise ratio by reducing background (287). Several available fluorophores conjugated to tyramide in the TSA system (Table 3) can be spectrally resolved in a composite multiplex image with dedicated software analysis programs. The TSA system has been successfully utilized in performing 3-plex fluorescent mIHC (286, 288).

While considerable effort has been dedicated to developing mIHC protocols for immunophenotyping in human tissue (289, 290), by 2017 relatively little progress had been made to develop mIHC protocols for FFPE murine tissues. This lagging development of mIHC in murine tissues was due, in part, to a more limited availability of antibodies against murine antigens. In addition, the issue of fixation-sensitive epitope detection in FFPE tissue had been resolved in human tissue (291-294); however, this issue persisted in FFPE murine tissues. In our study, we validated the use of TSA-based mIHC in murine tissue for sensitive epitopes (295), by optimizing the mIHC protocol for murine tissue. We compared multiple fixation and antigen retrieval methods, in order to optimize the use of TSA-based mIHC for detecting sensitive epitopes, such as CD4, CD8a, and CD19 in murine tissue.

There are many different protocols and fixatives to denature and cross-link tissue sections (296). Among the fixatives, 10% neutral buffered formalin (10% NBF) has been predominantly the fixative of choice. Although 10% NBF fixation and heat-mediated antigen retrieval had been used successfully for epitopes such as CD3, many formalin fixation-sensitive epitopes such as CD4 and CD8a are difficult to detect on murine

tissues. The detection of formalin-sensitive epitopes has mainly relied on frozen tissue, with the cost of intact tissue morphology. Periodate-lysine-paraformaldehyde (PLP) is a lysine residue cross-linking fixative that has been shown to be suitable for detecting many epitopes (297, 298). Zinc-based fixation has been also used as an alternative to formalin fixation to resolve epitope masking in human tissue (294, 299). To detect sensitive epitopes of CD4 and CD8a while maintaining the morphology of murine tissue, we examined PLP and zinc-based fixation methods compared to 10% NBF. We were able to detect only CD3 in murine spleen fixed with 10% NBF, but not CD4 or CD8a (Fig. 18). In PLP fixed murine spleen, we detected CD3 and CD4 with a weak intensity but not CD8a (Fig. 18). Interestingly, in murine spleen fixed with zinc-based fixation, we detected CD3, CD4, and CD8a epitopes with a good intensity (Fig. 18). The staining of CD4 and $CD8^+$ T cells were validated in CD4 and CD8 transgenic mouse spleen tissue (295). In addition, there was no noticeable difference in the integrity of tissue fixed with 10% NBF and zinc-based fixation (295).

To optimize TSA-based mIHC in murine tissue, the TSA-based mIHC protocol previously developed for human tissue was used as the starting protocol (300). The TSA-based mIHC protocol for human tissue sections includes: 1. antigen retrieval, 2. stain with a primary antibody against the antigen of interest, 3. stain with secondary antibody conjugated with HRP-polymers, and 4. stain with TSA conjugated to a fluorophore (Diagram 1). These steps were followed by heat-mediated antigen stripping to remove the primary and secondary antibodies, and then a new staining cycle was started. Heat-mediated antigen retrieval and the removal of primary and secondary antibodies between each staining cycle has been successful in human FFPE tissue. However, in mouse tissue

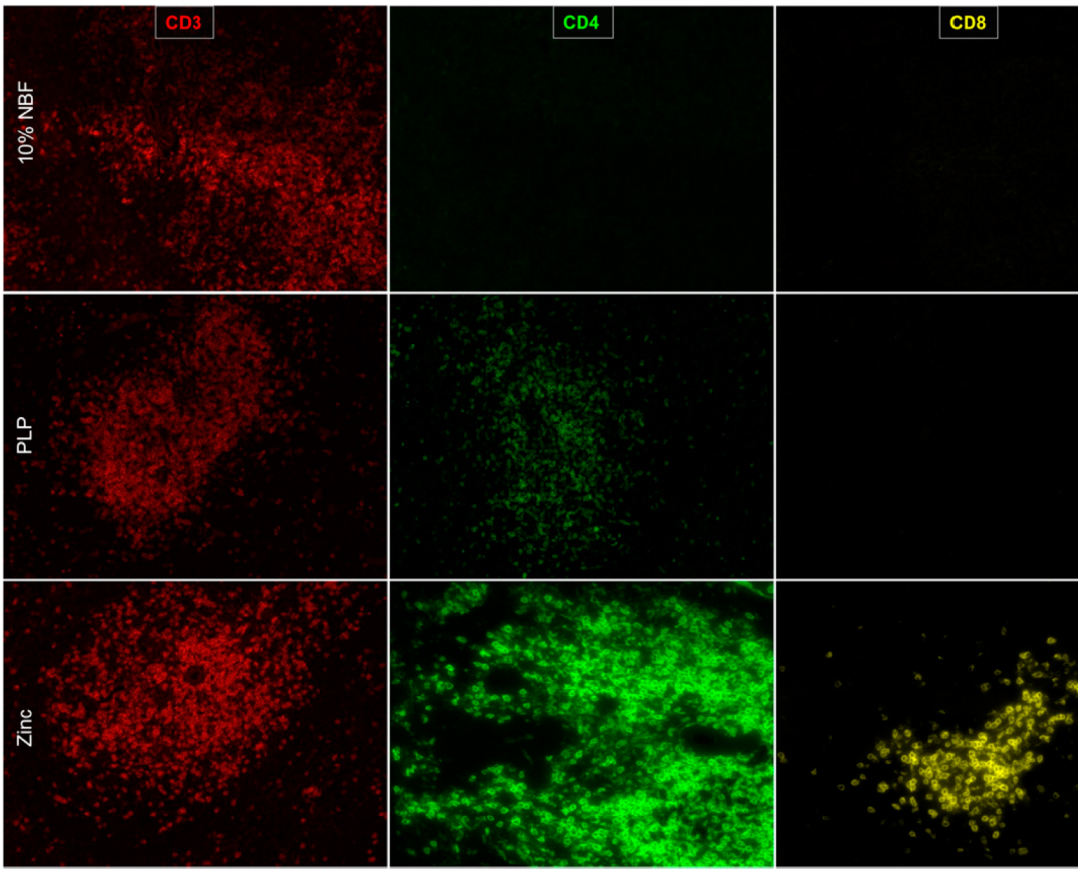

Figure 18. (Reprinted from Feng Z, et. al. *JI*, 2016) Zinc-based buffer is superior in detection of CD4 and CD8a. Spleen sections were fixed for 24 h in each condition and 4-mm sections were cut and prepared. Ag retrieval was performed on formalin-fixed tissues but not on PLP or zinc-fixed tissues. Tissue sections were imaged at 20X with a PerkinElmer Vectra platform.

heat-mediated antigen retrieval and antibody removal reduced CD3 staining and resulted in non-T cell CD8a staining, because after heat-mediated antigen retrieval, CD3 staining did not colocalize with CD8a staining. Similarly, after heat-mediated antibody stripping CD4 and CD19 also had incomplete detection (Fig. 19). Thus, to be able to use the TSA system in murine zinc-fixed tissue, we examined acidic (pH 2) and basic (pH 10) antibody stripping buffers to remove primary and secondary antibodies in order to resolve the heat-mediated antigen stripping issue. Using pH 10 antibody stripping buffer for antigen retrieval and removing primary and

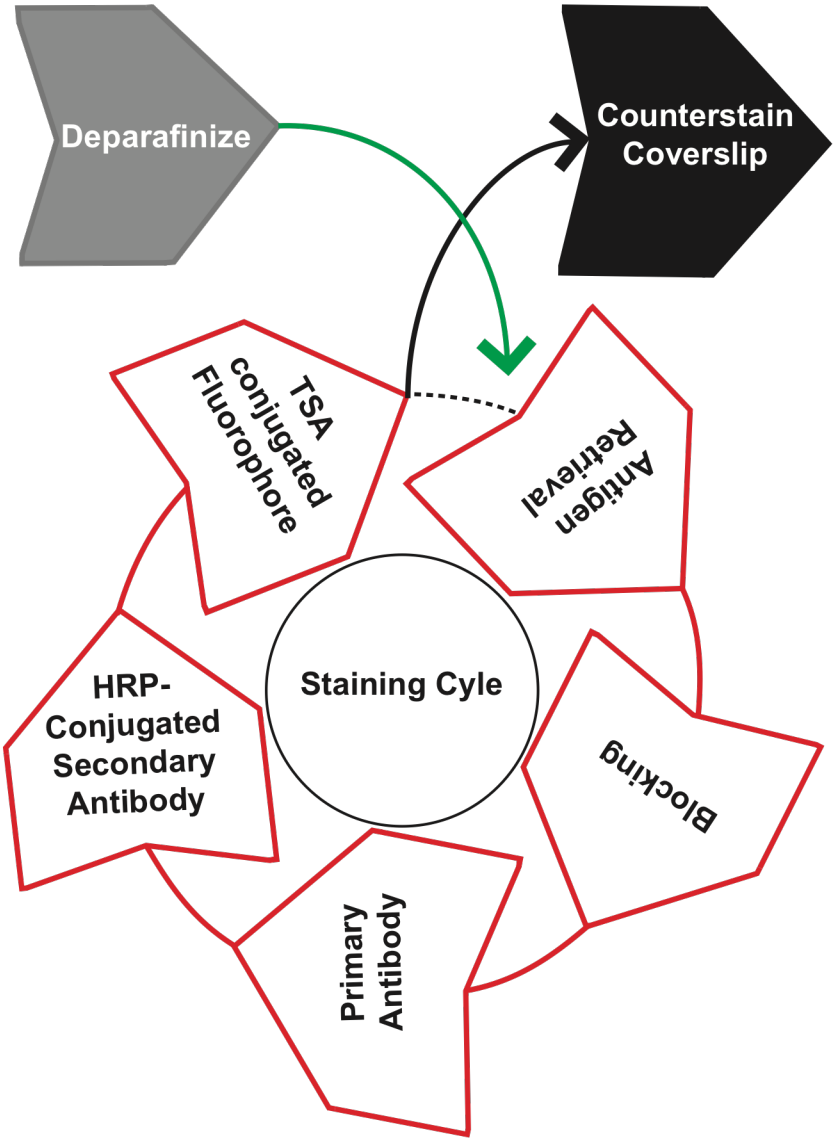

Diagram 1. TSA-based mIHC staining steps.

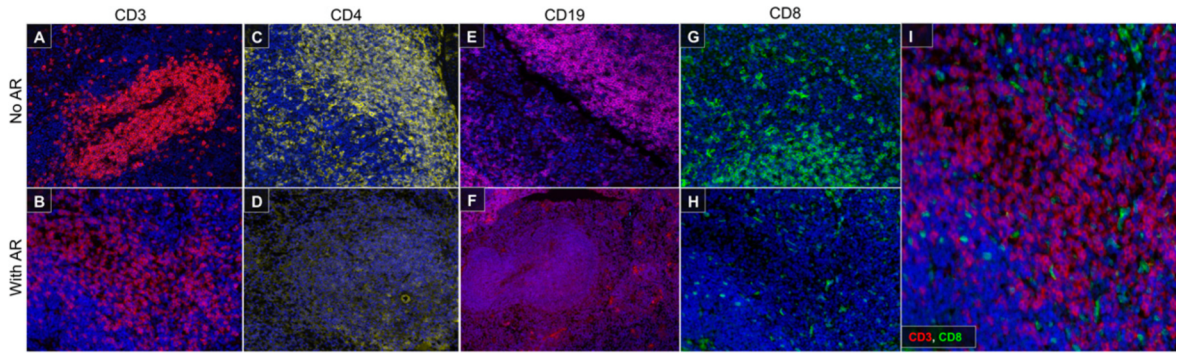

FIGURE 19. (Reprinted from Feng Z, et. al. *JI*, 2016) Heat-mediated Ag retrieval diminishes CD4, CD19, and CD8 staining. Heat-mediated Ag retrieval with Biogenex Citra buffer was performed using a microwave. Slides were microwaved for 25 s to bring to a boil on high power and maintained for 10 min on 10% power. Ab staining were performed with **(B, D, F, and H)** or without **(A, C, E, and G)** Ag retrieval. **(I)** Merge of CD3 and CD8 after Ag retrieval. Original magnification 200X.

secondary antibodies between each cycle of staining allowed for a superior detection and multiplexing CD4, CD8, and CD19 compared to pH 2 stripping buffer (Fig. 20). Thus, by optimizing the basic stripping buffer for antigen retrieval and antibody removal, we were able to perform subsequent staining cycles with the TSA-based mIHC in zinc-fixed murine tissues.

The TSA-based mIHC protocol for murine zinc-fixed tissues has been applied in order to develop several antibody panels for different tumor models. For example, we stained for CD3, CD4, CD8, FoxP3, and F4/80 using our TSA-based mIHC protocol in MCA310 (a sarcoma tumor model), and we stained for PD-L1, CD4, CD8, FoxP3, and DAPI in a SCCVII (squamous cell carcinoma) tumor model (295). In another study, to evaluate the TME of a mammary carcinoma model, TUBO, after combinatorial immunotherapy that included aOX40/aCTLA-4 and vaccination with anti-HER2/DEC-

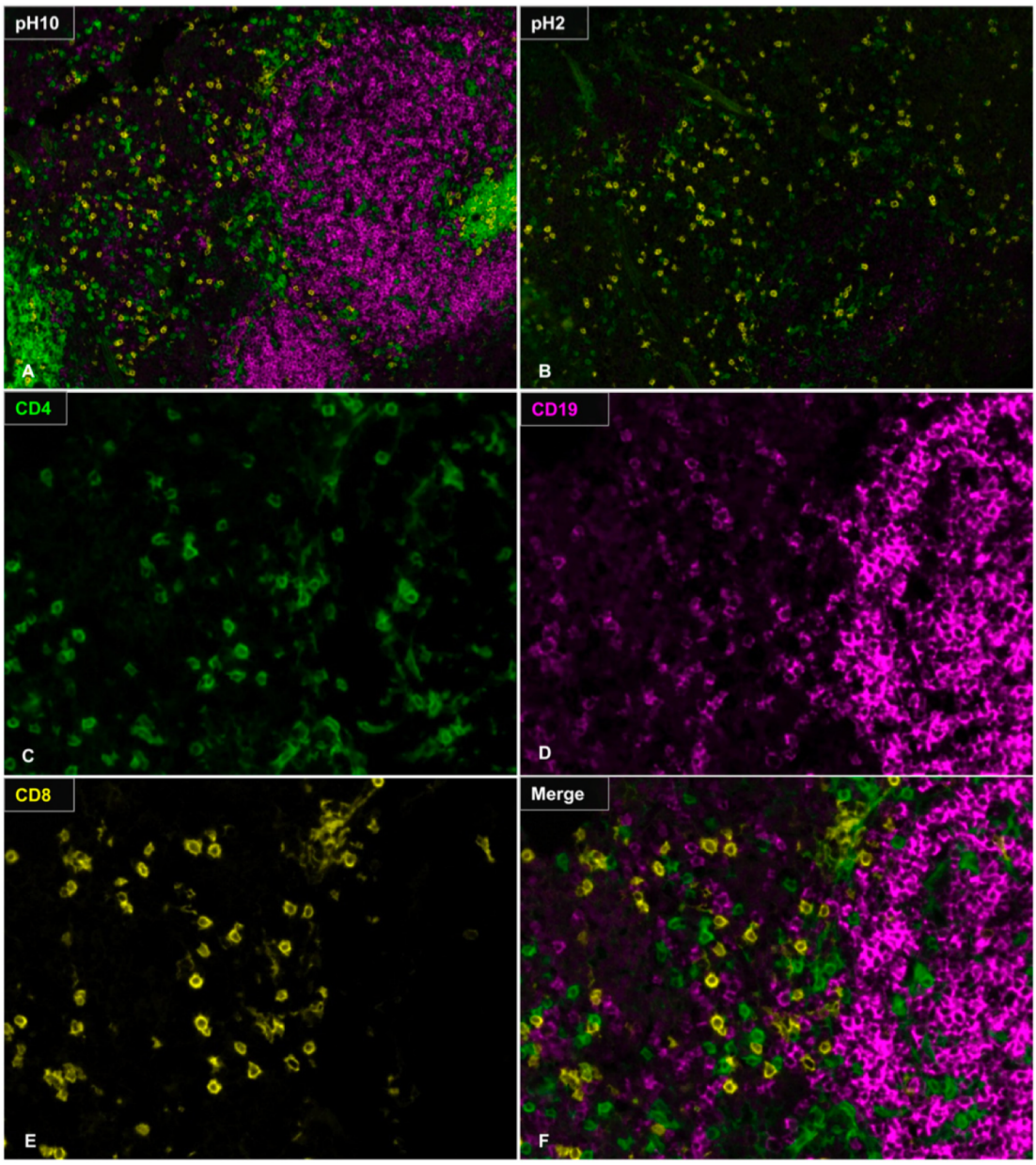

FIGURE 20: (Reprinted from Feng Z, et. al. *JI*, 2016) Multiplex IHC with CD4, CD8, and CD19. Slides were stained with CD8 (yellow) and exposed to Ag-stripping buffer (100 mM glycine, 0.5% Tween) of pH 10 **(A)** or pH 2 **(B)**. Slides were stained for CD4 (green), followed by Ag stripping and CD19 staining (magenta). **(C–F)** Higher magnification of the slides stripped with pH-10 buffer. Original magnification 200X.

205 mAb (dendritic and epithelial cells, 205 kDa)–HER2 (human epidermal growth factor receptor 2 vaccine), we stained the tumor for CD8 T cells using the TSA-based mIHC protocol for murine zinc-fixed tissues (301). This mIHC, in support of flow cytometry data, revealed that mice treated with combination immunotherapy plus HER2 vaccination increased $CD3^+$ lymphocyte infiltration throughout the tumors relative to mice treated with monotherapy or controls (Fig. 21). In another ongoing study, we evaluated the TME of MCA205 (a fibrosarcoma model) in a Eomes-GFP model after the treatment of combination immunotherapy comprised of aOX40/aCTLA-4 mAbs. We stained for CD3, CD4, CD8, GFP, and DAPI. Our mIHC data supported our flow cytometry data, showing the Eomes-GFP expressing $CD8^+$ T cell infiltration into the tumors (Fig. 22).

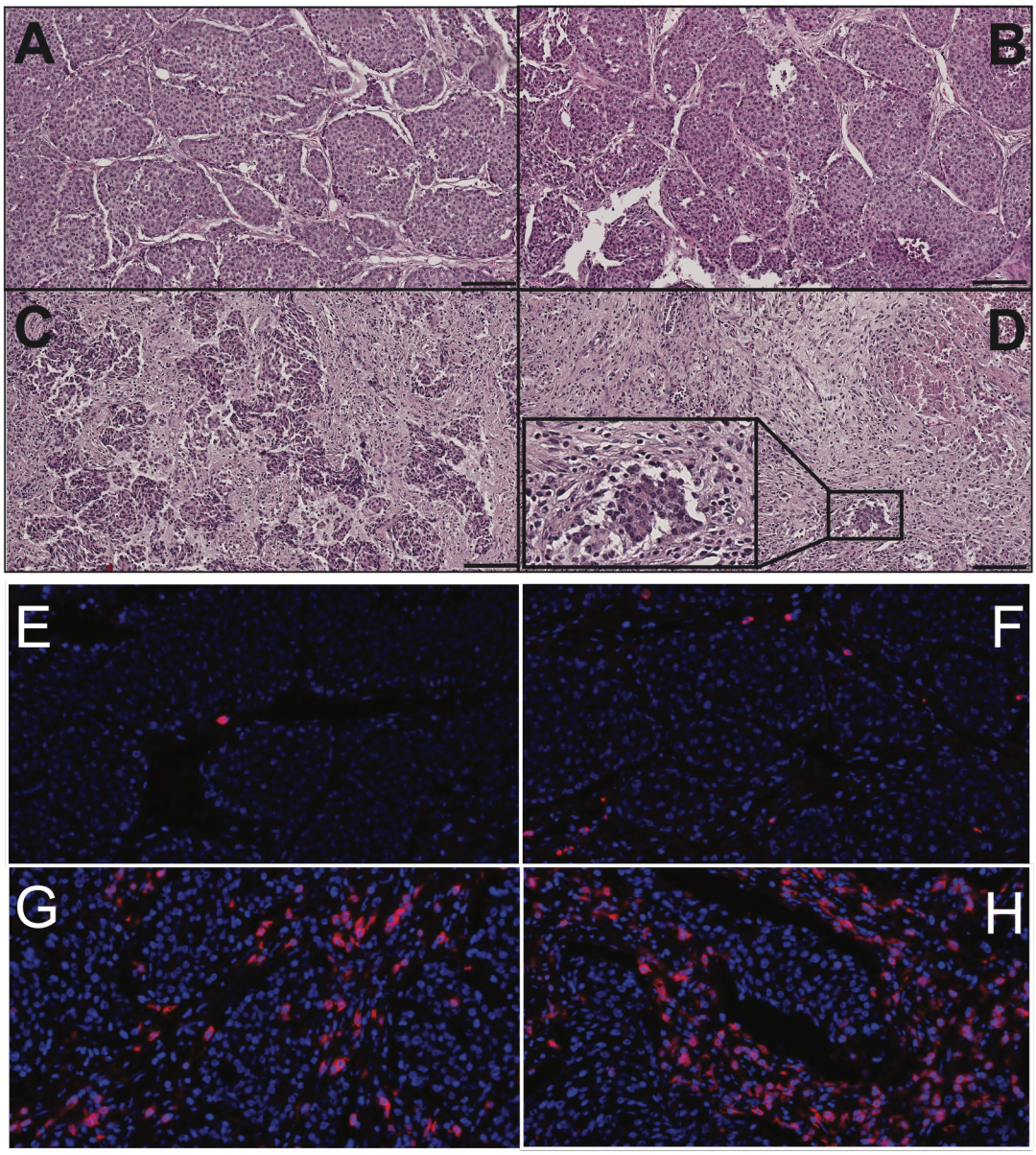

Figure 21: Combination therapy with vaccination induces robust effector T-cell infiltration into the tumor (adapted from Linch et. al.. PNAS, 2016). TUBO mammary carcinoma cells were implanted into the flanks of female BALB/c mice on day 0. Tumor-bearing mice were given control rat IgG on days 10 and 14 **(A and E)**, vaccine [anti–DEC 205/HER2/poly(I:C)] on days 10 and 14 **(B and F)**, combination immunotherapy with aOX40 on days 10 and 14/aCTLA-4 on days 10, 12, and 14 **(C and G)**, or both vaccine and combination immunotherapy (D and H). Tumors were harvested on day 21 and were analyzed by immunohistochemistry.Images depict sections of paraffin-embedded slides stained using H&E **(A–D)** or anti-CD3 plus DAPI **(E–H)**. A-D 20X and E-F magnification 200X.

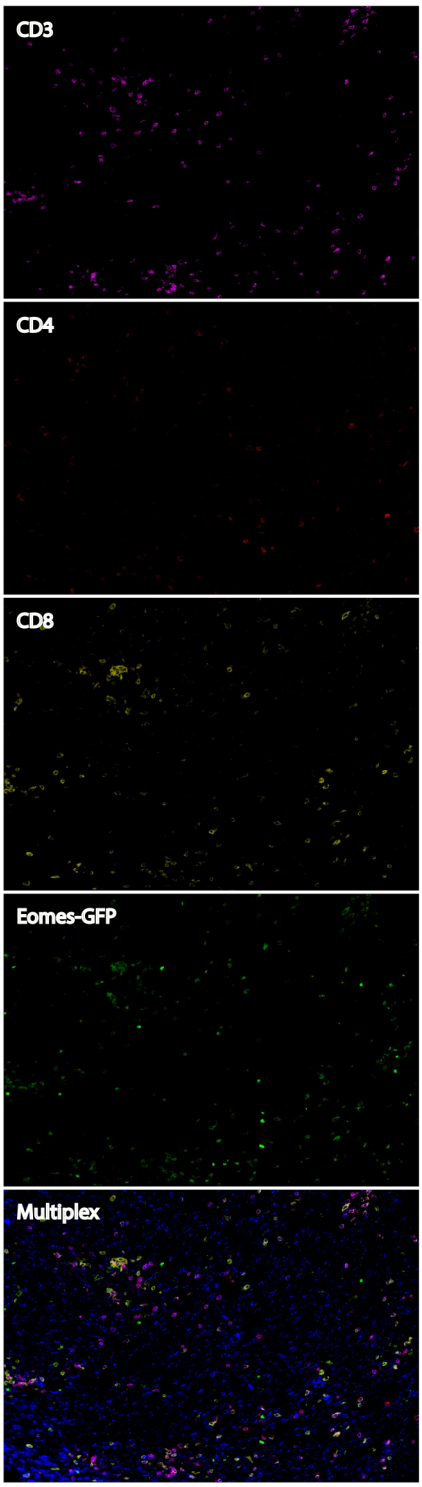

Figure 22. Tumors from aOX40/aCTLA-4 treated Eomes-GFP transgenic mice harvested and stained for CD3, CD4, CD8, GFP and DAPI using the mouse TSA-based mIHC protocol. Original magnification 200X

1.2 Multispectral image analysis

MSIs require software analysis capable of deconvolution, among other analysis tools. InForm (Perkin Elmer) was one of the first image analysis software platforms for TSA-based mIHC. InForm Tissue Finder package software is specifically designed for processing images taken by the Vectra microscope. The slides are scanned at 10X magnification in order to select for MSI at 20X using the Phenochart software which is part of the Vectra imaging software. InForm allows for unmixing MSI, manual tissue segmentation (tumor vs. stroma), setting signal thresholds, colocalization of different makers, cell segmentation, phenotyping, batch processing, and scoring. An algorithm is designed on a representative MSI based on pattern recognition of cytokeratin (CK)-positive tissue (tumor) and CK-negative tissue (stroma). After tissue segmentation, cells are segmented based on all cells' counterstain, DAPI. To phenotype the cells, 5 or more representative cells per phenotype (marker) need to be selected and cell selection needs to be repeated until the software recognizes and phenotypes all cells properly. Using the algorithm, batch analysis can be performed on all MSI.

Even though InForm is useful software for TME analysis, it is laborious and takes hours to train the algorithm on the representative MSI and even longer for processing about 10 MSI in a batch analysis. There has been a surge in the field of digital pathology in developing new systems that are capable of deconvoluting MSI produced by mIHC, segmenting tissues, phenotyping, and scoring faster and better. Currently, there are few automated digital pathology systems in use in the field that can analyze mIHC images with more than three color stains, such as HALO (Indica labs, Corrales, NM, USA), Aperio Color Deconvolution Algorithm or SlidePath (Leica Biosystems,Wetzlar,

Germany), Automated Cellular Imaging System (ACIS III, Dako, Glostrup, Denmark), BLISS workstation (Bacus Laboratories, Lombard, IL, USA), Mirax HistoQuant (3DHistech, Budapest, Hungary), and Tissue Studio® 4.0 (Definiens, Munich, Germany). However, big issues in the mIHC imaging software still persist; they are laborious, time-consuming, and most are limited to analysis of regions of interest only (6).

An open source imaging software, QuPath, has been developed and improved to allow researchers to visualize and annotate a whole slide in real time. QuPath is evolving through the contributions of users who face issues in analysis of complex tissue images and through the adding of the solutions and new algorithms to this platform (302). QuPath has resolved the two major issues of time and coverage of a whole tissue slide analysis (302). However, QuPath has not yet acquired the tool for deconvolution of multispectral images, and it is limited to processing only 4-color panels of mIHC MSI.

1.3 Discussion

1.3.1 mIHC in research and clinical trials

mIHC using the TSA technique has been implemented successfully by researchers for human and animal tissues (303, 304). TSA-based mIHC has also been successfully utilized to predict the success of culturing TIL from human melanoma samples (300). The TSA-based mIHC staining protocol from the melanoma study was used to examine TIL frequencies and PD-L1 expression in prostate cancer and non-small cell lung cancer (NSCLC) specimens. For the first time, evidence of the anti-tumor activity of PD-1 inhibitor (pembrolizumab) was shown in men who have metastatic castration-resistant prostate cancer (mCRPC) and who have shown progression with enzlutamide. TSA-

based mIHC showed the infiltration of $CD3^+CD8^+$ T cells and $CD163^+$ macrophages and expression of PD-L1 in the baseline biopsies of the two responders (Fig. 23, published Graff JN, *Oncotarget*, 2016). We observed differential TIL and PD-L1 expression between the liver and lymph node biopsies. There was pronounced T cell and macrophage infiltration and PD-L1 expression by CK^+ cells in the lymph node biopsy. While in the liver biopsy, there was a pronounced macrophage infiltration and PD-L1 expression associated with macrophages rather than CK^+ cells. Thus, these data provided evidence of pre-existing leukocyte infiltration in the baseline liver biopsy of one of the responders. The pronounced lymphocyte infiltration in the lymph node was difficult to interpret since lymphocytes reside in the lymph node. However, the presence of lymphocytes was detected in the tumor deposit itself (305), suggesting potential immune-mediated recognition of the cancer cells.

Another phase Ib clinical trial (NCT02523469) was designed to assess the safety of the combination of ALT-803 (a pharmacological grade IL-15/IL-15Rα complex fused to an IgG1 Fc) and nivolumab (anti-PD-1 monoclonal antibody), and their anti-tumor activity in patients with NSCLC. In ALT-803, IL-15 is mutated (asn72asp) to enhance the biological activity and agonism of the IL-2 and IL-15βγ receptors (306). This study used TSA-based mIHC to determine the expression of immune markers (CD3, CD8 and CD163), tumor (cytokeratin), and PD-L1. The multispectral images from TSA-based mIHC pre-treatment biopsy samples showed the relation between $CD8^+$ T cells and PD-L1-expressing tumor and immune cells (Fig. 24). This data supported the post-hoc analysis of patients based on PD-L1 positive and negative tumors, where the ALT-803

combined with anti-PD-1 monoclonal antibody might help overcome resistance to anti-PD-1 monoclonal antibody treatment in PD-1 refractory patients (307).

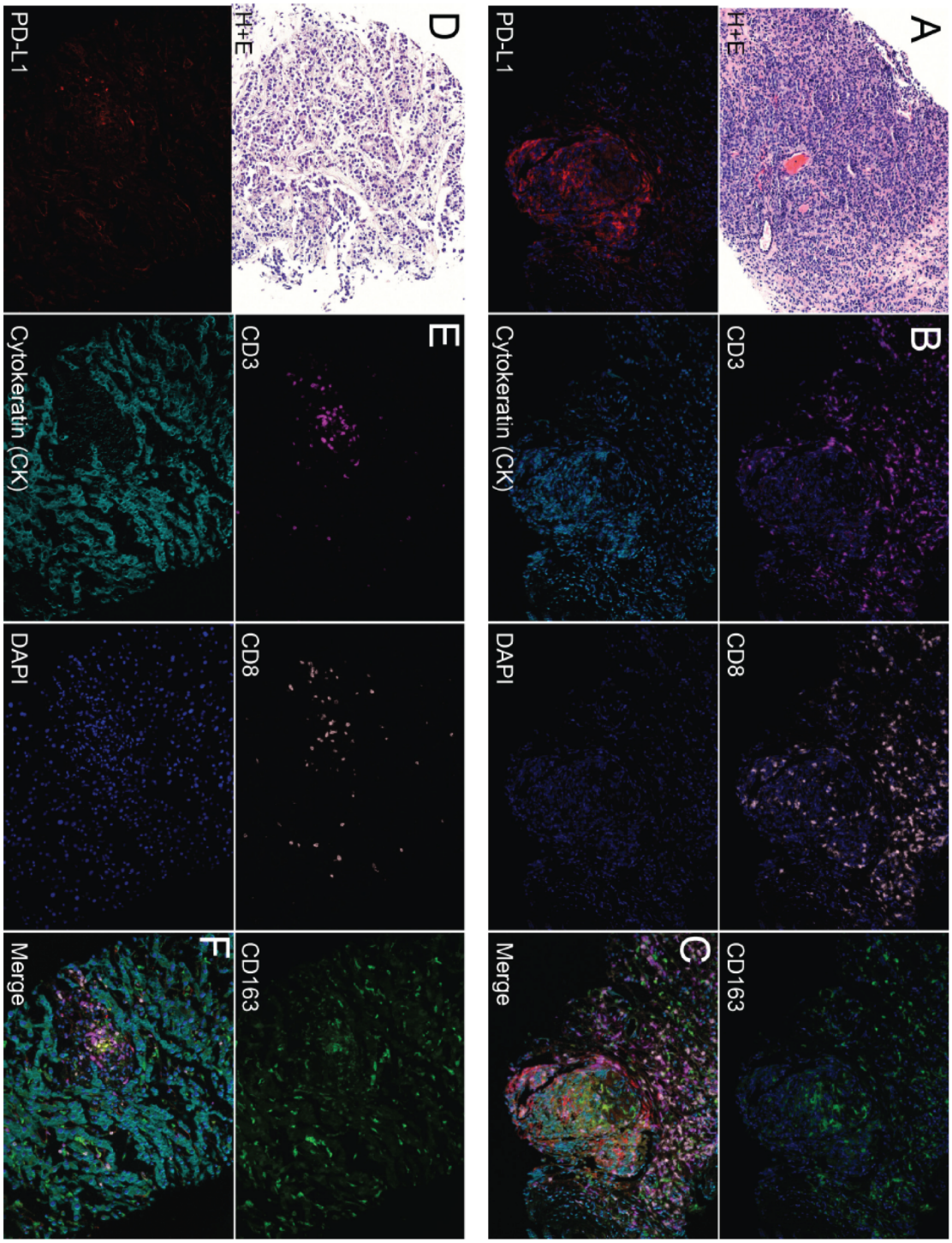

Figure 23: (Reprinted from Graff NJ, Oncotarget, 2016) Multi-spectral imaging reveals leukocyte infiltration in biopsies from men with metastatic castrate-resistant prostate cancer (mCRPC). A-C) Lymph node (LN) and **D-F)** liver biopsies were obtained from men with mCRPC. **A)** H+E and **B)** single-color images (plus nuclear stain; DAPI) of CD3, CD8, CD163, PD-L1, cytokeratin (CK), DAPI and **C)** merged image from a LN biopsy of patient A. **D)** H+E, E) single-color, and **F)** merged from a liver biopsy of patient B. Note: images depicted in (B-C and E-F) were selected from representative "hot spots" of leukocyte infiltrates in each biopsy. A, D) H+E images 20X; B, C, E, F) multi-spectral images 200X.

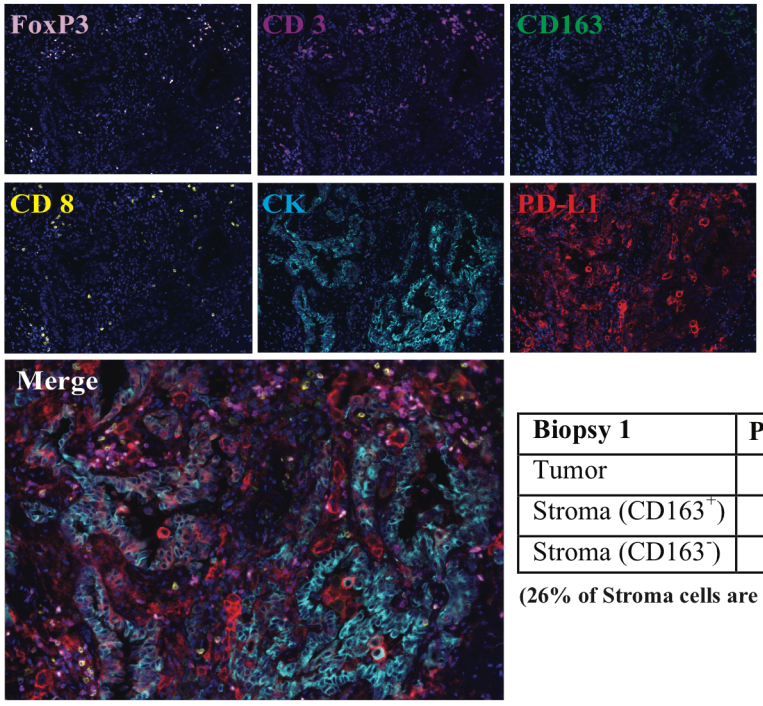

Biopsy 1	PD-L1^{+}
Tumor	66%
Stroma (CD163^{+})	71%
Stroma (CD163^{-})	49%

(26% of Stroma cells are CD163^{+})

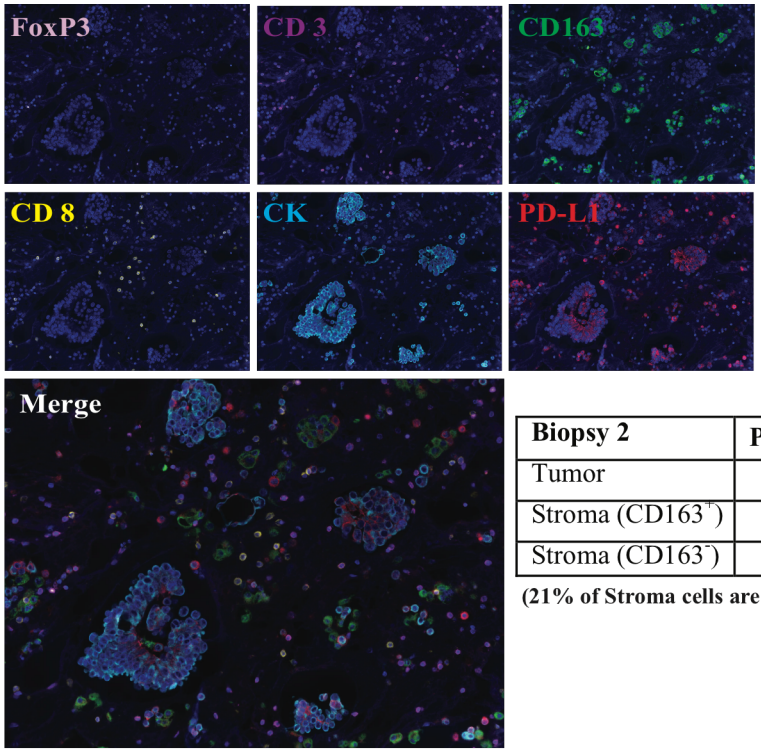

Biopsy 2	PD-L1^{+}
Tumor	91%
Stroma (CD163^{+})	27%
Stroma (CD163^{-})	4%

(21% of Stroma cells are CD163^{+})

Figure 24: (Reprinted from Wrangle JM, *Lancet*, 2018) Multi-spectral imaging of pre-treatment biopsies from patients with NSCLC. Tumor biopsies (FFPE) from two patients were obtained prior to treatment. Representative single- color images (plus DAPI) of CD3, CD8, CD163, FoxP3, PD-L1, and cytokeratin (CK) staining and merged images are shown. Images were selected from representative "hot spots" of leukocyte infiltrates in each biopsy. Quantification was determined using InForm analysis software (PerkinElmer). All images are 200X.

1.3.2 Advantages and limitations of mIHC

There has been tremendous effort to develop new and improved protocols for mIHC in human and murine tissue. Improved mIHC could be implemented in the TNM-I classification of tumors, and in diagnostic and prognostic routine clinical workflow. This would help obtain maximum data per tissue section, which is important due to the common issue of sample limitation. The ability of mIHC to provide co-expression analysis and single-cell quantification with the spatial relationships of different targets while preserving tissue integrity on the same section gives mIHC an edge over other multiplex approaches, such as MICSSS and fluorescent mIHC (276, 308). Chromogenic IHC and fluorescent mIHC face similar technical issues due to method similarities (309). Pre-analytic variables that still need to be still standardized, such as type of fixative, duration of fixation, dehydration, paraffin embedding, drying and storage of the slides are the potential challenges that mIHC faces (309, 310). Reproducibility is another hurdle which requires well-characterized antibodies that will not cross-react (311). For mIHC to be suitable for clinical use, there needs be a validated and characterized single staining positive tissue control for each marker due to tumors' cellular and spatial heterogeneity, and variation in immune cell's infiltration and immune markers, such as PD-L1 expression (312). Even the heterogeneity across the tumor alone calls for high resolution multiplexed analysis for the whole tumor sections rather than ROIs (264, 313). Automation of mIHC for routine use in a clinical setting is important, but has been proven to be a difficult task due to poor reproducibility.

1.3.3 Up and coming technological improvements on mIHC

Recently developed multiplexed technologies, such as multiplexed ion beam imaging (MIBI) (IONpath, Inc., Menlo Park, CA, USA), imaging mass cytometry (IMC-CyTOF) (Fluidigm, South San Francisco, CA, USA), and digital spatial profiling (DSP) technology (NanoString Technologies, Inc., Seattle, WA, USA) (308, 314, 315), could be a potential replacement for mIHC. MIBI and IMC-CyTOF are both platforms use secondary ion mass spectrometry to image antibodies tagged with isotopically pure elemental metals in FFPE tissue (314). Theoretically, MIBI and IMC-CyTOF capable of detecting more than 50 targets stained simultaneously (308). DSP technology uses target-specific barcodes conjugated either with primary antibodies via a UV-cleavable linker or nucleic acid probes that are liberated by a UV laser. Target-specific barcodes are counted using the nCounter platform and mapped back to tissue location, thus allowing for target detection. DSP is theoretically capable of detecting up to 800 targets simultaneously (308). These upcoming high throughput platforms will also face some challenges and limitations that need to be overcome, such as file sizes, data analysis, and visual verification of staining quality and specificity.

1.4 Material and Methods

1.4.1 Tissue fixation and processing

Calcium acetate (0.5 g), zinc acetate (5 g), zinc chloride (5 g), and Tris (0.1 M, pH 7.4) was added to 1L double distilled water and mixed to make 1L zinc-fixation buffer. The final pH of 1L zinc-fixation buffer was 6.5–7. PLP was prepared by mixing Lysine HCl solution (13.7 g Lysine HCl in 375 ml double distilled water pH was adjusted

to 7.4 with Na2HPO4 and 15.6 ml 16% paraformaldehyde). A total of 2.14 g sodium periodate was added, and the solution was brought up to 1L with 0.1 M phosphate buffer. Spleens and tumors were harvested and fixed for 24h at RT. Spleens and tumors were processed using a Tissue-Tek automated tissue processor for formalin (70% ethanol 30 min, 95% ethanol 30 min two times, 100% ethanol 30 min three times, xylene 40 min two times, paraffin 35 min four times), on Zinc setting for zinc- and PLP-fixed samples (the tissue process was started on 70% ethanol and skipped formalin fixation) and embedded with a Leica tissue embedder. The embedded paraffin blocks were chilled for 10 minutes before cutting 4μM thick sections using the microtome and floated onto Plus slides in a tissue flotation bath set at 40°C. Slides were allowed to dry at RT overnight and stored at 4°C until use.

1.4.2 Deparaffinization

To deparaffinize the slides for staining, slides were placed on a staining rack in a Leica autostainer, and a deparaffinization protocol was run. Samples were marked with ImmEdge hydrophobic pen and allowed to dry in order to prevent overflow of antibody, TSA and other solutions during staining steps.

1.4.3 TSA-based mIHC staining method for murine tissue

After deparaffinization, slides were transferred to a rack in double distilled water. Then, slides were rinsed once with 1X TBST (to make 10X TBST solution: 88g of Trizma base and 24g of NaCl was dissolved in double distilled water and adjusted the pH to 7.60 with 37% HCl (approximately 47.5mL for 1L 10X TBS)) and blocked with

Rodent Block M solution for 10 min. Primary Ab was diluted in Renaissance Ab diluent (PD905; Biocare Medical). The dilutions used were 1:50 for CD3 (SP7, M3074; Spring Bioscience), CD4 (RM4-5, 550280, BD Biosciences; GK1.5, 14-0041-85, eBioscience), CD8 (53-6.7, 550281; BD Biosciences), CD19 (1D3, 553783; BD Biosciences), and PD-L1 (ab58810; Abcam). Primary Abs were incubated for 45 min on an orbital shaker at RT. Abs were subsequently removed by vacuum, and slides were washed three times for 30 s in TBST. Anti-rabbit secondary Ab (87-9623; Life Technologies) or anti-rat (MP-7444-15; Vector Laboratories) was added drop-wise to slides to cover the tissue area. Slides were incubated for 10 min at RT and washed three times for 30 s in 1X TBST. TSA-conjugated fluorophore (NEL791001KT, PerkinElmer; T20950, Life Technologies) was added to slides at 1:100 dilution in Amplification plus buffer (NEL791001KT; PerkinElmer) and incubated for 10 min at RT; TSA-conjugated fluorophore was vacuumed off, and slides were washed three times for 30 s in 1X TBST. For multiplex imaging, antibody stripping buffer (100 mM glycine plus 0.5% Tween was adjusted to pH 10 using NaOH) was added to slides and incubated for 10 min at RT. Slides were rinsed with 1X TBST, blocked briefly with Rodent Block M solution, and incubated with primary Ab at the desired dilution and time. DAPI (D1306; Life Technologies, 1 mg/ml stock) was diluted 1:500 in 1X TBST and added to slides. Slides were incubated for 5 min at RT and washed twice for 30 s in 1X TBST. Slides were rinsed with double distilled water, coverslipped with VECTASHIELD Hard Mount, painted with nail polish and stored at 4°C in a covered slide box. Slides were imaged at 4X and 20X using Vectra imaging software, and phenotyped from 20X fields using inForm analysis software.

1.4.4 TSA-based mIHC staining protocol for human FFPE tissue

After deparaffinization, samples were bordered with ImmEdge hydrophobic pen and rinsed in double distilled water. Slides were then immersed in 1X Citra antigen retrieval buffer in a container, covered, and heated in the container for 1 min on 100% power, followed by 12 min on 10% power. The dish was let cool for at least 15 min. Slides were blocked with Ventana antibody diluent for 10 minutes. Approximately 100 µl, diluted Cell Signaling Technology rabbit anti-PD-L1 (E1L3N, 13684) antibody in Ventana antibody diluent at 1:250 ratio was added per slide and incubated for 30 minutes at RT, shaking at 110 rpm. After 30 min, the primary antibody was vacuumed off and washed the slides 3X for 3s in 1X TBST. Anti-rabbit secondary antibody was added drop wise to cover the tissue area and incubated for 10 min at RT, shaking at 110 rpm. After 10 min, secondary antibody was vacuumed off and washed the slides 3X for 3s in 1X TBST. TSA-conjugated fluorophore was diluted 1:75 in amplification buffer and added at approximately 100 µl per slide to cover the tissue and incubate for 10 min at RT, shaking at 110 rpm. The TSA was then vacuumed off and the slides were washed 3X for 3s in 1X TBST. The steps were repeated from antigen retrieval to TSA-conjugated fluorophores for all the markers. The markers and dilution were used in the following order after PD-L1 staining cycle: Spring Biosciences rabbit anti-CD8 antibody (SP239, M5394) 1:50, Abcam mouse anti-FoxP3 antibody (236A/E7, AB20034) 1:100, Spring Biosciences rabbit anti-CD3 antibody (SP7, M3070), Ventana mouse anti-CD163 antibody (MRQ-26, 760-4437) prediluted (100 µl), and DAKO mouse pan-cytokeratin (AE1/AE3) 1:50. After all the staining was done, DAPI (1 mg/ml stock) was diluted 1:500 in D-PBS and added at 100 µl per slide to cover the tissue area and was incubated for 5 min at RT, shaking at

110 rpm. DAPI was then vacuumed off and washed 3X for 30 s in 1X TBST. The slides were cover slipped with Vectra Shield Hard Mount and the edges of the slides were sealed with nail polish and stored slides at 40C in cover slide box.

Chapter 5: Conclusions

5.1 Summary

A better understanding of the immune system and discoveries about cellular and humoral immunity intensified the investigation of an immune-driven anti-tumor response. Specifically, the discovery of T lymphocytes and their key role in anti-tumor responses grabbed the attention of immunologists. Discoveries of checkpoint inhibitors and costimulatory receptors on T lymphocytes and their modulation with specific antibodies have led cancer immunotherapy to join surgery, cytotoxic chemotherapy, radiation, and targeted therapy as the fifth pillar of cancer therapy (135). It has been predicted that immunotherapy will be the leading cancer treatment for all cancers within a decade due to its ability to drive a response against cancers that do not respond to chemotherapy or radiation therapies, to improve anti-tumor responses in combination with other therapies, and to generate durable responses with potentially long-term tumor-specific immunity (136).

Cancer immunotherapies that are currently FDA approved include CAR T and B cell therapy and mAbs against checkpoint inhibitors CTLA-4, PD-1, and PD-L1. However, costimulators, such as OX40, 4-1BB, GITR, and ICOS, while not approved by the FDA, have had limited success in human clinical trials. The preclinical activity of surrogate OX40 agonists alone or in combination with other agents, such as immune checkpoint antibodies, targeted inhibitors, and cancer vaccines in murine tumor models led six different pharmaceutical companies to develop OX40 agonist antibodies that entered clinical trials in a short period of time (167, 172). However, in these cases, few objective clinical responses were observed. These studies raised the question of how to optimally combine OX40 with the other agents and achieve OX40-mediated anti-tumor responses

in humans. In clinical trials, dosing, scheduling and combinations also need to be carefully considered. A deeper understanding of the therapeutic mechanism of the OX40 pathway is required to achieve maximum therapeutic benefits of combinatorial therapies in patients.

Our studies from Chapter 3 contribute to a better understanding of OX40 agonists and a critical component of the OX40 pathway, Gal-3, in OX40-induced $CD8^+$ T cell development and survival. OX40-OX40L signaling induces the expansion and survival of memory $CD8^+$ T cells (72, 119, 245-247), and here we show that intracellular Gal-3 contributes to agonist aOX40-induced $CD8^+$ T cell survival and memory formation. Gal-$3^{-/-}$ $CD8^+$ T cells receiving aOX40 therapy underwent a similar expansion and activation as WT cells early in the response, however, Gal-$3^{-/-}$ $CD8^+$ T cells treated with aOX40 had significantly reduced survival by days 14 and 29, suggesting a crucial role for Gal-3 in regulating OX40-induced $CD8^+$ T cell survival (Fig. 8). The reduced survival of Gal-$3^{-/-}$ $CD8^+$ T cells later in the response was also observed following IL-2c therapy and attenuated *Lm*-OVA vaccination plus aOX40 therapy.

Agonist aOX40 has been shown to promote CD8 T cell memory formation (316). Interestingly, we observed a significantly higher percentage of Gal-$3^{-/-}$ $CD8^+$ T cells remained in an effector or effector memory phenotype by day 14 post-aOX40 therapy, indicating a key role for intracellular Gal-3 in facilitating the development of central memory $CD8^+$ T cells through an OX40-mediated pathway (Fig. 8). Moreover, Gal-$3^{-/-}$ $CD8^+$ T cells treated with aOX40 exhibited higher death by apoptosis compared to WT cells. We found a correlation between Gal-$3^{-/-}$ $CD8^+$ T cell apoptosis and higher

expression of *Erdr1* mRNA in Gal-3$^{-/-}$ CD8^{+} T cells compared to WT cells. However, we were not able to determine how Erdr1 induces apoptosis in Gal-3$^{-/-}$ CD8^{+} T cells.

CD8^{+} T cells are a key component of a robust anti-tumor response and CD8^{+} T cell memory formation is important for maintaining durable responses with potentially long-term tumor-specific immunity. Gal-3$^{-/-}$ CD8^{+} T cell-mediated adoptive therapy plus aOX40 treatment of B16-OVA tumor-bearing mice showed a significantly lower survival compared to WT CD8^{+} T cell adoptive therapy plus aOX40 treatment. These data suggest that the defect in memory development of Gal-3$^{-/-}$ CD8^{+} T cells and reduced survival of Gal-3$^{-/-}$ CD8^{+} T cells negatively affect the generation of an effective anti-tumor response (Fig. 12E).

Multiplex IHC, discussed in Chapter 4, is a vital tool for analyzing the TME. Multiplex IHC has made it possible to look at the extent of infiltration of different immune cells, markers, and cytokines within the TME *in situ*. This ability to better evaluate the TME immune milieu has led researchers to design better cancer immunotherapies. Our studies from Chapter 4 resulted in the development of the first protocol to perform successfully TSA-based mIHC in zinc-fixed paraffin embedded murine tissues. The TSA-based mIHC protocol for murine tissue has enabled a deeper understanding of the TME in murine tumor models in preclinical studies. Furthermore, TSA-based mIHC has the potential to play a crucial role in selecting cancer patients that will benefit the most from a particular immunotherapy or clinical trial.

5.2 Future directions

5.2.1 Does Gal-3 induced Akt phosphorylation contribute to OX40 induced survival?

OX40 has a critical role in mediating memory $CD8^+$ T cell formation following infection with pathogens including *Listeria monocytogenes* expressing OVA (*Lm*-OVA) or vaccinia virus (245, 252). One mechanism for OX40-induced survival is through engagement of the OX40 signaling pathway leading to expression of anti-apoptotic proteins that help the T cells survive long-term and transition into memory cells (124, 257-259). We show that OX40 ligation sustains Gal-3 mRNA expression over time (Fig. 6B) and in the absence of Gal-3, OX40 signaling does not induce the long-term survival of $CD8^+$ T cells, suggesting a connection between Gal-3 and $CD8^+$ T cell survival. Interestingly, both OX40 and Gal-3 contribute to Akt activity, which has an essential role in regulating T cell longevity (259); OX40 maintains Akt activity, and Gal-3 upregulates Akt phosphorylation (260). One possibility is that the connection between Gal-3 and OX40 induced survival is reliant on Akt-mediated signaling. Currently, whether there is a defect in the phosphorylation of Akt in Gal-$3^{-/-}$ $CD8^+$ T cells after aOX40 therapy is not known. The phosphorylation status of Akt in Gal-$3^{-/-}$ $CD8^+$ T cells can be determined through western blot or phospho-specific intracellular flow cytometry at different time points following aOX40 therapy. These experiments would reveal whether Akt activity is altered as a result of Gal-3 deficiency, which would be the first step in determining whether Gal-3 regulation of Akt phosphorylation following OX40 ligation contributes to increased $CD8^+$ T cell survival.

5.2.2 Do Gal-3$^{-/-}$ CD8^{+} T effector cells die or are they unable to transition to central memory cells?

Gal-3 can inhibit Fas-dependent apoptosis in Jurkat T cells (201) and, in addition, Gal-3 has been shown to suppress apoptosis through inhibition of caspase-9 and caspase-3 activation (197). Indeed, as expected based on Gal-3's role in the inhibition of apoptosis, we found Gal-3$^{-/-}$ CD8^{+} T cells to be significantly more apoptotic *in vitro* and *in vivo* (Fig. 15). Furthermore, the extent of Annexin V expression among the T_E, T_{EM} and T_{CM} Gal-3$^{-/-}$ CD8^{+} T cells subsets was significantly higher in the T_E subsets of Gal-3$^{-/-}$ CD8^{+} T cells treated with aOX40 compared to wild-type T_E CD8^{+} T cells (day 14). Thus, the increased apoptosis of Gal-3$^{-/-}$ CD8^{+} T cells appears to be associated with Gal-3$^{-/-}$ CD8^{+} T cell skewing towards a short-lived effector cell phenotype and failure to generate central memory cells (Fig. 8). However, whether reduced long-term survival of Gal-3$^{-/-}$ CD8^{+} T cells is due to increased cell death of the effector cell phenotype or if they are simply unable to develop into central memory cells following aOX40 therapy is unclear. Single cell gene expression profiling assays may be useful in elucidating the underlying mechanisms regulating the deficiencies in the generation of memory Gal-3$^{-/-}$ CD8^{+} T cells. This assay will allow to assess comprehensive sets of pro-apoptotic and pro survival genes in Gal-3$^{-/-}$ CD8^{+} T cells treated with aOX40 therapy early in the response (day 4) which will help in determining the fate of T effector cells. Assessment of T cell differentiation-associated gene expression in Gal-3$^{-/-}$ CD8^{+} T cells treated with aOX40 therapy would also help determine whether there is a defect in forming memory cells. Another way to determine whether the reduced long-term survival of Gal-3$^{-/-}$ CD8^{+} T cells is due to increased cell death of effector cells or if they are simply unable to develop

into central memory cells following aOX40 therapy is to produce inducible Gal-3 knockout mice. Gal-3 could be induced in these mice at different time points following aOX40 therapy and would help determine where the defect in the long-term survival of Gal-$3^{-/-}$ $CD8^+$ T cells lies. Knocking out Gal-3 early in the aOX40 therapy response in inducible Gal-3 knockout mice can be expected to mimic the reduced long-term survival in Gal-$3^{-/-}$ $CD8^+$ T cells as seen in our current model. If Gal-3 deficiency is causing a defect in $CD8^+$ T cells memory development, knocking out Gal-3 on day 7 post-aOX40 therapy should rescue $CD8^+$ T cell long-term survival since $CD8^+$ T cells would have already become memory cells or poised to become memory cells by then. If the defect in Gal-$3^{-/-}$ $CD8^+$ T cells is not in the memory development, then knocking out Gal-3 on day 7 post-aOX40 therapy would mimic the reduced long-term survival phenotype that we originally observed in Gal$3^{-/-}$ $CD8^+$ T cells.

5.2.3 Does Erdr1 trigger apoptosis in Gal-$3^{-/-}$ cells?

Erdr1 induces T cell apoptosis via a Fas-dependent pathway (256), while intracellular Gal-3 inhibits apoptosis in a Fas-dependent mechanism. Erdr1 mRNA expression is significantly increased in Gal-$3^{-/-}$ $CD8^+$ T cells, suggesting that higher levels of Erdr1 in Gal-$3^{-/-}$ $CD8^+$ T cells might be triggering apoptosis. However, it remains to be determined whether and how Erdr1 triggers apoptosis in Gal-$3^{-/-}$ $CD8^+$ T cells. To investigate this, one might determine Fas/FasL expression and its association with Erdr1 in Gal-$3^{-/-}$ $CD8^+$ T cells, which would shed light on whether Erdr1 acts through a Fas-dependent pathway to trigger apoptosis. Second, due to the reciprocal relation between Gal-3 and Erdr1 expression, knocking down the increased expression of

Erdr1 in Gal-3$^{-/-}$ CD8^{+} T cells via shRNA or similar techniques and then looking at changes in the extent of apoptosis should reveal whether the increased apoptosis in Gal-3$^{-/-}$ CD8^{+} T cells is induced by Erdr1. The opposing contribution of both Erdr1 (induces) and Gal-3 (prevents) to Fas-dependent apoptotic pathways suggest that there is a regulatory connection between Gal-3 and Erdr1. To determine this relationship, one could look upstream of Gal-3 and Erdr1 genes to see if there is transcription factor that potentially co-regulates these genes.

5.2.4 How are CD8^{+} T cell tumor responses affected by the lack of Gal-3?

We showed that Gal-3$^{-/-}$ CD8^{+} T cell-mediated adoptive therapy plus aOX40 treatment of B16-OVA tumor-bearing mice led to significantly reduced survival compared to WT CD8^{+} T-cells plus aOX40 treatment. It is not known whether Gal-3$^{-/-}$ CD8^{+} T cells are additionally influenced by other tumor induced immune suppressive mechanisms within the TME, such as expression of checkpoint ligands, secretion of inhibitory cytokines and inhibition of metabolic pathways. In addition, it will be crucial to see if Gal-3$^{-/-}$ CD8^{+} T cells traffic to the tumor and retain their effector function to a similar extent as wild-type CD8^{+} T cells. These questions can be answered by harvesting the TIL from tumor-bearing mice treated with Gal-3$^{-/-}$ vs. wild-type CD8^{+} T cells plus aOX40 at days 7, 14 and 29 post-transfer and then determining the phenotype and differentiation status of the donor CD8^{+} T cells.

5.3 Conclusions

The function and role of extracellular Gal-3 has been studied extensively in both tumors and immune cells, however, little is known about the intracellular function of Gal-3 in immune cells, especially $CD8^+$ T cells (reviewed in Chapter 2). Our studies in Chapter 3 are the first, to our knowledge, to describe the role of intracellular Gal-3 in OX40-induced survival and development in $CD8^+$ T cells. In contrast to the negative role of Gal-3 described in pathology, our studies point out the importance of intracellular Gal-3 in regulating $CD8^+$ T cell responses and warrants consideration in cancer therapies combined with modulation of intracellular Gal-3 to potentially improve $CD8^+$ T cell survival and the formation of long-lived memory cells. Overexpression of Gal-3 in $CD8^+$ T cells along with $CD8^+$ T cell costimulation could potentially enhance the $CD8^+$ T cell response and survival, thus supporting better anti-tumor efficacy.

Our studies raise the question about the role of Gal-3 in other costimulatory and checkpoint blocked therapies, especially PD-1/ PD-L1 and CTLA-4 therapies. PD-1, PD-L1, and CTLA-4 are all FDA approved drugs for multiple tumor types, but they do not work for every patient. Because we show a critical role for Gal-3 in aOX40-induced $CD8^+$ T cell memory formation and survival, it will be important to investigate the role of Gal-3 following checkpoint blockade immunotherapy. Future studies will be needed to address this important issue.

Reference:

1. Uhlen, M., L. Fagerberg, B. M. Hallstrom, C. Lindskog, P. Oksvold, A. Mardinoglu, A. Sivertsson, C. Kampf, E. Sjostedt, A. Asplund, I. Olsson, K. Edlund, E. Lundberg, S. Navani, C. A. Szigyarto, J. Odeberg, D. Djureinovic, J. O. Takanen, S. Hober, T. Alm, P. H. Edqvist, H. Berling, H. Tegel, J. Mulder, J. Rockberg, P. Nilsson, J. M. Schwenk, M. Hamsten, K. von Feilitzen, M. Forsberg, L. Persson, F. Johansson, M. Zwahlen, G. von Heijne, J. Nielsen, and F. Ponten. 2015. Proteomics. Tissue-based map of the human proteome. *Science (New York, N.Y.)* 347: 1260419.
2. Kammula, U. S., D. E. White, and S. A. Rosenberg. 1998. Trends in the safety of high dose bolus interleukin-2 administration in patients with metastatic cancer. *Cancer* 83: 797-805.
3. Hoffmann, J. A., F. C. Kafatos, C. A. Janeway, and R. A. Ezekowitz. 1999. Phylogenetic perspectives in innate immunity. *Science (New York, N.Y.)* 284: 1313-1318.
4. Pancer, Z., and M. D. Cooper. 2006. The evolution of adaptive immunity. *Annual review of immunology* 24: 497-518.
5. Janeway, C. A., Jr., and R. Medzhitov. 2002. Innate immune recognition. *Annual review of immunology* 20: 197-216.
6. Turvey, S. E., and D. H. Broide. 2010. Innate immunity. *The Journal of allergy and clinical immunology* 125: S24-32.
7. Tomar, N., and R. K. De. 2014. A brief outline of the immune system. *Methods in molecular biology (Clifton, N.J.)* 1184: 3-12.
8. Murphy, K. W., C. 2016. *Janeway's immunobiology.* Tylor & Francis, New York: Garland Science.
9. Nagasawa, T. 2006. Microenvironmental niches in the bone marrow required for B-cell development. *Nature reviews. Immunology* 6: 107-116.
10. Allman, D., J. Li, and R. R. Hardy. 1999. Commitment to the B lymphoid lineage occurs before DH-JH recombination. *The Journal of experimental medicine* 189: 735-740.
11. Nemazee, D. 2017. Mechanisms of central tolerance for B cells. *Nature reviews. Immunology* 17: 281-294.
12. Tiegs, S. L., D. M. Russell, and D. Nemazee. 1993. Receptor editing in self-reactive bone marrow B cells. *The Journal of experimental medicine* 177: 1009-1020.
13. Carsetti, R., G. Kohler, and M. C. Lamers. 1995. Transitional B cells are the target of negative selection in the B cell compartment. *The Journal of experimental medicine* 181: 2129-2140.
14. Pieper, K., B. Grimbacher, and H. Eibel. 2013. B-cell biology and development. *The Journal of allergy and clinical immunology* 131: 959-971.
15. Shlomchik, M. J., and F. Weisel. 2012. Germinal center selection and the development of memory B and plasma cells. *Immunological reviews* 247: 52-63.

16. Li, Z., C. J. Woo, M. D. Iglesias-Ussel, D. Ronai, and M. D. Scharff. 2004. The generation of antibody diversity through somatic hypermutation and class switch recombination. *Genes & development* 18: 1-11.
17. Blackburn, C. C., and N. R. Manley. 2004. Developing a new paradigm for thymus organogenesis. *Nature reviews. Immunology* 4: 278-289.
18. Robey, E., and B. J. Fowlkes. 1994. Selective events in T cell development. *Annual review of immunology* 12: 675-705.
19. Germain, R. N. 2002. T-cell development and the CD4-CD8 lineage decision. *Nature reviews. Immunology* 2: 309-322.
20. Janeway CA Jr, T. P., Walport M, Shlomchik MJ. 2001. *Immunobiology: The Immune System in Health and Disease.* Garland Science, New York.
21. Abdel-Aziz, H. O., Y. Murai, I. Takasaki, Y. Tabuchi, H. C. Zheng, K. Nomoto, H. Takahashi, K. Tsuneyama, I. Kato, D. K. Hsu, F. T. Liu, K. Hiraga, and Y. Takano. 2008. Targeted disruption of the galectin-3 gene results in decreased susceptibility to NNK-induced lung tumorigenesis: an oligonucleotide microarray study. *Journal of cancer research and clinical oncology* 134: 777-788.
22. Sawicka, M., G. L. Stritesky, J. Reynolds, N. Abourashchi, G. Lythe, C. Molina-Paris, and K. A. Hogquist. 2014. From pre-DP, post-DP, SP4, and SP8 Thymocyte Cell Counts to a Dynamical Model of Cortical and Medullary Selection. *Frontiers in immunology* 5: 19.
23. Petrie, H. T., and J. C. Zuniga-Pflucker. 2007. Zoned out: functional mapping of stromal signaling microenvironments in the thymus. *Annual review of immunology* 25: 649-679.
24. Takada, K., I. Ohigashi, M. Kasai, H. Nakase, and Y. Takahama. 2014. Development and function of cortical thymic epithelial cells. *Current topics in microbiology and immunology* 373: 1-17.
25. Palmer, E. 2003. Negative selection--clearing out the bad apples from the T-cell repertoire. *Nature reviews. Immunology* 3: 383-391.
26. Anderson, M. S., and M. A. Su. 2011. Aire and T cell development. *Current opinion in immunology* 23: 198-206.
27. Klein, L. 2009. Dead man walking: how thymocytes scan the medulla. *Nature immunology* 10: 809-811.
28. Elmore, S. 2007. Apoptosis: a review of programmed cell death. *Toxicol Pathol* 35: 495-516.
29. Golstein, P. 1998. Cell death in us and others. *Science (New York, N.Y.)* 281: 1283.
30. Kurtulus, S., P. Tripathi, J. T. Opferman, and D. A. Hildeman. 2010. Contracting the 'mus cells'--does down-sizing suit us for diving into the memory pool? *Immunological reviews* 236: 54-67.
31. Hernandez, J. B., R. H. Newton, and C. M. Walsh. 2010. Life and death in the thymus--cell death signaling during T cell development. *Current opinion in cell biology* 22: 865-871.
32. Kerr, J. F., C. M. Winterford, and B. V. Harmon. 1994. Apoptosis. Its significance in cancer and cancer therapy. *Cancer* 73: 2013-2026.

33. Reed, J. C., C. Stein, C. Subasinghe, S. Haldar, C. M. Croce, S. Yum, and J. Cohen. 1990. Antisense-mediated inhibition of BCL2 protooncogene expression and leukemic cell growth and survival: comparisons of phosphodiester and phosphorothioate oligodeoxynucleotides. *Cancer research* 50: 6565-6570.
34. Clem, R. J., and L. K. Miller. 1993. Apoptosis reduces both the in vitro replication and the in vivo infectivity of a baculovirus. *Journal of virology* 67: 3730-3738.
35. Kerr, J. F., A. H. Wyllie, and A. R. Currie. 1972. Apoptosis: a basic biological phenomenon with wide-ranging implications in tissue kinetics. *British journal of cancer* 26: 239-257.
36. Garcia-Martinez, V., D. Macias, Y. Ganan, J. M. Garcia-Lobo, M. V. Francia, M. A. Fernandez-Teran, and J. M. Hurle. 1993. Internucleosomal DNA fragmentation and programmed cell death (apoptosis) in the interdigital tissue of the embryonic chick leg bud. *Journal of cell science* 106 (Pt 1): 201-208.
37. Strasser, A., A. W. Harris, D. C. Huang, P. H. Krammer, and S. Cory. 1995. Bcl-2 and Fas/APO-1 regulate distinct pathways to lymphocyte apoptosis. *The EMBO journal* 14: 6136-6147.
38. Li, K.-P., S. Shanmuganad, K. Carroll, J. D. Katz, M. B. Jordan, and D. A. Hildeman. 2017. Dying to protect: cell death and the control of T-cell homeostasis. *Immunological reviews* 277: 21-43.
39. Wojciechowski, S., P. Tripathi, T. Bourdeau, L. Acero, H. L. Grimes, J. D. Katz, F. D. Finkelman, and D. A. Hildeman. 2007. Bim/Bcl-2 balance is critical for maintaining naive and memory T cell homeostasis. *The Journal of experimental medicine* 204: 1665-1675.
40. Willis, S. N., J. I. Fletcher, T. Kaufmann, M. F. van Delft, L. Chen, P. E. Czabotar, H. Ierino, E. F. Lee, W. D. Fairlie, P. Bouillet, A. Strasser, R. M. Kluck, J. M. Adams, and D. C. Huang. 2007. Apoptosis initiated when BH3 ligands engage multiple Bcl-2 homologs, not Bax or Bak. *Science (New York, N.Y.)* 315: 856-859.
41. Li, P., D. Nijhawan, I. Budihardjo, S. M. Srinivasula, M. Ahmad, E. S. Alnemri, and X. Wang. 1997. Cytochrome c and dATP-dependent formation of Apaf-1/caspase-9 complex initiates an apoptotic protease cascade. *Cell* 91: 479-489.
42. Yang, X., H. Y. Chang, and D. Baltimore. 1998. Autoproteolytic activation of pro-caspases by oligomerization. *Molecular cell* 1: 319-325.
43. Starr, T. K., S. C. Jameson, and K. A. Hogquist. 2003. Positive and negative selection of T cells. *Annual review of immunology* 21: 139-176.
44. Dunkle, A., I. Dzhagalov, and Y. W. He. 2010. Mcl-1 promotes survival of thymocytes by inhibition of Bak in a pathway separate from Bcl-2. *Cell death and differentiation* 17: 994-1002.
45. Bouillet, P., J. F. Purton, D. I. Godfrey, L. C. Zhang, L. Coultas, H. Puthalakath, M. Pellegrini, S. Cory, J. M. Adams, and A. Strasser. 2002. BH3-only Bcl-2 family member Bim is required for apoptosis of autoreactive thymocytes. *Nature* 415: 922-926.
46. Sohn, S. J., G. M. Lewis, and A. Winoto. 2008. Non-redundant function of the MEK5-ERK5 pathway in thymocyte apoptosis. *The EMBO journal* 27: 1896-1906.

47. Blattman, J. N., R. Antia, D. J. Sourdive, X. Wang, S. M. Kaech, K. Murali-Krishna, J. D. Altman, and R. Ahmed. 2002. Estimating the precursor frequency of naive antigen-specific CD8 T cells. *The Journal of experimental medicine* 195: 657-664.
48. Murali-Krishna, K., J. D. Altman, M. Suresh, D. J. Sourdive, A. J. Zajac, J. D. Miller, J. Slansky, and R. Ahmed. 1998. Counting antigen-specific CD8 T cells: a reevaluation of bystander activation during viral infection. *Immunity* 8: 177-187.
49. Kaech, S. M., and W. Cui. 2012. Transcriptional control of effector and memory CD8+ T cell differentiation. *Nature reviews. Immunology* 12: 749-761.
50. Bahl, K., S. K. Kim, C. Calcagno, D. Ghersi, R. Puzone, F. Celada, L. K. Selin, and R. M. Welsh. 2006. IFN-induced attrition of CD8 T cells in the presence or absence of cognate antigen during the early stages of viral infections. *Journal of immunology (Baltimore, Md. : 1950)* 176: 4284-4295.
51. Upton, J. W., and F. K. Chan. 2014. Staying alive: cell death in antiviral immunity. *Molecular cell* 54: 273-280.
52. Su, H. C., and M. J. Lenardo. 2008. Genetic defects of apoptosis and primary immunodeficiency. *Immunology and allergy clinics of North America* 28: 329-351, ix.
53. Zhang, H. G., M. Fleck, E. R. Kern, D. Liu, Y. Wang, H. C. Hsu, P. Yang, Z. Wang, D. T. Curiel, T. Zhou, and J. D. Mountz. 2000. Antigen presenting cells expressing Fas ligand down-modulate chronic inflammatory disease in Fas ligand-deficient mice. *The Journal of clinical investigation* 105: 813-821.
54. Olson, M. R., and S. M. Varga. 2009. Fas ligand is required for the development of respiratory syncytial virus vaccine-enhanced disease. *Journal of immunology (Baltimore, Md. : 1950)* 182: 3024-3031.
55. Balkow, S., A. Kersten, T. T. Tran, T. Stehle, P. Grosse, C. Museteanu, O. Utermohlen, H. Pircher, F. von Weizsacker, R. Wallich, A. Mullbacher, and M. M. Simon. 2001. Concerted action of the FasL/Fas and perforin/granzyme A and B pathways is mandatory for the development of early viral hepatitis but not for recovery from viral infection. *Journal of virology* 75: 8781-8791.
56. Singh, A., and M. Suresh. 2007. A role for TNF in limiting the duration of CTL effector phase and magnitude of CD8 T cell memory. *Journal of leukocyte biology* 82: 1201-1211.
57. Redmond, W. L., C. H. Wei, H. T. Kreuwel, and L. A. Sherman. 2008. The apoptotic pathway contributing to the deletion of naive CD8 T cells during the induction of peripheral tolerance to a cross-presented self-antigen. *Journal of immunology (Baltimore, Md. : 1950)* 180: 5275-5282.
58. Liao, W., J. X. Lin, and W. J. Leonard. 2011. IL-2 family cytokines: new insights into the complex roles of IL-2 as a broad regulator of T helper cell differentiation. *Current opinion in immunology* 23: 598-604.
59. Bouillet, P., D. Metcalf, D. C. Huang, D. M. Tarlinton, T. W. Kay, F. Kontgen, J. M. Adams, and A. Strasser. 1999. Proapoptotic Bcl-2 relative Bim required for certain apoptotic responses, leukocyte homeostasis, and to preclude autoimmunity. *Science (New York, N.Y.)* 286: 1735-1738.

60. Weant, A. E., R. D. Michalek, I. U. Khan, B. C. Holbrook, M. C. Willingham, and J. M. Grayson. 2008. Apoptosis regulators Bim and Fas function concurrently to control autoimmunity and CD8+ T cell contraction. *Immunity* 28: 218-230.
61. Tripathi, P., B. Koss, J. T. Opferman, and D. A. Hildeman. 2013. Mcl-1 antagonizes Bax/Bak to promote effector CD4(+) and CD8(+) T-cell responses. *Cell death and differentiation* 20: 998-1007.
62. Kane, L. P., J. Lin, and A. Weiss. 2000. Signal transduction by the TCR for antigen. *Current opinion in immunology* 12: 242-249.
63. Lathrop, S. K., C. A. Huddleston, P. A. Dullforce, M. J. Montfort, A. D. Weinberg, and D. C. Parker. 2004. A signal through OX40 (CD134) allows anergic, autoreactive T cells to acquire effector cell functions. *Journal of immunology (Baltimore, Md. : 1950)* 172: 6735-6743.
64. Kuo, C. T., and J. M. Leiden. 1999. Transcriptional regulation of T lymphocyte development and function. *Annual review of immunology* 17: 149-187.
65. Li, Y., Q. Yu, Z. Zhang, J. Wang, S. Li, J. Zhang, and G. Liu. 2016. TH9 cell differentiation, transcriptional control and function in inflammation, autoimmune diseases and cancer. *Oncotarget* 7: 71001-71012.
66. Masopust, D., and J. M. Schenkel. 2013. The integration of T cell migration, differentiation and function. *Nature reviews. Immunology* 13: 309-320.
67. Yao, Z., Y. Kanno, M. Kerenyi, G. Stephens, L. Durant, W. T. Watford, A. Laurence, G. W. Robinson, E. M. Shevach, R. Moriggl, L. Hennighausen, C. Wu, and J. J. O'Shea. 2007. Nonredundant roles for Stat5a/b in directly regulating Foxp3. *Blood* 109: 4368-4375.
68. Springer, T. A. 1994. Traffic signals for lymphocyte recirculation and leukocyte emigration: the multistep paradigm. *Cell* 76: 301-314.
69. Budhu, S., J. D. Loike, A. Pandolfi, S. Han, G. Catalano, A. Constantinescu, R. Clynes, and S. C. Silverstein. 2010. CD8+ T cell concentration determines their efficiency in killing cognate antigen-expressing syngeneic mammalian cells in vitro and in mouse tissues. *The Journal of experimental medicine* 207: 223-235.
70. Curtsinger, J. M., D. C. Lins, and M. F. Mescher. 2003. Signal 3 determines tolerance versus full activation of naive CD8 T cells: dissociating proliferation and development of effector function. *The Journal of experimental medicine* 197: 1141-1151.
71. Gerritsen, B., and A. Pandit. 2016. The memory of a killer T cell: models of CD8(+) T cell differentiation. *Immunology and cell biology* 94: 236-241.
72. Bansal-Pakala, P., B. S. Halteman, M. H. Cheng, and M. Croft. 2004. Costimulation of CD8 T cell responses by OX40. *Journal of immunology (Baltimore, Md. : 1950)* 172: 4821-4825.
73. Sallusto, F., D. Lenig, R. Forster, M. Lipp, and A. Lanzavecchia. 1999. Two subsets of memory T lymphocytes with distinct homing potentials and effector functions. *Nature* 401: 708-712.
74. Kallies, A. 2008. Distinct regulation of effector and memory T-cell differentiation. *Immunology and cell biology* 86: 325-332.

75. Mahnke, Y. D., T. M. Brodie, F. Sallusto, M. Roederer, and E. Lugli. 2013. The who's who of T-cell differentiation: human memory T-cell subsets. *European journal of immunology* 43: 2797-2809.
76. Rochman, Y., R. Spolski, and W. J. Leonard. 2009. New insights into the regulation of T cells by gamma(c) family cytokines. *Nature reviews. Immunology* 9: 480-490.
77. Zhang, J. M., and J. An. 2007. Cytokines, inflammation, and pain. *International anesthesiology clinics* 45: 27-37.
78. Lucey, D. R., M. Clerici, and G. M. Shearer. 1996. Type 1 and type 2 cytokine dysregulation in human infectious, neoplastic, and inflammatory diseases. *Clinical microbiology reviews* 9: 532-562.
79. Leonard, W. J., J. X. Lin, and J. J. O'Shea. 2019. The gammac Family of Cytokines: Basic Biology to Therapeutic Ramifications. *Immunity* 50: 832-850.
80. Waldmann, T. A. 2006. The biology of interleukin-2 and interleukin-15: implications for cancer therapy and vaccine design. *Nature reviews. Immunology* 6: 595-601.
81. McNamara, M. J., M. J. Kasiewicz, S. N. Linch, C. Dubay, and W. L. Redmond. 2014. Common gamma chain (gammac) cytokines differentially potentiate TNFR family signaling in antigen-activated CD8(+) T cells. *J Immunother Cancer* 2: 28.
82. Shuai, K., and B. Liu. 2003. Regulation of JAK-STAT signalling in the immune system. *Nature reviews. Immunology* 3: 900-911.
83. D'Souza, W. N., and L. Lefrancois. 2003. IL-2 is not required for the initiation of CD8 T cell cycling but sustains expansion. *Journal of immunology (Baltimore, Md. : 1950)* 171: 5727-5735.
84. Hatakeyama, M., T. Kono, N. Kobayashi, A. Kawahara, S. D. Levin, R. M. Perlmutter, and T. Taniguchi. 1991. Interaction of the IL-2 receptor with the src-family kinase p56lck: identification of novel intermolecular association. *Science (New York, N.Y.)* 252: 1523-1528.
85. Delespine-Carmagnat, M., G. Bouvier, G. Allee, R. Fagard, and J. Bertoglio. 1999. Biochemical analysis of interleukin-2 receptor beta chain phosphorylation by p56(lck). *FEBS letters* 447: 241-246.
86. Ross, S. H., C. Rollings, K. E. Anderson, P. T. Hawkins, L. R. Stephens, and D. A. Cantrell. 2016. Phosphoproteomic Analyses of Interleukin 2 Signaling Reveal Integrated JAK Kinase-Dependent and -Independent Networks in CD8(+) T Cells. *Immunity* 45: 685-700.
87. Miyazaki, T., A. Kawahara, H. Fujii, Y. Nakagawa, Y. Minami, Z. J. Liu, I. Oishi, O. Silvennoinen, B. A. Witthuhn, J. N. Ihle, and et al. 1994. Functional activation of Jak1 and Jak3 by selective association with IL-2 receptor subunits. *Science (New York, N.Y.)* 266: 1045-1047.
88. Lin, J. X., and W. J. Leonard. 2000. The role of Stat5a and Stat5b in signaling by IL-2 family cytokines. *Oncogene* 19: 2566-2576.
89. Malek, T. R., and I. Castro. 2010. Interleukin-2 receptor signaling: at the interface between tolerance and immunity. *Immunity* 33: 153-165.

90. O'Shea, J. J., D. M. Schwartz, A. V. Villarino, M. Gadina, I. B. McInnes, and A. Laurence. 2015. The JAK-STAT pathway: impact on human disease and therapeutic intervention. *Annual review of medicine* 66: 311-328.
91. Snow, J. W., N. Abraham, M. C. Ma, B. G. Herndier, A. W. Pastuszak, and M. A. Goldsmith. 2003. Loss of tolerance and autoimmunity affecting multiple organs in STAT5A/5B-deficient mice. *Journal of immunology (Baltimore, Md. : 1950)* 171: 5042-5050.
92. Yang, X. P., K. Ghoreschi, S. M. Steward-Tharp, J. Rodriguez-Canales, J. Zhu, J. R. Grainger, K. Hirahara, H. W. Sun, L. Wei, G. Vahedi, Y. Kanno, J. J. O'Shea, and A. Laurence. 2011. Opposing regulation of the locus encoding IL-17 through direct, reciprocal actions of STAT3 and STAT5. *Nature immunology* 12: 247-254.
93. Stittrich, A. B., C. Haftmann, E. Sgouroudis, A. A. Kuhl, A. N. Hegazy, I. Panse, R. Riedel, M. Flossdorf, J. Dong, F. Fuhrmann, G. A. Heinz, Z. Fang, N. Li, U. Bissels, F. Hatam, A. Jahn, B. Hammoud, M. Matz, F. M. Schulze, R. Baumgrass, A. Bosio, H. J. Mollenkopf, J. Grun, A. Thiel, W. Chen, T. Hofer, C. Loddenkemper, M. Lohning, H. D. Chang, N. Rajewsky, A. Radbruch, and M. F. Mashreghi. 2010. The microRNA miR-182 is induced by IL-2 and promotes clonal expansion of activated helper T lymphocytes. *Nature immunology* 11: 1057-1062.
94. Ravichandran, K. S., and S. J. Burakoff. 1994. The adapter protein Shc interacts with the interleukin-2 (IL-2) receptor upon IL-2 stimulation. *The Journal of biological chemistry* 269: 1599-1602.
95. Hodi, F. S., S. J. O'Day, D. F. McDermott, R. W. Weber, J. A. Sosman, J. B. Haanen, R. Gonzalez, C. Robert, D. Schadendorf, J. C. Hassel, W. Akerley, A. J. van den Eertwegh, J. Lutzky, P. Lorigan, J. M. Vaubel, G. P. Linette, D. Hogg, C. H. Ottensmeier, C. Lebbe, C. Peschel, I. Quirt, J. I. Clark, J. D. Wolchok, J. S. Weber, J. Tian, M. J. Yellin, G. M. Nichol, A. Hoos, and W. J. Urba. 2010. Improved survival with ipilimumab in patients with metastatic melanoma. *The New England journal of medicine* 363: 711-723.
96. Reif, K., L. Buday, J. Downward, and D. A. Cantrell. 1994. SH3 domains of the adapter molecule Grb2 complex with two proteins in T cells: the guanine nucleotide exchange protein Sos and a 75-kDa protein that is a substrate for T cell antigen receptor-activated tyrosine kinases. *The Journal of biological chemistry* 269: 14081-14087.
97. Ray, J. P., M. M. Staron, J. A. Shyer, P. C. Ho, H. D. Marshall, S. M. Gray, B. J. Laidlaw, K. Araki, R. Ahmed, S. M. Kaech, and J. Craft. 2015. The Interleukin-2-mTORc1 Kinase Axis Defines the Signaling, Differentiation, and Metabolism of T Helper 1 and Follicular B Helper T Cells. *Immunity* 43: 690-702.
98. Saxton, R. A., and D. M. Sabatini. 2017. mTOR Signaling in Growth, Metabolism, and Disease. *Cell* 168: 960-976.
99. Finlay, D. K., E. Rosenzweig, L. V. Sinclair, C. Feijoo-Carnero, J. L. Hukelmann, J. Rolf, A. A. Panteleyev, K. Okkenhaug, and D. A. Cantrell. 2012. PDK1 regulation of mTOR and hypoxia-inducible factor 1 integrate metabolism and migration of CD8+ T cells. *The Journal of experimental medicine* 209: 2441-2453.

100. Hukelmann, J. L., K. E. Anderson, L. V. Sinclair, K. M. Grzes, A. B. Murillo, P. T. Hawkins, L. R. Stephens, A. I. Lamond, and D. A. Cantrell. 2016. The cytotoxic T cell proteome and its shaping by the kinase mTOR. *Nature immunology* 17: 104-112.
101. Franke, T. F., D. R. Kaplan, and L. C. Cantley. 1997. PI3K: downstream AKTion blocks apoptosis. *Cell* 88: 435-437.
102. Boise, L. H., A. J. Minn, P. J. Noel, C. H. June, M. A. Accavitti, T. Lindsten, and C. B. Thompson. 1995. CD28 costimulation can promote T cell survival by enhancing the expression of Bcl-XL. *Immunity* 3: 87-98.
103. Salomon, B., and J. A. Bluestone. 2001. Complexities of CD28/B7: CTLA-4 costimulatory pathways in autoimmunity and transplantation. *Annual review of immunology* 19: 225-252.
104. Redmond, W. L., C. E. Ruby, and A. D. Weinberg. 2009. The role of OX40-mediated co-stimulation in T-cell activation and survival. *Critical reviews in immunology* 29: 187-201.
105. Dustin, M. L., and D. Depoil. 2011. New insights into the T cell synapse from single molecule techniques. *Nature reviews. Immunology* 11: 672-684.
106. Melero, I., D. Hirschhorn-Cymerman, A. Morales-Kastresana, M. F. Sanmamed, and J. D. Wolchok. 2013. Agonist antibodies to TNFR molecules that costimulate T and NK cells. *Clinical cancer research : an official journal of the American Association for Cancer Research* 19: 1044-1053.
107. An, H. J., Y. J. Kim, D. H. Song, B. S. Park, H. M. Kim, J. D. Lee, S. G. Paik, J. O. Lee, and H. Lee. 2011. Crystallographic and mutational analysis of the CD40-CD154 complex and its implications for receptor activation. *The Journal of biological chemistry* 286: 11226-11235.
108. Croft, M. 2009. The role of TNF superfamily members in T-cell function and diseases. *Nature reviews. Immunology* 9: 271-285.
109. Wu, H. 2004. Assembly of post-receptor signaling complexes for the tumor necrosis factor receptor superfamily. *Advances in protein chemistry* 68: 225-279.
110. Snell, L. M., G. H. Lin, A. J. McPherson, T. J. Moraes, and T. H. Watts. 2011. T-cell intrinsic effects of GITR and 4-1BB during viral infection and cancer immunotherapy. *Immunological reviews* 244: 197-217.
111. al-Shamkhani, A., M. L. Birkeland, M. Puklavec, M. H. Brown, W. James, and A. N. Barclay. 1996. OX40 is differentially expressed on activated rat and mouse T cells and is the sole receptor for the OX40 ligand. *European journal of immunology* 26: 1695-1699.
112. Baum, P. R., R. B. Gayle, 3rd, F. Ramsdell, S. Srinivasan, R. A. Sorensen, M. L. Watson, M. F. Seldin, E. Baker, G. R. Sutherland, K. N. Clifford, and et al. 1994. Molecular characterization of murine and human OX40/OX40 ligand systems: identification of a human OX40 ligand as the HTLV-1-regulated protein gp34. *The EMBO journal* 13: 3992-4001.
113. Paterson, D. J., W. A. Jefferies, J. R. Green, M. R. Brandon, P. Corthesy, M. Puklavec, and A. F. Williams. 1987. Antigens of activated rat T lymphocytes

including a molecule of 50,000 Mr detected only on CD4 positive T blasts. *Molecular immunology* 24: 1281-1290.
114. Manickasingham, S. P., S. M. Anderton, C. Burkhart, and D. C. Wraith. 1998. Qualitative and quantitative effects of CD28/B7-mediated costimulation on naive T cells in vitro. *Journal of immunology (Baltimore, Md. : 1950)* 161: 3827-3835.
115. Bour-Jordan, H., and J. A. Bluestone. 2009. Regulating the regulators: costimulatory signals control the homeostasis and function of regulatory T cells. *Immunological reviews* 229: 41-66.
116. Verdeil, G., D. Puthier, C. Nguyen, A. M. Schmitt-Verhulst, and N. Auphan-Anezin. 2006. STAT5-mediated signals sustain a TCR-initiated gene expression program toward differentiation of CD8 T cell effectors. *Journal of immunology (Baltimore, Md. : 1950)* 176: 4834-4842.
117. Gramaglia, I., A. Jember, S. D. Pippig, A. D. Weinberg, N. Killeen, and M. Croft. 2000. The OX40 costimulatory receptor determines the development of CD4 memory by regulating primary clonal expansion. *Journal of immunology (Baltimore, Md. : 1950)* 165: 3043-3050.
118. Evans, D. E., R. A. Prell, C. J. Thalhofer, A. A. Hurwitz, and A. D. Weinberg. 2001. Engagement of OX40 enhances antigen-specific CD4(+) T cell mobilization/memory development and humoral immunity: comparison of alphaOX-40 with alphaCTLA-4. *Journal of immunology (Baltimore, Md. : 1950)* 167: 6804-6811.
119. Ruby, C. E., W. L. Redmond, D. Haley, and A. D. Weinberg. 2007. Anti-OX40 stimulation in vivo enhances CD8+ memory T cell survival and significantly increases recall responses. *European journal of immunology* 37: 157-166.
120. Takeda, I., S. Ine, N. Killeen, L. C. Ndhlovu, K. Murata, S. Satomi, K. Sugamura, and N. Ishii. 2004. Distinct roles for the OX40-OX40 ligand interaction in regulatory and nonregulatory T cells. *Journal of immunology (Baltimore, Md. : 1950)* 172: 3580-3589.
121. Compaan, D. M., and S. G. Hymowitz. 2006. The crystal structure of the costimulatory OX40-OX40L complex. *Structure (London, England : 1993)* 14: 1321-1330.
122. Flynn, S., K. M. Toellner, C. Raykundalia, M. Goodall, and P. Lane. 1998. CD4 T cell cytokine differentiation: the B cell activation molecule, OX40 ligand, instructs CD4 T cells to express interleukin 4 and upregulates expression of the chemokine receptor, Blr-1. *The Journal of experimental medicine* 188: 297-304.
123. Ohshima, Y., Y. Tanaka, H. Tozawa, Y. Takahashi, C. Maliszewski, and G. Delespesse. 1997. Expression and function of OX40 ligand on human dendritic cells. *Journal of immunology (Baltimore, Md. : 1950)* 159: 3838-3848.
124. Rogers, P. R., J. Song, I. Gramaglia, N. Killeen, and M. Croft. 2001. OX40 promotes Bcl-xL and Bcl-2 expression and is essential for long-term survival of CD4 T cells. *Immunity* 15: 445-455.
125. Song, J., T. So, M. Cheng, X. Tang, and M. Croft. 2005. Sustained survivin expression from OX40 costimulatory signals drives T cell clonal expansion. *Immunity* 22: 621-631.

126. Ribatti, D. 2017. The concept of immune surveillance against tumors. The first theories. *Oncotarget* 8: 7175-7180.
127. Gross, L. 1943. Intradermal Immunization of C3H Mice against a Sarcoma That Originated in an Animal of the Same Line. *Cancer research* 3: 326-333.
128. Foley, E. J. 1953. Antigenic properties of methylcholanthrene-induced tumors in mice of the strain of origin. *Cancer research* 13: 835-837.
129. Dunn, G. P., L. J. Old, and R. D. Schreiber. 2004. The three Es of cancer immunoediting. *Annual review of immunology* 22: 329-360.
130. Dunn, G. P., A. T. Bruce, H. Ikeda, L. J. Old, and R. D. Schreiber. 2002. Cancer immunoediting: from immunosurveillance to tumor escape. *Nature immunology* 3: 991-998.
131. Gasser, S., and D. H. Raulet. 2006. The DNA damage response arouses the immune system. *Cancer research* 66: 3959-3962.
132. Hanahan, D., and L. M. Coussens. 2012. Accessories to the crime: functions of cells recruited to the tumor microenvironment. *Cancer cell* 21: 309-322.
133. Balkwill, F. 2004. Cancer and the chemokine network. *Nature reviews. Cancer* 4: 540-550.
134. Witsch, E., M. Sela, and Y. Yarden. 2010. Roles for growth factors in cancer progression. *Physiology (Bethesda, Md.)* 25: 85-101.
135. Oiseth, S., and M. Aziz. 2017. Cancer immunotherapy: a brief review of the history, possibilities, and challenges ahead. *Journal of Cancer Metastasis and Treatment* 3: 250.
136. Ledford, H. 2014. Cancer treatment: The killer within. *Nature* 508: 24-26.
137. Sharma, P., and J. P. Allison. 2015. The future of immune checkpoint therapy. *Science (New York, N.Y.)* 348: 56-61.
138. Mitchison, N. A. 1955. Studies on the immunological response to foreign tumor transplants in the mouse. I. The role of lymph node cells in conferring immunity by adoptive transfer. *The Journal of experimental medicine* 102: 157-177.
139. Morgan, D. A., F. W. Ruscetti, and R. Gallo. 1976. Selective in vitro growth of T lymphocytes from normal human bone marrows. *Science (New York, N.Y.)* 193: 1007-1008.
140. Lotze, M. T., L. W. Frana, S. O. Sharrow, R. J. Robb, and S. A. Rosenberg. 1985. In vivo administration of purified human interleukin 2. I. Half-life and immunologic effects of the Jurkat cell line-derived interleukin 2. *Journal of immunology (Baltimore, Md. : 1950)* 134: 157-166.
141. Devos, R., G. Plaetinck, H. Cheroutre, G. Simons, W. Degrave, J. Tavernier, E. Remaut, and W. Fiers. 1983. Molecular cloning of human interleukin 2 cDNA and its expression in E. coli. *Nucleic acids research* 11: 4307-4323.
142. Rosenberg, S. A., E. A. Grimm, M. McGrogan, M. Doyle, E. Kawasaki, K. Koths, and D. F. Mark. 1984. Biological activity of recombinant human interleukin-2 produced in Escherichia coli. *Science (New York, N.Y.)* 223: 1412-1414.
143. Rosenberg, S. A., J. J. Mule, P. J. Spiess, C. M. Reichert, and S. L. Schwarz. 1985. Regression of established pulmonary metastases and subcutaneous tumor

mediated by the systemic administration of high-dose recombinant interleukin 2. *The Journal of experimental medicine* 161: 1169-1188.
144. Rosenberg, S. A., M. T. Lotze, L. M. Muul, S. Leitman, A. E. Chang, S. E. Ettinghausen, Y. L. Matory, J. M. Skibber, E. Shiloni, J. T. Vetto, and et al. 1985. Observations on the systemic administration of autologous lymphokine-activated killer cells and recombinant interleukin-2 to patients with metastatic cancer. *The New England journal of medicine* 313: 1485-1492.
145. Rosenberg, S. A., M. T. Lotze, L. M. Muul, A. E. Chang, F. P. Avis, S. Leitman, W. M. Linehan, C. N. Robertson, R. E. Lee, J. T. Rubin, and et al. 1987. A progress report on the treatment of 157 patients with advanced cancer using lymphokine-activated killer cells and interleukin-2 or high-dose interleukin-2 alone. *The New England journal of medicine* 316: 889-897.
146. Rosenberg, S. A. 2014. IL-2: the first effective immunotherapy for human cancer. *Journal of immunology (Baltimore, Md. : 1950)* 192: 5451-5458.
147. Greenwald, R. J., G. J. Freeman, and A. H. Sharpe. 2005. The B7 family revisited. *Annual review of immunology* 23: 515-548.
148. Zou, W., and L. Chen. 2008. Inhibitory B7-family molecules in the tumour microenvironment. *Nature reviews. Immunology* 8: 467-477.
149. Pardoll, D. M. 2012. The blockade of immune checkpoints in cancer immunotherapy. *Nature reviews. Cancer* 12: 252-264.
150. Thompson, C. B., and J. P. Allison. 1997. The emerging role of CTLA-4 as an immune attenuator. *Immunity* 7: 445-450.
151. Francisco, L. M., P. T. Sage, and A. H. Sharpe. 2010. The PD-1 pathway in tolerance and autoimmunity. *Immunological reviews* 236: 219-242.
152. Spranger, S., R. M. Spaapen, Y. Zha, J. Williams, Y. Meng, T. T. Ha, and T. F. Gajewski. 2013. Up-regulation of PD-L1, IDO, and T(regs) in the melanoma tumor microenvironment is driven by CD8(+) T cells. *Science translational medicine* 5: 200ra116.
153. Walker, L. S., and D. M. Sansom. 2011. The emerging role of CTLA4 as a cell-extrinsic regulator of T cell responses. *Nature reviews. Immunology* 11: 852-863.
154. Wei, S. C., J. H. Levine, A. P. Cogdill, Y. Zhao, N. A. S. Anang, M. C. Andrews, P. Sharma, J. Wang, J. A. Wargo, D. Pe'er, and J. P. Allison. 2017. Distinct Cellular Mechanisms Underlie Anti-CTLA-4 and Anti-PD-1 Checkpoint Blockade. *Cell* 170: 1120-1133.e1117.
155. De Sousa Linhares, A., J. Leitner, K. Grabmeier-Pfistershammer, and P. Steinberger. 2018. Not All Immune Checkpoints Are Created Equal. *Frontiers in immunology* 9: 1909.
156. Robert, C., L. Thomas, I. Bondarenko, S. O'Day, J. Weber, C. Garbe, C. Lebbe, J. F. Baurain, A. Testori, J. J. Grob, N. Davidson, J. Richards, M. Maio, A. Hauschild, W. H. Miller, Jr., P. Gascon, M. Lotem, K. Harmankaya, R. Ibrahim, S. Francis, T. T. Chen, R. Humphrey, A. Hoos, and J. D. Wolchok. 2011. Ipilimumab plus dacarbazine for previously untreated metastatic melanoma. *The New England journal of medicine* 364: 2517-2526.

157. Robert, C., G. V. Long, B. Brady, C. Dutriaux, M. Maio, L. Mortier, J. C. Hassel, P. Rutkowski, C. McNeil, E. Kalinka-Warzocha, K. J. Savage, M. M. Hernberg, C. Lebbe, J. Charles, C. Mihalcioiu, V. Chiarion-Sileni, C. Mauch, F. Cognetti, A. Arance, H. Schmidt, D. Schadendorf, H. Gogas, L. Lundgren-Eriksson, C. Horak, B. Sharkey, I. M. Waxman, V. Atkinson, and P. A. Ascierto. 2015. Nivolumab in previously untreated melanoma without BRAF mutation. *The New England journal of medicine* 372: 320-330.
158. Robert, C., J. Schachter, G. V. Long, A. Arance, J. J. Grob, L. Mortier, A. Daud, M. S. Carlino, C. McNeil, M. Lotem, J. Larkin, P. Lorigan, B. Neyns, C. U. Blank, O. Hamid, C. Mateus, R. Shapira-Frommer, M. Kosh, H. Zhou, N. Ibrahim, S. Ebbinghaus, and A. Ribas. 2015. Pembrolizumab versus Ipilimumab in Advanced Melanoma. *The New England journal of medicine* 372: 2521-2532.
159. Wieder, T., T. Eigentler, E. Brenner, and M. Rocken. 2018. Immune checkpoint blockade therapy. *The Journal of allergy and clinical immunology* 142: 1403-1414.
160. Hargadon, K. M., C. E. Johnson, and C. J. Williams. 2018. Immune checkpoint blockade therapy for cancer: An overview of FDA-approved immune checkpoint inhibitors. *International immunopharmacology* 62: 29-39.
161. Helmink, B. A., P. O. Gaudreau, and J. A. Wargo. 2018. Immune Checkpoint Blockade across the Cancer Care Continuum. *Immunity* 48: 1077-1080.
162. Marcus, L., S. J. Lemery, P. Keegan, and R. Pazdur. 2019. FDA Approval Summary: Pembrolizumab for the Treatment of Microsatellite Instability-High Solid Tumors. *Clinical cancer research : an official journal of the American Association for Cancer Research* 25: 3753-3758.
163. Gide, T. N., J. S. Wilmott, R. A. Scolyer, and G. V. Long. 2018. Primary and Acquired Resistance to Immune Checkpoint Inhibitors in Metastatic Melanoma. *Clinical cancer research : an official journal of the American Association for Cancer Research* 24: 1260-1270.
164. Zhai, K., J. Chang, C. Wu, N. Lu, L. M. Huang, T. W. Zhang, D. K. Yu, W. Tan, and D. X. Lin. 2012. Association between genetic variations in tumor necrosis factor receptor genes and survival of patients with T-cell lymphoma. *Chinese journal of cancer* 31: 335-341.
165. Weiguang, Y., L. Dalin, X. Lidan, C. Yonggang, C. Shuang, L. Yanhong, X. Fengyan, F. Zhenkun, P. Da, and L. Dianjun. 2012. Association of OX40L polymorphisms with sporadic breast cancer in northeast Chinese Han population. *PloS one* 7: e41277.
166. Watts, T. H. 2005. TNF/TNFR family members in costimulation of T cell responses. *Annual review of immunology* 23: 23-68.
167. Mayes, P. A., K. W. Hance, and A. Hoos. 2018. The promise and challenges of immune agonist antibody development in cancer. *Nature reviews. Drug discovery* 17: 509-527.
168. Shimizu, J., S. Yamazaki, T. Takahashi, Y. Ishida, and S. Sakaguchi. 2002. Stimulation of CD25(+)CD4(+) regulatory T cells through GITR breaks immunological self-tolerance. *Nature immunology* 3: 135-142.

169. Kjaergaard, J., J. Tanaka, J. A. Kim, K. Rothchild, A. Weinberg, and S. Shu. 2000. Therapeutic efficacy of OX-40 receptor antibody depends on tumor immunogenicity and anatomic site of tumor growth. *Cancer research* 60: 5514-5521.
170. Aspeslagh, S., S. Postel-Vinay, S. Rusakiewicz, J. C. Soria, L. Zitvogel, and A. Marabelle. 2016. Rationale for anti-OX40 cancer immunotherapy. *European journal of cancer (Oxford, England : 1990)* 52: 50-66.
171. Weinberg, A. D., N. P. Morris, M. Kovacsovics-Bankowski, W. J. Urba, and B. D. Curti. 2011. Science gone translational: the OX40 agonist story. *Immunological reviews* 244: 218-231.
172. Linch, S. N., M. J. McNamara, and W. L. Redmond. 2015. OX40 Agonists and Combination Immunotherapy: Putting the Pedal to the Metal. *Frontiers in oncology* 5: 34.
173. Curti, B. D., M. Kovacsovics-Bankowski, N. Morris, E. Walker, L. Chisholm, K. Floyd, J. Walker, I. Gonzalez, T. Meeuwsen, B. A. Fox, T. Moudgil, W. Miller, D. Haley, T. Coffey, B. Fisher, L. Delanty-Miller, N. Rymarchyk, T. Kelly, T. Crocenzi, E. Bernstein, R. Sanborn, W. J. Urba, and A. D. Weinberg. 2013. OX40 is a potent immune-stimulating target in late-stage cancer patients. *Cancer research* 73: 7189-7198.
174. Guo, Z., X. Wang, D. Cheng, Z. Xia, M. Luan, and S. Zhang. 2014. PD-1 blockade and OX40 triggering synergistically protects against tumor growth in a murine model of ovarian cancer. *PloS one* 9: e89350.
175. Polesso, F., A. D. Weinberg, and A. E. Moran. 2019. Late-Stage Tumor Regression after PD-L1 Blockade Plus a Concurrent OX40 Agonist. *Cancer immunology research* 7: 269-281.
176. Shrimali, R. K., S. Ahmad, V. Verma, P. Zeng, S. Ananth, P. Gaur, R. M. Gittelman, E. Yusko, C. Sanders, H. Robins, S. A. Hammond, J. E. Janik, M. Mkrtichyan, S. Gupta, and S. N. Khleif. 2017. Concurrent PD-1 Blockade Negates the Effects of OX40 Agonist Antibody in Combination Immunotherapy through Inducing T-cell Apoptosis. *Cancer immunology research* 5: 755-766.
177. Messenheimer, D. J., S. M. Jensen, M. E. Afentoulis, K. W. Wegmann, Z. Feng, D. J. Friedman, M. J. Gough, W. J. Urba, and B. A. Fox. 2017. Timing of PD-1 Blockade Is Critical to Effective Combination Immunotherapy with Anti-OX40. *Clinical cancer research : an official journal of the American Association for Cancer Research* 23: 6165-6177.
178. Dawicki, W., and T. H. Watts. 2004. Expression and function of 4-1BB during CD4 versus CD8 T cell responses in vivo. *European journal of immunology* 34: 743-751.
179. Starck, L., C. Scholz, B. Dorken, and P. T. Daniel. 2005. Costimulation by CD137/4-1BB inhibits T cell apoptosis and induces Bcl-xL and c-FLIP(short) via phosphatidylinositol 3-kinase and AKT/protein kinase B. *European journal of immunology* 35: 1257-1266.

180. Melero, I., W. W. Shuford, S. A. Newby, A. Aruffo, J. A. Ledbetter, K. E. Hellstrom, R. S. Mittler, and L. Chen. 1997. Monoclonal antibodies against the 4-1BB T-cell activation molecule eradicate established tumors. *Nature medicine* 3: 682-685.
181. Nam, K. O., H. Kang, S. M. Shin, K. H. Cho, B. Kwon, B. S. Kwon, S. J. Kim, and H. W. Lee. 2005. Cross-linking of 4-1BB activates TCR-signaling pathways in CD8+ T lymphocytes. *Journal of immunology (Baltimore, Md. : 1950)* 174: 1898-1905.
182. Li, B., J. Lin, M. Vanroey, M. Jure-Kunkel, and K. Jooss. 2007. Established B16 tumors are rejected following treatment with GM-CSF-secreting tumor cell immunotherapy in combination with anti-4-1BB mAb. *Clinical immunology (Orlando, Fla.)* 125: 76-87.
183. Curran, M. A., M. Kim, W. Montalvo, A. Al-Shamkhani, and J. P. Allison. 2011. Combination CTLA-4 blockade and 4-1BB activation enhances tumor rejection by increasing T-cell infiltration, proliferation, and cytokine production. *PloS one* 6: e19499.
184. Dubrot, J., F. Milheiro, C. Alfaro, A. Palazon, I. Martinez-Forero, J. L. Perez-Gracia, A. Morales-Kastresana, J. L. Romero-Trevejo, M. C. Ochoa, S. Hervas-Stubbs, J. Prieto, M. Jure-Kunkel, L. Chen, and I. Melero. 2010. Treatment with anti-CD137 mAbs causes intense accumulations of liver T cells without selective antitumor immunotherapeutic effects in this organ. *Cancer immunology, immunotherapy : CII* 59: 1223-1233.
185. Fisher, T. S., C. Kamperschroer, T. Oliphant, V. A. Love, P. D. Lira, R. Doyonnas, S. Bergqvist, S. M. Baxi, A. Rohner, A. C. Shen, C. Huang, S. A. Sokolowski, and L. L. Sharp. 2012. Targeting of 4-1BB by monoclonal antibody PF-05082566 enhances T-cell function and promotes anti-tumor activity. *Cancer immunology, immunotherapy : CII* 61: 1721-1733.
186. Tolcher, A. W., M. Sznol, S. Hu-Lieskovan, K. P. Papadopoulos, A. Patnaik, D. W. Rasco, D. Di Gravio, B. Huang, D. Gambhire, Y. Chen, A. D. Thall, N. Pathan, E. V. Schmidt, and L. Q. M. Chow. 2017. Phase Ib Study of Utomilumab (PF-05082566), a 4-1BB/CD137 Agonist, in Combination with Pembrolizumab (MK-3475) in Patients with Advanced Solid Tumors. *Clinical cancer research : an official journal of the American Association for Cancer Research* 23: 5349-5357.
187. van der Stegen, S. J., M. Hamieh, and M. Sadelain. 2015. The pharmacology of second-generation chimeric antigen receptors. *Nature reviews. Drug discovery* 14: 499-509.
188. Maude, S. L., N. Frey, P. A. Shaw, R. Aplenc, D. M. Barrett, N. J. Bunin, A. Chew, V. E. Gonzalez, Z. Zheng, S. F. Lacey, Y. D. Mahnke, J. J. Melenhorst, S. R. Rheingold, A. Shen, D. T. Teachey, B. L. Levine, C. H. June, D. L. Porter, and S. A. Grupp. 2014. Chimeric antigen receptor T cells for sustained remissions in leukemia. *The New England journal of medicine* 371: 1507-1517.
189. Rabinovich, G. A., and D. O. Croci. 2012. Regulatory circuits mediated by lectin-glycan interactions in autoimmunity and cancer. *Immunity* 36: 322-335.
190. Granier, C., E. De Guillebon, C. Blanc, H. Roussel, C. Badoual, E. Colin, A. Saldmann, A. Gey, S. Oudard, and E. Tartour. 2017. Mechanisms of action and rationale for the use of checkpoint inhibitors in cancer. *ESMO open* 2: e000213.

191. Pulluri, B., A. Kumar, M. Shaheen, J. Jeter, and S. Sundararajan. 2017. Tumor microenvironment changes leading to resistance of immune checkpoint inhibitors in metastatic melanoma and strategies to overcome resistance. *Pharmacological research* 123: 95-102.
192. Anderson, K. G., I. M. Stromnes, and P. D. Greenberg. 2017. Obstacles Posed by the Tumor Microenvironment to T cell Activity: A Case for Synergistic Therapies. *Cancer cell* 31: 311-325.
193. Chen, H. Y., A. Fermin, S. Vardhana, I. C. Weng, K. F. Lo, E. Y. Chang, E. Maverakis, R. Y. Yang, D. K. Hsu, M. L. Dustin, and F. T. Liu. 2009. Galectin-3 negatively regulates TCR-mediated CD4+ T-cell activation at the immunological synapse. *Proceedings of the National Academy of Sciences of the United States of America* 106: 14496-14501.
194. Grigorian, A., and M. Demetriou. 2010. Manipulating cell surface glycoproteins by targeting N-glycan-galectin interactions. *Methods in enzymology* 480: 245-266.
195. Barondes, S. H., V. Castronovo, D. N. Cooper, R. D. Cummings, K. Drickamer, T. Feizi, M. A. Gitt, J. Hirabayashi, C. Hughes, K. Kasai, and et al. 1994. Galectins: a family of animal beta-galactoside-binding lectins. *Cell* 76: 597-598.
196. Houzelstein, D., I. R. Goncalves, A. J. Fadden, S. S. Sidhu, D. N. Cooper, K. Drickamer, H. Leffler, and F. Poirier. 2004. Phylogenetic analysis of the vertebrate galectin family. *Molecular biology and evolution* 21: 1177-1187.
197. Dumic, J., S. Dabelic, and M. Flogel. 2006. Galectin-3: an open-ended story. *Biochimica et biophysica acta* 1760: 616-635.
198. Ahmed, H., and D. M. AlSadek. 2015. Galectin-3 as a Potential Target to Prevent Cancer Metastasis. *Clinical Medicine Insights. Oncology* 9: 113-121.
199. Ahmad, N., H. J. Gabius, S. Andre, H. Kaltner, S. Sabesan, R. Roy, B. Liu, F. Macaluso, and C. F. Brewer. 2004. Galectin-3 precipitates as a pentamer with synthetic multivalent carbohydrates and forms heterogeneous cross-linked complexes. *The Journal of biological chemistry* 279: 10841-10847.
200. Obermann, J., C. S. Priglinger, J. Merl-Pham, A. Geerlof, S. Priglinger, M. Gotz, and S. M. Hauck. 2017. Proteome-wide Identification of Glycosylation-dependent Interactors of Galectin-1 and Galectin-3 on Mesenchymal Retinal Pigment Epithelial (RPE) Cells. *Molecular & cellular proteomics : MCP* 16: 1528-1546.
201. Yang, R. Y., D. K. Hsu, and F. T. Liu. 1996. Expression of galectin-3 modulates T-cell growth and apoptosis. *Proceedings of the National Academy of Sciences of the United States of America* 93: 6737-6742.
202. Hsu, D. K., R. Y. Yang, J. Saegusa, and F. T. Liu. 2015. Analysis of the intracellular role of galectins in cell growth and apoptosis. *Methods in molecular biology (Clifton, N.J.)* 1207: 451-463.
203. Poirier, F., and E. J. Robertson. 1993. Normal development of mice carrying a null mutation in the gene encoding the L14 S-type lectin. *Development (Cambridge, England)* 119: 1229-1236.
204. Fowlis, D., C. Colnot, M. A. Ripoche, and F. Poirier. 1995. Galectin-3 is expressed in the notochord, developing bones, and skin of the postimplantation mouse

embryo. *Developmental dynamics : an official publication of the American Association of Anatomists* 203: 241-251.
205. Van den Brule, F. A., P. L. Fernandez, C. Buicu, F. T. Liu, P. Jackers, R. Lambotte, and V. Castronovo. 1997. Differential expression of galectin-1 and galectin-3 during first trimester human embryogenesis. *Developmental dynamics : an official publication of the American Association of Anatomists* 209: 399-405.
206. Joo, H. G., P. S. Goedegebuure, N. Sadanaga, M. Nagoshi, W. von Bernstorff, and T. J. Eberlein. 2001. Expression and function of galectin-3, a beta-galactoside-binding protein in activated T lymphocytes. *Journal of leukocyte biology* 69: 555-564.
207. Stillman, B. N., D. K. Hsu, M. Pang, C. F. Brewer, P. Johnson, F. T. Liu, and L. G. Baum. 2006. Galectin-3 and galectin-1 bind distinct cell surface glycoprotein receptors to induce T cell death. *Journal of immunology (Baltimore, Md. : 1950)* 176: 778-789.
208. Hsu, D. K., H. Y. Chen, and F. T. Liu. 2009. Galectin-3 regulates T-cell functions. *Immunological reviews* 230: 114-127.
209. Melief, S. M., M. Visser, S. H. van der Burg, and E. M. E. Verdegaal. 2017. IDO and galectin-3 hamper the ex vivo generation of clinical grade tumor-specific T cells for adoptive cell therapy in metastatic melanoma. *Cancer immunology, immunotherapy : CII* 66: 913-926.
210. Radosavljevic, G., I. Jovanovic, I. Majstorovic, M. Mitrovic, V. J. Lisnic, N. Arsenijevic, S. Jonjic, and M. L. Lukic. 2011. Deletion of galectin-3 in the host attenuates metastasis of murine melanoma by modulating tumor adhesion and NK cell activity. *Clinical & experimental metastasis* 28: 451-462.
211. Demotte, N., V. Stroobant, P. J. Courtoy, P. Van Der Smissen, D. Colau, I. F. Luescher, C. Hivroz, J. Nicaise, J. L. Squifflet, M. Mourad, D. Godelaine, T. Boon, and P. van der Bruggen. 2008. Restoring the association of the T cell receptor with CD8 reverses anergy in human tumor-infiltrating lymphocytes. *Immunity* 28: 414-424.
212. Demotte, N., G. Wieers, P. Van Der Smissen, M. Moser, C. Schmidt, K. Thielemans, J. L. Squifflet, B. Weynand, J. Carrasco, C. Lurquin, P. J. Courtoy, and P. van der Bruggen. 2010. A galectin-3 ligand corrects the impaired function of human CD4 and CD8 tumor-infiltrating lymphocytes and favors tumor rejection in mice. *Cancer research* 70: 7476-7488.
213. Kouo, T., L. Huang, A. B. Pucsek, M. Cao, S. Solt, T. Armstrong, and E. Jaffee. 2015. Galectin-3 Shapes Antitumor Immune Responses by Suppressing CD8+ T Cells via LAG-3 and Inhibiting Expansion of Plasmacytoid Dendritic Cells. *Cancer immunology research* 3: 412-423.
214. Mantovani, A., A. Sica, and M. Locati. 2007. New vistas on macrophage differentiation and activation. *European journal of immunology* 37: 14-16.
215. Norling, L. V., M. Perretti, and D. Cooper. 2009. Endogenous galectins and the control of the host inflammatory response. *The Journal of endocrinology* 201: 169-184.

216. Liu, F. T., D. K. Hsu, R. I. Zuberi, I. Kuwabara, E. Y. Chi, and W. R. Henderson, Jr. 1995. Expression and function of galectin-3, a beta-galactoside-binding lectin, in human monocytes and macrophages. *The American journal of pathology* 147: 1016-1028.
217. Sano, H., D. K. Hsu, L. Yu, J. R. Apgar, I. Kuwabara, T. Yamanaka, M. Hirashima, and F. T. Liu. 2000. Human galectin-3 is a novel chemoattractant for monocytes and macrophages. *Journal of immunology (Baltimore, Md. : 1950)* 165: 2156-2164.
218. MacKinnon, A. C., S. L. Farnworth, P. S. Hodkinson, N. C. Henderson, K. M. Atkinson, H. Leffler, U. J. Nilsson, C. Haslett, S. J. Forbes, and T. Sethi. 2008. Regulation of alternative macrophage activation by galectin-3. *Journal of immunology (Baltimore, Md. : 1950)* 180: 2650-2658.
219. Novak, R., S. Dabelic, and J. Dumic. 2012. Galectin-1 and galectin-3 expression profiles in classically and alternatively activated human macrophages. *Biochimica et biophysica acta* 1820: 1383-1390.
220. Shanshiashvili, L., E. Tsitsilashvili, N. Dabrundashvili, I. Kalandadze, and D. Mikeladze. 2017. Metabotropic glutamate receptor 5 may be involved in macrophage plasticity. *Biological research* 50: 4.
221. Cardoso, A. C., L. N. Andrade, S. O. Bustos, and R. Chammas. 2016. Galectin-3 Determines Tumor Cell Adaptive Strategies in Stressed Tumor Microenvironments. *Frontiers in oncology* 6: 127.
222. Ebrahim, A. H., Z. Alalawi, L. Mirandola, R. Rakhshanda, S. Dahlbeck, D. Nguyen, M. Jenkins, F. Grizzi, E. Cobos, J. A. Figueroa, and M. Chiriva-Internati. 2014. Galectins in cancer: carcinogenesis, diagnosis and therapy. *Annals of translational medicine* 2: 88.
223. Glinsky, V. V., G. V. Glinsky, O. V. Glinskii, V. H. Huxley, J. R. Turk, V. V. Mossine, S. L. Deutscher, K. J. Pienta, and T. P. Quinn. 2003. Intravascular metastatic cancer cell homotypic aggregation at the sites of primary attachment to the endothelium. *Cancer research* 63: 3805-3811.
224. Compagno, D., L. D. Gentilini, F. M. Jaworski, I. G. Perez, G. Contrufo, and D. J. Laderach. 2014. Glycans and galectins in prostate cancer biology, angiogenesis and metastasis. *Glycobiology* 24: 899-906.
225. Merseburger, A. S., M. W. Kramer, J. Hennenlotter, P. Simon, J. Knapp, J. T. Hartmann, A. Stenzl, J. Serth, and M. A. Kuczyk. 2008. Involvement of decreased Galectin-3 expression in the pathogenesis and progression of prostate cancer. *The Prostate* 68: 72-77.
226. Ahmed, H., P. P. Banerjee, and G. R. Vasta. 2007. Differential expression of galectins in normal, benign and malignant prostate epithelial cells: silencing of galectin-3 expression in prostate cancer by its promoter methylation. *Biochemical and biophysical research communications* 358: 241-246.
227. Knapp, J. S., S. D. Lokeshwar, U. Vogel, J. Hennenlotter, C. Schwentner, M. W. Kramer, A. Stenzl, and A. S. Merseburger. 2013. Galectin-3 expression in prostate cancer and benign prostate tissues: correlation with biochemical recurrence. *World journal of urology* 31: 351-358.

228. Wang, Y., P. Nangia-Makker, L. Tait, V. Balan, V. Hogan, K. J. Pienta, and A. Raz. 2009. Regulation of prostate cancer progression by galectin-3. *The American journal of pathology* 174: 1515-1523.
229. Nakajima, K., D. H. Kho, T. Yanagawa, Y. Harazono, V. Hogan, W. Chen, R. Ali-Fehmi, R. Mehra, and A. Raz. 2016. Galectin-3 Cleavage Alters Bone Remodeling: Different Outcomes in Breast and Prostate Cancer Skeletal Metastasis. *Cancer research* 76: 1391-1402.
230. Nangia-Makker, P., Y. Wang, T. Raz, L. Tait, V. Balan, V. Hogan, and A. Raz. 2010. Cleavage of galectin-3 by matrix metalloproteases induces angiogenesis in breast cancer. *International journal of cancer* 127: 2530-2541.
231. Ochieng, J., B. Green, S. Evans, O. James, and P. Warfield. 1998. Modulation of the biological functions of galectin-3 by matrix metalloproteinases. *Biochimica et biophysica acta* 1379: 97-106.
232. Yoshimura, A., A. Gemma, Y. Hosoya, E. Komaki, Y. Hosomi, T. Okano, K. Takenaka, K. Matuda, M. Seike, K. Uematsu, S. Hibino, M. Shibuya, T. Yamada, S. Hirohashi, and S. Kudoh. 2003. Increased expression of the LGALS3 (galectin 3) gene in human non-small-cell lung cancer. *Genes, chromosomes & cancer* 37: 159-164.
233. Chung, L. Y., S. J. Tang, Y. C. Wu, G. H. Sun, H. Y. Liu, and K. H. Sun. 2015. Galectin-3 augments tumor initiating property and tumorigenicity of lung cancer through interaction with beta-catenin. *Oncotarget* 6: 4936-4952.
234. Dange, M. C., N. Srinivasan, S. K. More, S. M. Bane, A. Upadhya, A. D. Ingle, R. P. Gude, R. Mukhopadhyaya, and R. D. Kalraiya. 2014. Galectin-3 expressed on different lung compartments promotes organ specific metastasis by facilitating arrest, extravasation and organ colonization via high affinity ligands on melanoma cells. *Clinical & experimental metastasis* 31: 661-673.
235. Liang, Y., H. Li, S. C. Hou, B. Hu, J. B. Miao, T. Li, B. You, L. X. Yu, L. Wang, Q. R. Chen, and X. Chen. 2009. [The expression of galectin-3 and osteopontin in occult metastasis of non-small cell lung cancer]. *Zhonghua wai ke za zhi [Chinese journal of surgery]* 47: 1061-1063.
236. Szoke, T., K. Kayser, J. D. Baumhakel, I. Trojan, J. Furak, L. Tiszlavicz, A. Horvath, K. Szluha, H. J. Gabius, and S. Andre. 2005. Prognostic significance of endogenous adhesion/growth-regulatory lectins in lung cancer. *Oncology* 69: 167-174.
237. Erez, N., M. Truitt, P. Olson, S. T. Arron, and D. Hanahan. 2010. Cancer-Associated Fibroblasts Are Activated in Incipient Neoplasia to Orchestrate Tumor-Promoting Inflammation in an NF-kappaB-Dependent Manner. *Cancer cell* 17: 135-147.
238. Linch, S., M. J. Kasiewicz, M. McNamara, I. Hilgart, M. Farhad, and W. Redmond. 2015. Galectin-3 inhibition using novel inhibitor GR-MD-02 improves survival and immune function while reducing tumor vasculature. *Journal for ImmunoTherapy of Cancer* 3: P306.
239. Linch., S. N., M. J. Kasiewicz., P. G. Traber., and W. L. Redmond. 2013. Dual Role for Galectin-3 in CD8 T cell Function. *Keystone Cancer Immunotherapy*.

240. Cotter, F., D. A. Smith, T. E. Boyd, D. A. Richards, C. Alemany, D. Loesch, G. Salogub, G. F. Tidmarsh, G. M. Gammon, and J. Gribben. 2009. Single-agent activity of GCS-100, a first-in-class galectin-3 antagonist, in elderly patients with relapsed chronic lymphocytic leukemia. *Journal of Clinical Oncology* 27: 7006-7006.
241. Grous, J. J., C. H. Redfern, D. Mahadevan, and J. Schindler. 2006. GCS-100, a galectin-3 antagonist, in refractory solid tumors: A phase I study. *Journal of Clinical Oncology* 24: 13023-13023.
242. Seguin, L., M. F. Camargo, H. I. Wettersten, S. Kato, J. S. Desgrosellier, T. von Schalscha, K. C. Elliott, E. Cosset, J. Lesperance, S. M. Weis, and D. A. Cheresh. 2017. Galectin-3, a Druggable Vulnerability for KRAS-Addicted Cancers. *Cancer discovery* 7: 1464-1479.
243. Sakaguchi, S., T. Yamaguchi, T. Nomura, and M. Ono. 2008. Regulatory T cells and immune tolerance. *Cell* 133: 775-787.
244. Marrack, P., J. Scott-Browne, and M. K. MacLeod. 2010. Terminating the immune response. *Immunological reviews* 236: 5-10.
245. Salek-Ardakani, S., M. Moutaftsi, S. Crotty, A. Sette, and M. Croft. 2008. OX40 drives protective vaccinia virus-specific CD8 T cells. *Journal of immunology (Baltimore, Md. : 1950)* 181: 7969-7976.
246. Yu, Q., F. Y. Yue, X. X. Gu, H. Schwartz, C. M. Kovacs, and M. A. Ostrowski. 2006. OX40 ligation of CD4+ T cells enhances virus-specific CD8+ T cell memory responses independently of IL-2 and CD4+ T regulatory cell inhibition. *Journal of immunology (Baltimore, Md. : 1950)* 176: 2486-2495.
247. Redmond, W. L., M. J. Gough, B. Charbonneau, T. L. Ratliff, and A. D. Weinberg. 2007. Defects in the acquisition of CD8 T cell effector function after priming with tumor or soluble antigen can be overcome by the addition of an OX40 agonist. *Journal of immunology (Baltimore, Md. : 1950)* 179: 7244-7253.
248. Williams, C. A., S. E. Murray, A. D. Weinberg, and D. C. Parker. 2007. OX40-mediated differentiation to effector function requires IL-2 receptor signaling but not CD28, CD40, IL-12Rbeta2, or T-bet. *Journal of immunology (Baltimore, Md. : 1950)* 178: 7694-7702.
249. Redmond, W. L., T. Triplett, K. Floyd, and A. D. Weinberg. 2012. Dual anti-OX40/IL-2 therapy augments tumor immunotherapy via IL-2R-mediated regulation of OX40 expression. *PLoS One* 7: e34467.
250. Kaur, M., D. Kumar, V. Butty, S. Singh, A. Esteban, G. R. Fink, H. L. Ploegh, and S. Sehrawat. 2018. Galectin-3 Regulates gamma-Herpesvirus Specific CD8 T Cell Immunity. *iScience* 9: 101-119.
251. Sarkar, S., V. Kalia, W. N. Haining, B. T. Konieczny, S. Subramaniam, and R. Ahmed. 2008. Functional and genomic profiling of effector CD8 T cell subsets with distinct memory fates. *The Journal of experimental medicine* 205: 625-640.
252. Mousavi, S. F., P. Soroosh, T. Takahashi, Y. Yoshikai, H. Shen, L. Lefrancois, J. Borst, K. Sugamura, and N. Ishii. 2008. OX40 costimulatory signals potentiate the memory commitment of effector CD8+ T cells. *Journal of immunology (Baltimore, Md. : 1950)* 181: 5990-6001.

253. Joshi, N. S., W. Cui, A. Chandele, H. K. Lee, D. R. Urso, J. Hagman, L. Gapin, and S. M. Kaech. 2007. Inflammation directs memory precursor and short-lived effector CD8(+) T cell fates via the graded expression of T-bet transcription factor. *Immunity* 27: 281-295.
254. Mostbock, S., M. E. Lutsiak, D. E. Milenic, K. Baidoo, J. Schlom, and H. Sabzevari. 2008. IL-2/anti-IL-2 antibody complex enhances vaccine-mediated antigen-specific CD8+ T cell responses and increases the ratio of effector/memory CD8+ T cells to regulatory T cells. *Journal of immunology (Baltimore, Md. : 1950)* 180: 5118-5129.
255. Letourneau, S., E. M. van Leeuwen, C. Krieg, C. Martin, G. Pantaleo, J. Sprent, C. D. Surh, and O. Boyman. 2010. IL-2/anti-IL-2 antibody complexes show strong biological activity by avoiding interaction with IL-2 receptor alpha subunit CD25. *Proceedings of the National Academy of Sciences of the United States of America* 107: 2171-2176.
256. Soto, R., C. Petersen, C. L. Novis, J. L. Kubinak, R. Bell, W. Z. Stephens, T. E. Lane, R. S. Fujinami, A. Bosque, R. M. O'Connell, and J. L. Round. 2017. Microbiota promotes systemic T-cell survival through suppression of an apoptotic factor. *Proceedings of the National Academy of Sciences of the United States of America* 114: 5497-5502.
257. Salek-Ardakani, S., and M. Croft. 2006. Regulation of CD4 T cell memory by OX40 (CD134). *Vaccine* 24: 872-883.
258. Song, A., X. Tang, K. M. Harms, and M. Croft. 2005. OX40 and Bcl-xL promote the persistence of CD8 T cells to recall tumor-associated antigen. *Journal of immunology (Baltimore, Md. : 1950)* 175: 3534-3541.
259. Song, J., S. Salek-Ardakani, P. R. Rogers, M. Cheng, L. Van Parijs, and M. Croft. 2004. The costimulation-regulated duration of PKB activation controls T cell longevity. *Nature immunology* 5: 150-158.
260. Saegusa, J., D. K. Hsu, W. Liu, I. Kuwabara, Y. Kuwabara, L. Yu, and F. T. Liu. 2008. Galectin-3 protects keratinocytes from UVB-induced apoptosis by enhancing AKT activation and suppressing ERK activation. *The Journal of investigative dermatology* 128: 2403-2411.
261. Dai, Z., B. T. Konieczny, and F. G. Lakkis. 2000. The dual role of IL-2 in the generation and maintenance of CD8+ memory T cells. *Journal of immunology (Baltimore, Md. : 1950)* 165: 3031-3036.
262. Song, J., T. So, and M. Croft. 2008. Activation of NF-kappaB1 by OX40 contributes to antigen-driven T cell expansion and survival. *Journal of immunology (Baltimore, Md. : 1950)* 180: 7240-7248.
263. Liu, L., T. Sakai, N. Sano, and K. Fukui. 2004. Nucling mediates apoptosis by inhibiting expression of galectin-3 through interference with nuclear factor kappaB signalling. *The Biochemical journal* 380: 31-41.
264. Christgen, M., S. von Ahsen, H. Christgen, F. Langer, and H. Kreipe. 2015. The region-of-interest size impacts on Ki67 quantification by computer-assisted image analysis in breast cancer. *Human pathology* 46: 1341-1349.

265. Urruticoechea, A., R. Alemany, J. Balart, A. Villanueva, F. Vinals, and G. Capella. 2010. Recent advances in cancer therapy: an overview. *Current pharmaceutical design* 16: 3-10.
266. Housman, G., S. Byler, S. Heerboth, K. Lapinska, M. Longacre, N. Snyder, and S. Sarkar. 2014. Drug resistance in cancer: an overview. *Cancers* 6: 1769-1792.
267. Wittekind, C., C. C. Compton, F. L. Greene, and L. H. Sobin. 2002. TNM residual tumor classification revisited. *Cancer* 94: 2511-2516.
268. Finn, O. J. 2008. Cancer immunology. *The New England journal of medicine* 358: 2704-2715.
269. Galon, J., F. Pagès, F. M. Marincola, M. Thurin, G. Trinchieri, B. A. Fox, T. F. Gajewski, and P. A. Ascierto. 2012. The immune score as a new possible approach for the classification of cancer. *J Transl Med* 10: 1-1.
270. Galon, J., B. Mlecnik, G. Bindea, H. K. Angell, A. Berger, C. Lagorce, A. Lugli, I. Zlobec, A. Hartmann, C. Bifulco, I. D. Nagtegaal, R. Palmqvist, G. V. Masucci, G. Botti, F. Tatangelo, P. Delrio, M. Maio, L. Laghi, F. Grizzi, M. Asslaber, C. D'Arrigo, F. Vidal-Vanaclocha, E. Zavadova, L. Chouchane, P. S. Ohashi, S. Hafezi-Bakhtiari, B. G. Wouters, M. Roehrl, L. Nguyen, Y. Kawakami, S. Hazama, K. Okuno, S. Ogino, P. Gibbs, P. Waring, N. Sato, T. Torigoe, K. Itoh, P. S. Patel, S. N. Shukla, Y. Wang, S. Kopetz, F. A. Sinicrope, V. Scripcariu, P. A. Ascierto, F. M. Marincola, B. A. Fox, and F. Pages. 2014. Towards the introduction of the 'Immunoscore' in the classification of malignant tumours. *The Journal of pathology* 232: 199-209.
271. Chan, J. K. 2014. The wonderful colors of the hematoxylin-eosin stain in diagnostic surgical pathology. *International journal of surgical pathology* 22: 12-32.
272. Carvajal-Hausdorf, D. E., K. A. Schalper, V. M. Neumeister, and D. L. Rimm. 2015. Quantitative measurement of cancer tissue biomarkers in the lab and in the clinic. *Laboratory investigation; a journal of technical methods and pathology* 95: 385-396.
273. Zhang, D., W. He, C. Wu, Y. Tan, Y. He, B. Xu, L. Chen, Q. Li, and J. Jiang. 2019. Scoring System for Tumor-Infiltrating Lymphocytes and Its Prognostic Value for Gastric Cancer. *Frontiers in immunology* 10: 71.
274. van der Loos, C. M. 2008. Multiple immunoenzyme staining: methods and visualizations for the observation with spectral imaging. *The journal of histochemistry and cytochemistry : official journal of the Histochemistry Society* 56: 313-328.
275. Lu, S., J. E. Stein, D. L. Rimm, D. W. Wang, J. M. Bell, D. B. Johnson, J. A. Sosman, K. A. Schalper, R. A. Anders, H. Wang, C. Hoyt, D. M. Pardoll, L. Danilova, and J. M. Taube. 2019. Comparison of Biomarker Modalities for Predicting Response to PD-1/PD-L1 Checkpoint Blockade: A Systematic Review and Meta-analysis. *JAMA oncology*.
276. Hofman, P., C. Badoual, F. Henderson, L. Berland, M. Hamila, E. Long-Mira, S. Lassalle, H. Roussel, V. Hofman, E. Tartour, and M. Ilie. 2019. Multiplexed Immunohistochemistry for Molecular and Immune Profiling in Lung Cancer-Just About Ready for Prime-Time? *Cancers* 11.

277. Johnson, D. B., J. Bordeaux, J. Y. Kim, C. Vaupel, D. L. Rimm, T. H. Ho, R. W. Joseph, A. I. Daud, R. M. Conry, E. M. Gaughan, L. F. Hernandez-Aya, A. Dimou, P. Funchain, J. Smithy, J. S. Witte, S. B. McKee, J. Ko, J. M. Wrangle, B. Dabbas, S. Tangri, J. Lameh, J. Hall, J. Markowitz, J. M. Balko, and N. Dakappagari. 2018. Quantitative Spatial Profiling of PD-1/PD-L1 Interaction and HLA-DR/IDO-1 Predicts Improved Outcomes of Anti-PD-1 Therapies in Metastatic Melanoma. *Clinical cancer research : an official journal of the American Association for Cancer Research* 24: 5250-5260.
278. Stack, E. C., C. Wang, K. A. Roman, and C. C. Hoyt. 2014. Multiplexed immunohistochemistry, imaging, and quantitation: a review, with an assessment of Tyramide signal amplification, multispectral imaging and multiplex analysis. *Methods (San Diego, Calif.)* 70: 46-58.
279. Pirici, D., L. Mogoanta, S. Kumar-Singh, I. Pirici, C. Margaritescu, C. Simionescu, and R. Stanescu. 2009. Antibody elution method for multiple immunohistochemistry on primary antibodies raised in the same species and of the same subtype. *The journal of histochemistry and cytochemistry : official journal of the Histochemistry Society* 57: 567-575.
280. Remark, R., T. Merghoub, N. Grabe, G. Litjens, D. Damotte, J. D. Wolchok, M. Merad, and S. Gnjatic. 2016. In-depth tissue profiling using multiplexed immunohistochemical consecutive staining on single slide. *Science immunology* 1: aaf6925.
281. Mason, D. Y., K. Micklem, and M. Jones. 2000. Double immunofluorescence labelling of routinely processed paraffin sections. *The Journal of pathology* 191: 452-461.
282. Peng, C. W., X. L. Liu, C. Chen, X. Liu, X. Q. Yang, D. W. Pang, X. B. Zhu, and Y. Li. 2011. Patterns of cancer invasion revealed by QDs-based quantitative multiplexed imaging of tumor microenvironment. *Biomaterials* 32: 2907-2917.
283. Osman, T. A., G. Oijordsbakken, D. E. Costea, and A. C. Johannessen. 2013. Successful triple immunoenzymatic method employing primary antibodies from same species and same immunoglobulin subclass. *European journal of histochemistry : EJH* 57: e22.
284. Glass, G., J. A. Papin, and J. W. Mandell. 2009. SIMPLE: a sequential immunoperoxidase labeling and erasing method. *The journal of histochemistry and cytochemistry : official journal of the Histochemistry Society* 57: 899-905.
285. Bobrow, M. N., T. D. Harris, K. J. Shaughnessy, and G. J. Litt. 1989. Catalyzed reporter deposition, a novel method of signal amplification. Application to immunoassays. *Journal of immunological methods* 125: 279-285.
286. Toth, Z. E., and E. Mezey. 2007. Simultaneous visualization of multiple antigens with tyramide signal amplification using antibodies from the same species. *The journal of histochemistry and cytochemistry : official journal of the Histochemistry Society* 55: 545-554.
287. Bobrow, M. N., K. J. Shaughnessy, and G. J. Litt. 1991. Catalyzed reporter deposition, a novel method of signal amplification. II. Application to membrane immunoassays. *Journal of immunological methods* 137: 103-112.

288. Mitchell, R. T., M. Camacho-Moll, J. Macdonald, R. A. Anderson, C. J. Kelnar, M. O'Donnell, R. M. Sharpe, L. B. Smith, K. M. Grigor, W. H. B. Wallace, H. Stoop, K. P. Wolffenbuttel, R. Donat, P. T. Saunders, and L. H. Looijenga. 2014. Intratubular germ cell neoplasia of the human testis: heterogeneous protein expression and relation to invasive potential. *Modern pathology : an official journal of the United States and Canadian Academy of Pathology, Inc* 27: 1255-1266.
289. Carstens, J. L., P. Correa de Sampaio, D. Yang, S. Barua, H. Wang, A. Rao, J. P. Allison, V. S. LeBleu, and R. Kalluri. 2017. Spatial computation of intratumoral T cells correlates with survival of patients with pancreatic cancer. *Nature communications* 8: 15095.
290. Vasaturo, A., S. Di Blasio, D. Verweij, W. A. Blokx, J. H. van Krieken, I. J. de Vries, and C. G. Figdor. 2017. Multispectral imaging for highly accurate analysis of tumour-infiltrating lymphocytes in primary melanoma. *Histopathology* 70: 643-649.
291. Shi, S. R., M. E. Key, and K. L. Kalra. 1991. Antigen retrieval in formalin-fixed, paraffin-embedded tissues: an enhancement method for immunohistochemical staining based on microwave oven heating of tissue sections. *The journal of histochemistry and cytochemistry : official journal of the Histochemistry Society* 39: 741-748.
292. Shin, R. W., T. Iwaki, T. Kitamoto, and J. Tateishi. 1991. Hydrated autoclave pretreatment enhances tau immunoreactivity in formalin-fixed normal and Alzheimer's disease brain tissues. *Laboratory investigation; a journal of technical methods and pathology* 64: 693-702.
293. Collings, L. A., L. W. Poulter, and G. Janossy. 1984. The demonstration of cell surface antigens on T cells, B cells and accessory cells in paraffin-embedded human tissues. *Journal of immunological methods* 75: 227-239.
294. Beckstead, J. H. 1994. A simple technique for preservation of fixation-sensitive antigens in paraffin-embedded tissues. *The journal of histochemistry and cytochemistry : official journal of the Histochemistry Society* 42: 1127-1134.
295. Feng, Z., S. M. Jensen, D. J. Messenheimer, M. Farhad, M. Neuberger, C. B. Bifulco, and B. A. Fox. 2016. Multispectral Imaging of T and B Cells in Murine Spleen and Tumor. *Journal of immunology (Baltimore, Md. : 1950)* 196: 3943-3950.
296. Howat, W. J., and B. A. Wilson. 2014. Tissue fixation and the effect of molecular fixatives on downstream staining procedures. *Methods (San Diego, Calif.)* 70: 12-19.
297. McLean, I. W., and P. K. Nakane. 1974. Periodate-lysine-paraformaldehyde fixative. A new fixation for immunoelectron microscopy. *The journal of histochemistry and cytochemistry : official journal of the Histochemistry Society* 22: 1077-1083.
298. Brenes, F., S. Harris, M. O. Paz, L. M. Petrovic, and P. J. Scheuer. 1986. PLP fixation for combined routine histology and immunocytochemistry of liver biopsies. *Journal of clinical pathology* 39: 459-463.

299. Hicks, D. J., L. Johnson, S. M. Mitchell, J. Gough, W. A. Cooley, R. M. La Ragione, Y. I. Spencer, and A. Wangoo. 2006. Evaluation of zinc salt based fixatives for preserving antigenic determinants for immunohistochemical demonstration of murine immune system cell markers. *Biotechnic & histochemistry : official publication of the Biological Stain Commission* 81: 23-30.
300. Feng, Z., S. Puri, T. Moudgil, W. Wood, C. C. Hoyt, C. Wang, W. J. Urba, B. D. Curti, C. B. Bifulco, and B. A. Fox. 2015. Multispectral imaging of formalin-fixed tissue predicts ability to generate tumor-infiltrating lymphocytes from melanoma. *J Immunother Cancer* 3: 47.
301. Linch, S. N., M. J. Kasiewicz, M. J. McNamara, I. F. Hilgart-Martiszus, M. Farhad, and W. L. Redmond. 2016. Combination OX40 agonism/CTLA-4 blockade with HER2 vaccination reverses T-cell anergy and promotes survival in tumor-bearing mice. *Proceedings of the National Academy of Sciences of the United States of America* 113: E319-327.
302. Bankhead, P., M. B. Loughrey, J. A. Fernandez, Y. Dombrowski, D. G. McArt, P. D. Dunne, S. McQuaid, R. T. Gray, L. J. Murray, H. G. Coleman, J. A. James, M. Salto-Tellez, and P. W. Hamilton. 2017. QuPath: Open source software for digital pathology image analysis. *Scientific reports* 7: 16878.
303. Gorris, M. A. J., A. Halilovic, K. Rabold, A. van Duffelen, I. N. Wickramasinghe, D. Verweij, I. M. N. Wortel, J. C. Textor, I. J. M. de Vries, and C. G. Figdor. 2018. Eight-Color Multiplex Immunohistochemistry for Simultaneous Detection of Multiple Immune Checkpoint Molecules within the Tumor Microenvironment. *Journal of immunology (Baltimore, Md. : 1950)* 200: 347-354.
304. Yarilin, D., K. Xu, M. Turkekul, N. Fan, Y. Romin, S. Fijisawa, A. Barlas, and K. Manova-Todorova. 2015. Machine-based method for multiplex in situ molecular characterization of tissues by immunofluorescence detection. *Scientific reports* 5: 9534.
305. Graff, J. N., J. J. Alumkal, C. G. Drake, G. V. Thomas, W. L. Redmond, M. Farhad, J. P. Cetnar, F. S. Ey, R. C. Bergan, R. Slottke, and T. M. Beer. 2016. Early evidence of anti-PD-1 activity in enzalutamide-resistant prostate cancer. *Oncotarget* 7: 52810-52817.
306. Rhode, P. R., J. O. Egan, W. Xu, H. Hong, G. M. Webb, X. Chen, B. Liu, X. Zhu, J. Wen, L. You, L. Kong, A. C. Edwards, K. Han, S. Shi, S. Alter, J. B. Sacha, E. K. Jeng, W. Cai, and H. C. Wong. 2016. Comparison of the Superagonist Complex, ALT-803, to IL15 as Cancer Immunotherapeutics in Animal Models. *Cancer immunology research* 4: 49-60.
307. Wrangle, J. M., V. Velcheti, M. R. Patel, E. Garrett-Mayer, E. G. Hill, J. G. Ravenel, J. S. Miller, M. Farhad, K. Anderton, K. Lindsey, M. Taffaro-Neskey, C. Sherman, S. Suriano, M. Swiderska-Syn, A. Sion, J. Harris, A. R. Edwards, J. A. Rytlewski, C. M. Sanders, E. C. Yusko, M. D. Robinson, C. Krieg, W. L. Redmond, J. O. Egan, P. R. Rhode, E. K. Jeng, A. D. Rock, H. C. Wong, and M. P. Rubinstein. 2018. ALT-803, an IL-15 superagonist, in combination with nivolumab in patients with metastatic non-small cell lung cancer: a non-randomised, open-label, phase 1b trial. *The Lancet. Oncology* 19: 694-704.

308. Decalf, J., M. L. Albert, and J. Ziai. 2019. New tools for pathology: a user's review of a highly multiplexed method for in situ analysis of protein and RNA expression in tissue. *The Journal of pathology* 247: 650-661.
309. Rimm, D. L. 2014. Next-gen immunohistochemistry. *Nature methods* 11: 381-383.
310. Magaki, S., S. A. Hojat, B. Wei, A. So, and W. H. Yong. 2019. An Introduction to the Performance of Immunohistochemistry. *Methods in molecular biology (Clifton, N.J.)* 1897: 289-298.
311. Torlakovic, E. E., C. C. Cheung, C. D'Arrigo, M. Dietel, G. D. Francis, C. B. Gilks, J. A. Hall, J. L. Hornick, M. Ibrahim, A. Marchetti, K. Miller, J. H. van Krieken, S. Nielsen, P. E. Swanson, M. Vyberg, X. Zhou, and C. R. Taylor. 2017. Evolution of Quality Assurance for Clinical Immunohistochemistry in the Era of Precision Medicine. Part 3: Technical Validation of Immunohistochemistry (IHC) Assays in Clinical IHC Laboratories. *Applied immunohistochemistry & molecular morphology : AIMM* 25: 151-159.
312. Ilie, M., E. Long-Mira, C. Bence, C. Butori, S. Lassalle, L. Bouhlel, L. Fazzalari, K. Zahaf, S. Lalvee, K. Washetine, J. Mouroux, N. Venissac, M. Poudenx, J. Otto, J. C. Sabourin, C. H. Marquette, V. Hofman, and P. Hofman. 2016. Comparative study of the PD-L1 status between surgically resected specimens and matched biopsies of NSCLC patients reveal major discordances: a potential issue for anti-PD-L1 therapeutic strategies. *Annals of oncology : official journal of the European Society for Medical Oncology* 27: 147-153.
313. Barnes, M., C. Srinivas, I. Bai, J. Frederick, W. Liu, A. Sarkar, X. Wang, Y. Nie, B. Portier, M. Kapadia, O. Sertel, E. Little, B. Sabata, and J. Ranger-Moore. 2017. Whole tumor section quantitative image analysis maximizes between-pathologists' reproducibility for clinical immunohistochemistry-based biomarkers. *Laboratory investigation; a journal of technical methods and pathology* 97: 1508-1515.
314. Angelo, M., S. C. Bendall, R. Finck, M. B. Hale, C. Hitzman, A. D. Borowsky, R. M. Levenson, J. B. Lowe, S. D. Liu, S. Zhao, Y. Natkunam, and G. P. Nolan. 2014. Multiplexed ion beam imaging of human breast tumors. *Nature medicine* 20: 436-442.
315. Giesen, C., H. A. Wang, D. Schapiro, N. Zivanovic, A. Jacobs, B. Hattendorf, P. J. Schuffler, D. Grolimund, J. M. Buhmann, S. Brandt, Z. Varga, P. J. Wild, D. Gunther, and B. Bodenmiller. 2014. Highly multiplexed imaging of tumor tissues with subcellular resolution by mass cytometry. *Nature methods* 11: 417-422.
316. Redmond, W. L., and A. D. Weinberg. 2007. Targeting OX40 and OX40L for the treatment of autoimmunity and cancer. *Critical reviews in immunology* 27: 415-436.